Report No. UMTA-MD-06-0022-77-2

A STATE-CONSTRAINED APPROACH TO VEHICLE-FOLLOWER CONTROL FOR SHORT-HEADWAY AGT SYSTEMS

A. J. PUE

TECHNICAL REPORT

AUGUST 1977

Prepared for

DEPARTMENT OF TRANSPORTATION
URBAN MASS TRANSPORTATION ADMINISTRATION

Office of Research and Development
Washington, D.C. 20590

NOTICE

This document is disseminated under the sponsorship of the Department of Transportation in the interest of information exchange. The United States Government assumes no liability for its contents or use thereof.

Technical Report Documentation Page

1. Report No.	2. Government Accession No.	3. Recipient's Catalog No.
UMTA-MD-06-0022-77-2		

4. Title and Subtitle	5. Report Date
A State-Constrained Approach To Vehicle-Follower Control For Short-Headway AGT Systems	6. Performing Organization Code
	8. Performing Organization Report No.
7. Author(s) J. A. Pue	
9. Performing Organization Name and Address The Johns Hopkins University Applied Physics Laboratory Johns Hopkins Road Laurel, Maryland 20810	10. Work Unit No. (TRAIS) 11. Contract or Grant No. DOT-UT-60042T
12. Sponsoring Agency Name and Address Department of Transportation Urban Mass Transportation Administration 2100 Second Street, SW Washington, DC 20590	13. Type of Report and Period Covered Final Report 14. Sponsoring Agency Code

15. Supplementary Notes

16. Abstract

Vehicle-following in an automated-guideway transit (AGT) system is a longitudinal control scheme where the state of a given vehicle is determined by the behavior of the preceding vehicle. At short time headways (0.5 to 3 s) a kinematic constraint on vehicle operation arises as a consequence of the velocity, acceleration, and jerk limits imposed to assure passenger comfort. This constraint requires a trailing vehicle to maintain a spacing such that it may react to nominal (nonemergency) preceding-vehicle maneuvers without collision and without exceeding service jerk and acceleration limits. A nonlinear feedback controller is designed to force the vehicle to follow the kinematically required spacing until the desired headway is attained. The design is based on a technique that uses an approximately optimal feedback control with state constraints. In addition, several suboptimal controls with reduced informational requirements are presented, thus producing an easily instrumentable controller that properly responds to all possible nominal maneuvers of a preceding vehicle.

17. Key Words	18. Distribution Statement
Optimal Control Automated-Guideway Transit Nonlinear Control Vehicle-Follower Control	This document is available to the public from the National Technical Information Service, Springfield, VA 22161.

19. Security Classif. (of this report)	20. Security Classif. (of this page)	21. No. of Pages	22. Price
Unclasified	Unclassified	128	

ABSTRACT

Vehicle-following in an automated-guideway transit (AGT) system is a longitudinal control scheme where the state of a given vehicle is determined by the behavior of the preceding vehicle. At short time headways (0.5 to 3 s) a kinematic constraint on vehicle operation arises as a consequence of the velocity, acceleration, and jerk limits imposed to assure passenger comfort. This constraint requires a trailing vehicle to maintain a spacing such that it may react to nominal (nonemergency) preceding-vehicle maneuvers without collision and without exceeding service jerk and acceleration limits. A nonlinear feedback controller is designed to force the vehicle to follow the kinematically required spacing until the desired headway is attained. The design is based on a technique that uses an approximately optimal feedback control with state constraints. In addition, several suboptimal controls with reduced informational requirements are presented, thus producing an easily instrumentable controller that properly responds to all possible nominal maneuvers of a preceding vehicle.

FOREWORD

This report documents an investigation into the automatic longitudinal control of vehicles using a vehicle-follower strategy in the short-headway range of operation (0.5 to 3 s). The work was carried out as part of the Automated Guideway Transit Technology Program under UMTA contract DOT-UT-60042T.

CONTENTS

ILLUSTRATIONS

TABLES

1. BACKGROUND

Two basic philosophies for the longitudinal control of vehicles on a guideway have been proposed for the design of an automated-guideway transit (AGT) system. One philosophy, known as point-following, assigns a cell (or slot) to each vehicle. These cells are propagated along the guideway network at predetermined velocities and spacings while propulsion commands are generated to keep each vehicle in its assigned cell. The other philosophy, an approach termed "vehicle-following," was considered in this study. Vehicle-following employs communication between vehicles, so as to allow a vehicle to control its motion in accordance with the motion of its neighbors.

Several investigators have shown the feasibility of this approach by using a linear, time-invariant regulator to control perturbations from a nominal operating condition. Levine and Athans (Ref. 1) use the linear optimal regulator to design a system in which each vehicle generates propulsion commands based on information from all other vehicles in a string. In Ref. 2, Athans et al. reduce the complexity of this technique by applying the optimization procedure to smaller overlapping strings. Finally, Cunningham and Hinman (Ref. 3) reduce the scheme to one in which vehicle control is based only on vehicle state and the state of the immediately preceding vehicle. This vehicle-following strategy is pursued by Brown in Ref. 4, while Ref. 5 deals with

---

Ref. 1. W. S. Levine and M. Athans, "On the Optimal Error Regulation of a String of Moving Vehicles," IEEE Trans. Autom. Control, Vol. AC-11, No. 3, July 1966.

Ref. 2. M. Athans, W. S. Levine, and A. H. Levis, "On the Optimal and Suboptimal Position and Velocity Control of a String of High Speed Moving Trains," MIT Electronic Systems Laboratory Report PB 173640, November 1966.

Ref. 3. E. P. Cunningham and E. J. Hinman, "Approach to Velocity/Spacing Regulation and the Merging Problem in Automated Transportation," Joint Transportation Engineering Conference, Chicago, IL, October 1970.

Ref. 4. S. J. Brown, Jr., "Design of Car-Follower Type Control Systems with Finite Bandwidth Plants," Proc. Seventh Annual Princeton Conference on Information Sciences and Systems, March 1973.

Ref. 5. R. E. Fenton et al., "Fundamental Studies in the Automatic Longitudinal Control of Vehicles," DOT-TST-76-79, July 1975.

the design and testing of hardware systems. Recently it has been recognized (Ref. 6) that additional problems occur at very short time headways (i.e., the time between successive vehicles passing a fixed point on the guideway) when one considers the large initial conditions that may be present in a real system.

Stupp, Chiu, and Brown (Ref. 6) have investigated the feasibility of a vehicle-following system for headways of 0.4 to 3 s and speeds from 8 to 24 m/s. Their analysis was formulated in terms of a dual-mode control that uses an open-loop velocity command to some desired line speed when vehicles are widely spaced and a closed-loop control for regulation when vehciles are closely spaced. In addition, each vehicle was required to observe specified jerk and acceleration limits in order to assure passenger safety and comfort. The limits were known a priori by each vehicle although future maneuvers by a preceding vehicle were unknown to the trailing vehicle. As a result, a fundamental kinematic constraing arises due to the bounds on vehicle motion. This constraint dictates a minimum allowable spacing between vehicles that is a function of trailing vehicle state, preceding vehicle state, and the future maneuver capability of each vehicle. The kinematic constraint had not been detected by earlier investigators primarily because they had not considered the overtaking situation at very short headways.

It is also shown (Ref. 6) that the kinematic constraint determines the point at which a vehicle must switch from a velocity-command mode to the closed-loop regulation mode of operation. As a result, the bandwidth requirement for the closed-loop regulator at short headways was inconsistent with the large initial values of vehicle motion. That is, the system response to these initial conditions typically led to violation of comfort criteria and the kinematically required spacing. Inclusion of local acceleration and jerk limits in a time-invariant controller would, under certain conditions, lead to limit-cycle oscillations of the regulator. Consequently, a time-varied gain approach was attempted in conjunction with the local acceleration and jerk limits. Because no systematic design procedure could be found to serve as a basis for this design, it met with limited success. However, despite the inability of the time-varied controller to achieve the kinematically required minimum spacing, the mathematical formulation of this constraint (Ref.6) appears to be a notable contribution to the definition of short-headway control problems. The key to the state-constrained approach to vehicle-follower control presented in this study is the explicit incorporation of this constraint function into the control law. The procedure used and the results of this investigation are summarized in Section 2.

Ref. 6. G. B. Stupp, H. Y. Chiu, and S. J. Brown, "Feasibility of Vehicle-Follower Controls for Short-Headway AGT Systems," APL/JHU TPR-035, June 1976.

2. SUMMARY

Any control system design requires an adequate formulation of the problem to ensure the proper system response in a realistic situation. A comprehensive mathematical description of the problem may then be used to select an appropriate design technique. However, the solution must be commensurate with the ability of present technology to provide the accuracies necessary to meet the requirements of the original problem formulation.

The first step in applying this procedure to the design of a vehicle-following control system is to establish criteria for evaluating vehicle performance. Because of the high cost of guideway construction, one measure of performance is the capacity of the system or the ability to transport a given number of passengers per unit time along a given section of guideway. The specification of a short time headway (0.5 to 3 s between successive vehicles) is aimed at meeting this condition. A second criterion is that of passenger comfort, which is generally expressed in terms of limits on vehicle acceleration and jerk. Finally, the most important performance measure is passenger safety, thus placing collision avoidance as the chief goal during normal operation (emergency situations may allow controlled collision).

A typical approach taken by a control system designer is to express the above criteria in terms of physical variables that are related through differential equations. A quadratic performance index is often used to weigh relatively the deviation from ideal performance versus the levels of control in the form of one composite expression. Optimal control theory then yields a solution that minimizes the quadratic performance index subject to the constraints imposed by the differential equations describing the physical properties of the system.

The principal focus of this study is the recognition that the kinematic constraint (i.e., an inequality constraint on the state variables) must be included in the above problem formulation. Moreover, a convenient feature of the kinematic constraint is that it is compatible with all of the performance criteria described above. As discussed in Section 1, the kinematic constraint is a result of the fact that future maneuvers of a preceding vehicle are unknown by the trailing vehicle. Thus, the trailing vehicle must anticipate a worst-case maneuver under nominal operating conditions on the part of a preceding vehicle. A worst-case maneuver consists of a minimum-time deceleration to minimum line speed using

service limits (i.e., the jerk and acceleration limits that assure passenger comfort). Hence, worst case is defined here for normal operation rather than emergency conditions. This anticipation of a worst-case maneuver translates to a required spacing such that the trailing vehicle may avoid collision by using its own full service-braking capability. Consequently, the kinematic constraint has all of the ingredients of our stated performance criteria. It allows the smallest possible spacing (or largest system capacity) in order to prevent a vehicle from exceeding service limits in a nonemergency situation and avoid collision. We now see that the kinematic constraint is, in fact, a precise mathematical statement of our performance measures.

The procedure used in this study is to combine the kinematic constraint (our performance criterion for transient phenomena, principally the overtaking situation) and a quadratic performance index (the criterion for steady-state perturbational phenomena) into an optimal control problem. However, the solution to such a problem is complex and requires a good deal of computation. Hence, in accordance with our stated requirement of finding a solution in view of existing technology, an approximate solution is sought with the use of a previously derived technique (Ref. 7). The method is based on a dual solution that may be summarized as follows.

When the states of the trailing and preceding vehicle are such that violation of the kinematic constraint is not imminent, we use the well-known solution to the optimal control problem with quadratic performance index — a constant-gain linear regulator that ignores the kinematic constraint. When conditions change such that the kinematic constraint may be violated, a control that causes the vehicle to follow precisely the kinematically required spacing is inplemented until it is determined that regulator control would again satisfy the constraint. A further approximation is presented whereby the linear regulator portion of the controller is eliminated. This requires some modification of the kinematic constraint but simplifies the control aspects with little degradation in performance. However, even with this simplification, the informational requirements for precisely maintaining the kinematically required spacing include preceding vehicle velocity, acceleration, and jerk. To overcome this drawback, several suboptimal controllers are derived with the intent of simplifying the kinematic constraint so that the resulting control will always keep the vehicle outside the actual kinematic boundary, while requiring less computation and information.

Ref. 7. G.N. Saridis and Z. V. Rekasius, "Design of Approximately Optimal Feedback Controllers for Systems with Bounded States," IEEE Trans. Autom. Control, Vol. AC-12, No. 4, August 1965.

The final result is an easily instrumentable controller requiring only spacing and its derivatives (relative velocity and acceleration).

Simulation studies are used to verify the effectiveness of the approach. First, the performance of the optimal and suboptimal controls are compared in a typical overtaking maneuver. For example, one maneuver is considered where two vehicles are initially spaced at 100 m with the preceding vehicle traveling at 10 m/s and the trailing vehicle traveling at 20 m/s (i.e., an initial headway of 5 s). For a desired headway of 0.5 s the optimal control requires 11.4 s to attain a headway of 0.55 s. Suboptimal control I, which requires the same information as the optimal control but with reduced computational complexity, performs the maneuver in 15.0 s. Suboptimal control II is even less complex computationally and, in addition, requires only information of spacing, relative velocity, and relative acceleration, with a time of 21.5 s required to reach the 0.55-s headway. Finally, suboptimal control III is a simplification over suboptimal control II in that one multiplication is removed from the computation. The time to reach the 0.55-s headway using suboptimal control III is 32.5 s. These results, in conjunction with other test cases in the study, point to suboptimal control II as the best choice in terms of the trade-off between performance and complexity.

In addition to the overtaking maneuver, the various control laws are tested in a situation where the vehicles are initially at the desired headway with a velocity of 10 m/s. The preceding vehicle then accelerates at the jerk and acceleration limits to a velocity of 25 m/s and immediately decelerates back to 10 m/s. In all cases the trailing vehicle successfully follows the preceding vehicle maneuver. The performance of the controllers in a five-vehicle string is the final subject of evaluation. Again, all maneuvers are performed in a smooth and satisfactory manner under a variety of circumstances.

The principal accomplishments of this work may be summarized as follows.

1. For the first time the state constraints inherent in a vehicle-following strategy are expressed as part of the control scheme. The resulting control is a nonlinear function of states that constitutes a natural way to conduct the transition between the modes of operation normally designed into a vehicle-following system. Thus, it affords a general formulation and systematic approach that designers may adapt for future work in this area.

2. Near-optimal performance may be obtained in that the spacing between vehicles is the minimum that allows safe and comfortable operation for all possible nominal maneuvers of a preceding vehicle.

3. An easily instrumentable controller is designed through simplification of the kinematic constraint. A particular control law is selected based on the trade-off between vehicle performance and controller complexity.

4. Simulation studies have verified the effectiveness of the controllers in a variety of situations.

The study represents the initial phase of an investigation that must be continued in order to determine the feasibility of implementing a state-constrained vehicle-following controller into a real system. Thus, further work would include the following areas:

1. Simulation studies with a realistic vehicle model to determine the effects of parameter variation and external forces such as wind gust, grade, and loading;

2. Selection of sampling rates, quantization levels, and time delays that may be tolerated while maintaining acceptable performance, including the design of an onboard digital controller using current microprocessor technology;

3. Study of the manner in which state measurements are obtained, the requirements on the accuracy of these measurements, and the design of a wayside computer and communications system; and

4. Application of this technique to other situations, such as merging and the injection of vehicles onto the guideway.

The contents of this report are as follows: In Section 3 the kinematic constraint is described in terms of two possible vehicle maneuvers, which yields a minimum allowable spacing as a function of vehicle states. Section 4 presents the design problem by explicitly considering the jerk, acceleration, and kinematic constraints. An approximately optimal regulator is then introduced as an easily instrumentable solution to the vehicle-following problem. The optimal control law on the kinematic boundary is formulated and then modified so the kinematic

boundary coincides with the desired spacing. Hence, the transition controller will act as a regulator at the nominal headway. In Section 5 three suboptimal control laws are derived from simplification of the kinematic constraint. These controls are suboptimal in the sense of reduced complexity and information requirements, but they also result in reduced performance. A describing-function analysis is used in Section 6 to validate the closed-loop stability of the suboptimal controls. The results of simulated test cases are presented in Section 7. The headway profiles using the optimal and suboptimal controls are compared for several overtaking maneuvers. Here, the trade-off between vehicle performance and controller complexity is determined. The suboptimal controls are then implemented in the regulator mode and in a five-vehicle string.

3. KINEMATIC BOUNDARY CONSTRAINT

This section provides a mathematical description of the kinematic constraint so that the resulting constraint function may be incorporated into the control law. The kinematic constraint becomes, in effect, the operating philosophy of a short-headway vehicle-following system and hence, because of its importance, the assumptions leading to its derivation will first be reviewed.

The kinematic constraint is the result of fundamental characteristics of vehicle following; that is, future maneuvers of a preceding vehicle are unknown by a trailing vehicle. Thus, safety considerations require that the trailing vehicle controller anticipate a nonemergency minimum-time deceleration to minimum line speed by the preceding vehicle at any time. A minimum-time deceleration is determined by the velocity, acceleration, and jerk limits imposed on the system for passenger safety and comfort. Consequently, the maneuver capability of a given vehicle as defined by these limits yields a time and distance required for a vehicle to decelerate to a given speed. In view of this fact, a trailing vehicle traveling at a higher velocity than a preceding vehicle (i.e., overtaking) will require a greater distance than the preceding vehicle to decelerate to minimum line speed. As a result, the trailing vehicle must maintain a spacing such that if the preceding vehicle should perform a minimum-time deceleration maneuver, the trailing vehicle can avoid collision by using its full service-braking capability. An underlying assumption in this argument is that the trailing vehicle adheres to its service limits. If the preceding vehicle brakes at service limits, the trailing vehicle can avoid collision by applying emergency braking. However, it is desirable to avoid the use of emergency limits in nonemergency situations; therefore, the kinematic constraint described above is constructed.

To illustrate the significance of the kinematic constraint, consider two vehicles arbitrarily spaced at 25 m with the preceding vehicle traveling at 15 m/s and the trailing vehicle traveling at 25 m/s (Fig. 1a). If both vehicles decelerate at their service limits to minimum line speed, the trailing vehicle reaches 10 m/s at 6.77 s (Fig. 1b). However, since the distance required for the trailing vehicle to reach 10 m/s is greater than the distance required for the preceding vehicle, a collision would occur. As a result, an initial spacing of 48.5 m is required (Fig. 2a). If both vehicles then decelerate to a minimum line speed, the final spacing at 6.77 s is 5 m (precisely the desired headway of 0.5 s) as shown in Fig. 2b. Thus, for any spacing less than 48.5 m the

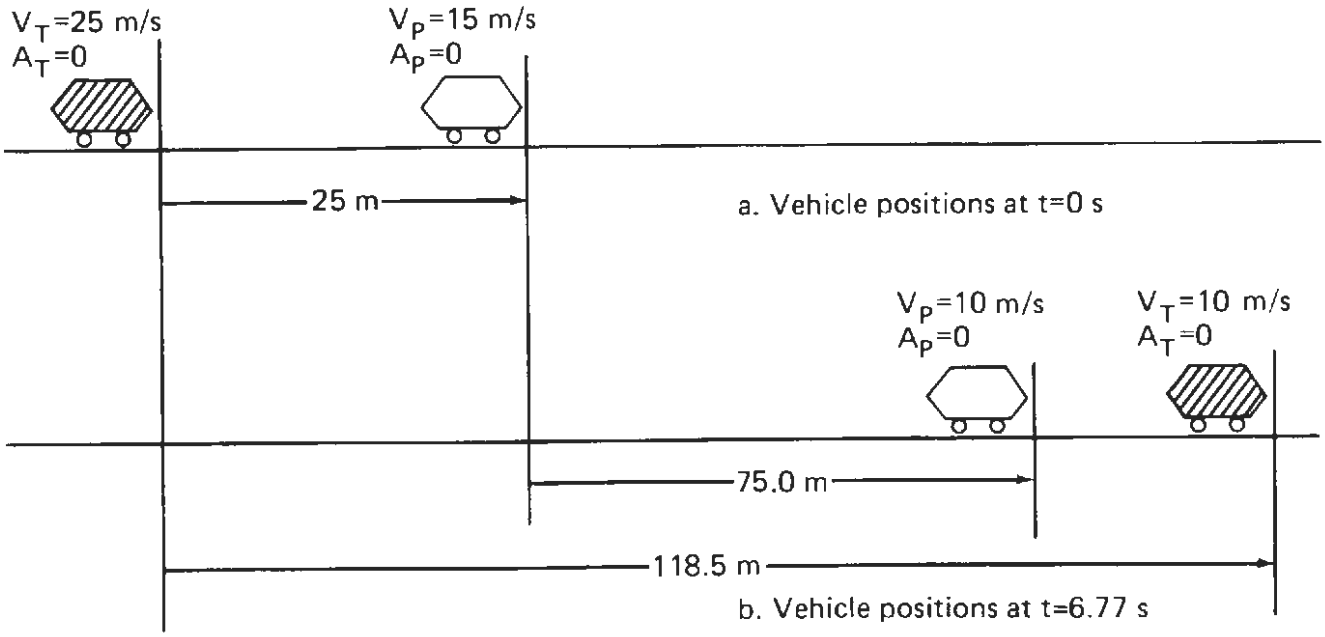

Fig. 1 Example Violating the Kinematic Constraint

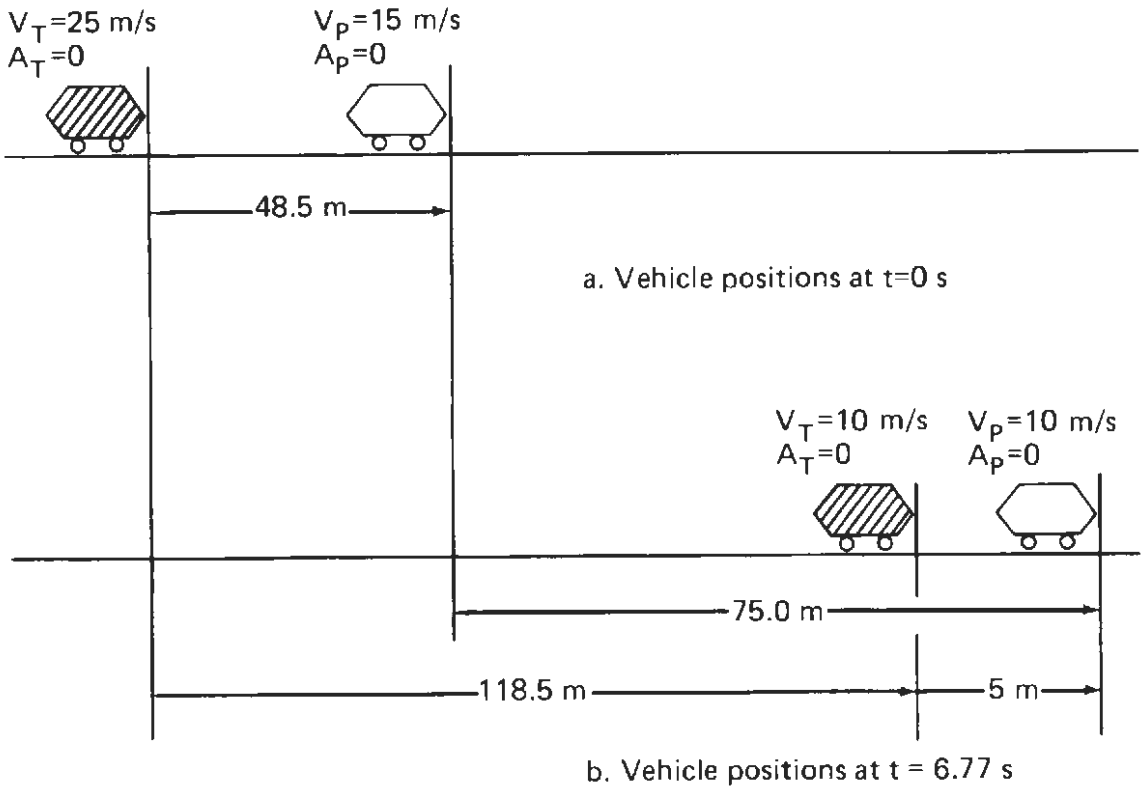

Fig. 2 Example Satisfying the Kinematic Constraint

trailing vehicle cannot attain the desired 0.5-s headway. For spacings less than 46.5 m emergency limits would be required to prevent a collision (assuming a vehicle length of 3 m). However, the use of emergency limits may be avoided if the trailing vehicle maintains the spacing as required for a given set of vehicle states.

VEHICLE MANEUVER CAPABILITIES

To develop a mathematical description of the kinematic constraint, we first examine the maneuver capability of a given vehicle. As discussed above this maneuver capability is a function of the limits imposed on the system. These limits have been specified for this study as follows:

Service acceleration limit, $A_s = 2.6$ m/s^2

Service jerk limit, $J_s = 2.6$ m/s^3

Maximum guideway speed, $V_{max} = 25$ m/s

Minimum guideway speed, $V_{min} = 10$ m/s

Although the above limits are somewhat higher than those presently achievable in a real system, it is felt they represent a good test for a controller design.

Since both acceleration and jerk limits have been specified, there are two possible minimum-time maneuver profiles that may occur when a vehicle decelerates to a lower speed. They are shown as Maneuvers 1 and 2 in Fig. 3. In Maneuver 1 the initial acceleration may be positive or negative and the acceleration profile always reaches the negative acceleration limit. In the case of Maneuver 2 the initial acceleration is again either positive or negative but the profile does not reach the negative acceleration limit. For a given set of vehicle states (acceleration and velocity) only one of the two possible maneuvers is applicable. This is shown in Fig. 3c, where each maneuver is associated with a region in the A-V plane. The acceptable region is bounded by the acceleration limits (A_s and $-A_s$) and the velocity limits (V_{min} and V_{max}). In addition, there are bounds near $-A_s$ and V_{min} and near A_s and V_{max} that are associated with the jerk limits. The latter bound results from the fact that if the vehicle is at the maximum acceleration limit, A_s, braking must be applied at the negative jerk limit at some velocity less than V_{max} in order not to exceed V_{max}. The trajectory that satisfies this condition is shown in Fig. 3c and is given by the relationship

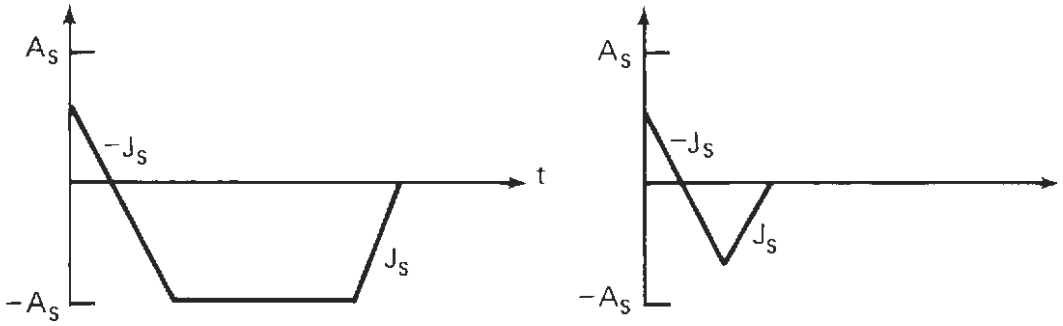

a. Maneuver 1

b. Maneuver 2

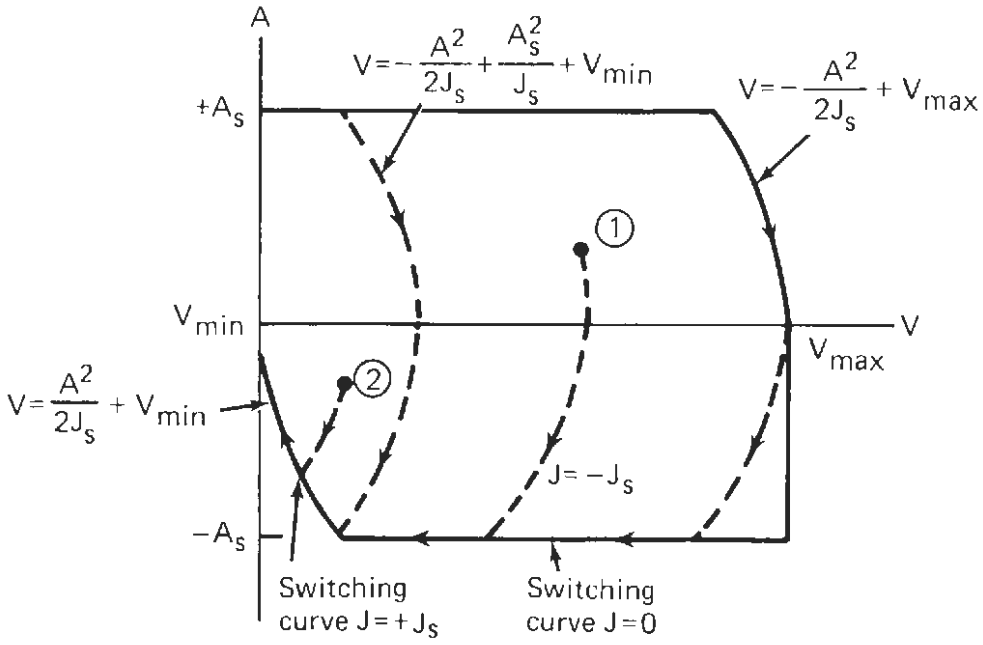

c. Minimum-time phase trajectory

Fig. 3 Minimum-Time Deceleration Maneuvers

$$V = -\frac{A^2}{2J_s} + V_{max} \quad .$$

Similarly, if a vehicle is at the negative acceleration limit, it must begin accelerating at the positive jerk limit in order not to drop below minimum line speed. This condition is satisfied by the trajectory given by

$$V = \frac{A^2}{2J_s} + V_{min} \quad .$$

Various minimum-time trajectories are indicated by dashed lines in Fig. 3c. Suppose, for example, a vehicle has the acceleration and velocity as shown by point 1. In order to decelerate to V_{min} in minimum time, the vehicle is immediately decelerated at the negative jerk limit and follows the parabolic trajectory shown. When the vehicle reaches the lower boundary of the acceptable region, the jerk is switched to 0 and the vehicle follows the negative acceleration limit until the lower left boundary of the acceptable region is reached. At this point the positive jerk limit is applied until the vehicle reaches minimum line speed. If the vehicle has an acceleration and velocity given by point 2 in the figure, the minimum-time trajectory does not include the switching curve corresponding to zero jerk. Consequently, any combination of acceleration and velocity that results in a maneuver just touching the negative acceleration limit specifies the trajectory separating Maneuvers 1 and 2. This trajectory (Fig. 3c) is given by the relationship

$$V = -\frac{A^2}{2J_s} + \frac{A_s^2}{J_s} + V_{min} \quad .$$

The kinematic constraint may now be formulated with the aid of the above description of vehicle maneuverability.

FUNCTIONAL DESCRIPTION

In order to describe functionally the kinematic requirement it is necessary to determine the distance in which a vehicle performs a minimum-time deceleration to minimum line speed as a

function of current velocity and acceleration. This may be found by a repeated integration of the curves shown in Fig. 3. The resulting time and distance for each maneuver is given in Appendix A.

Figure 4 illustrates the kinematic requirement as the required spacing to prevent collision in the event of a minimum-time deceleration by the preceding vehicle. As shown in Fig. 4, this spacing is given in terms of the distance required for each vehicle to complete a maneuver to minimum line speed and the time in which each vehicle accomplishes the maneuver. Consequently, the minimum required spacing is given by

$$S_{min} = X_P - X_T$$

$$= d_r^T - d_r^P - V_{min} (t_r^T - t_r^P) + hV_{min} \quad . \qquad (1)$$

The values of d_r^T, d_r^P, t_r^T, and t_r^P are given by the relations in Appendix A and are a function of each vehicle's current velocity and acceleration.

In the overtaking situation the preceding vehicle is at a lower velocity than the trailing vehicle and will complete its maneuver to minimum line speed before the trailing vehicle reaches V_{min}. Thus, the term $V_{min} (t_r^T - t_r^P)$ represents the distance traveled by the preceding vehicle at minimum line speed while the trailing vehicle is still in the process of accomplishing its deceleration maneuver. If, on the other hand, the trailing vehicle is at a lower velocity, this term will subtract from the overall required spacing.

The term hV_{min} represents the desired spacing when both vehicles are at V_{min} with no acceleration. Hence, it constitutes a residual term which specifies the desired spacing when the kinematically required spacing is 0. As a result, any suitable factor may be used (not necessarily hV_{min}). In fact, it will be shown that using hV_T rather than hV_{min} simplifies the control problem. Moreover, other vehicle-following strategies may be employed (e.g., a policy of constant K-factor) through inclusion of the appropriate term in the constraint function.

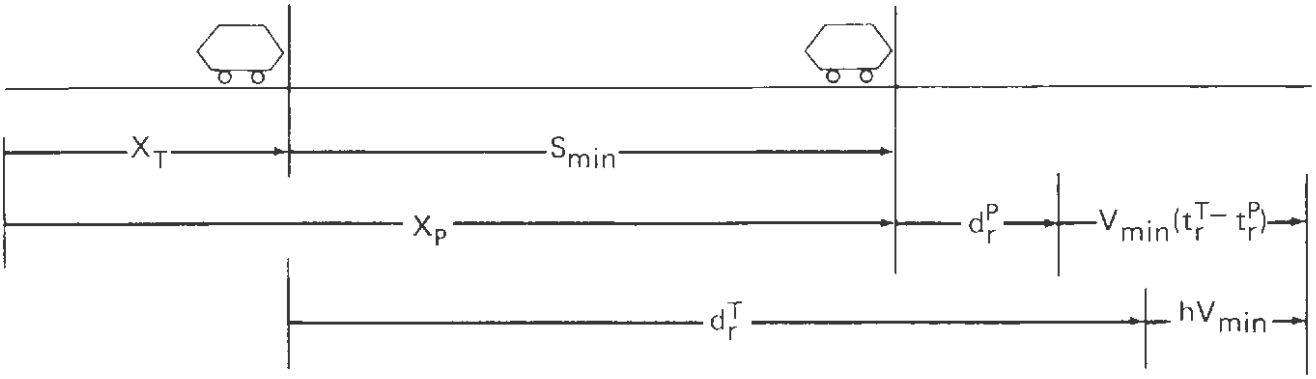

Fig. 4 Minimum Spacing as Required by Kinematics

Consequently, the kinematic constraint may be formulated in terms of vehicle spacing, S, as follows:

$$S_{min} - S \leq 0 \quad , \tag{2}$$

where S_{min} is given by Eq. 1.

In summary, for a given set of vehicle states and assuming that vehicles are constrained to operate within service jerk and acceleration limits, there is a minimum safe spacing between the trailing and preceding vehicle. If the spacing between vehicles is less than this spacing, the kinematic constraint is violated and there is a possibility of collision. That is, if the preceding vehicle should perform a minimum-time maneuver to minimum line speed, the trailing vehicle cannot attain the desired headway using service limits. Clearly, a controller must be designed to regulate to the desired headway but at the same time is must maintain the proper spacing between vehicles when velocity errors become significant. The development in the following sections will demonstrate how the kinematic constraint may be explicitly incorporated into the control law and thus satisfy this objective.

4. OPTIMAL REGULATOR WITH STATE CONSTRAINTS

The vehicle-following problem may be formulated into the optimal regulator solution with a linear plant and an infinite time integral quadratic performance index (Ref. 6). That is, a plant of the form

$$\dot{\underline{x}} = A\underline{x} + bu \tag{3}$$

is assumed where $\underline{x}$ is the n-dimensional state vector, u is the scalar control, A is a constant $n \times n$ matrix and b is a constant n-dimensional vector. The performance index is of the standard form

$$I = \int_0^\infty (\underline{x}^T Q \underline{x} + \frac{1}{2} u^2)\, dt \ , \tag{4}$$

where Q is a constant positive semidefinite $n \times n$ matrix. The resulting regulator is a feedback controller designed to maintain the system within an acceptable deviation from a nominal condition using acceptable amounts of control. This has been shown to produce satisfactory results for small initial conditions (Ref. 6). However, in the mode-transition (e.g., overtaking) problem where large initial condition errors are present, the resulting controller produces a response that exceeds the desired jerk, acceleration, and kinematic limits. This is due to the large bandwidth requirements for short-headway operation (Ref. 6).

Consequently, in designing a controller for the mode-transition problem, the jerk and acceleration limits and, in particular, the kinematic constraint must be explicitly considered. Hence, the design problem may be described in terms of Eqs. 3 and 4 and a constraint vector denoted by

$$\underline{g}\,(\underline{x}) \leq \underline{\alpha} \ , \tag{5}$$

where $g(x)$ is a 3×1 vector consisting of the kinematic constraint, vehicle acceleration, and vehicle jerk, and $\underline{\alpha}$ is a 3×1 constant vector.

The kinematic constraint is described by Eqs. 1 and 2. As a result, the constraint vector is given by

$$g(\underline{x}) = \begin{bmatrix} c(\underline{x}) \\ |A_T| \\ |J_T| \end{bmatrix} \leq \begin{bmatrix} 0 \\ A_s \\ J_s \end{bmatrix} = \underline{\alpha} \quad , \tag{6}$$

where $c(\underline{x}) = S_{min} - S$ (see Eqs. 1 and 2). However, recall that d_r^T and t_r^T as well as d_r^P and t_r^P are determined from one of two possible maneuvers (Fig. 3). Thus, the function $c(\underline{x})$ comprises four distinct forms, since each vehicle may have an acceleration and velocity that dictate either of the two maneuver profiles. Note that only one form is applicable for a given set of vehicle states.

The minimization of Eq. 4 subject to Eqs. 3 and 6 necessitates computational complexity that would likely become prohibitive in terms of an on-board controller. Consequently, an alternative solution that produces a near-optimal controller is proposed in the following section.

APPROXIMATELY OPTIMAL FEEDBACK CONTROLLER WITH STATE CONSTRAINTS

The transition controller is required to bring the system to a desired final state without exceeding predetermined bounds. Saridis (Refs. 7 and 8) presents a procedure based on observations of the geometric features of the optimal constrained trajectories. The general method will be summarized below; application to vehicle-following control will be presented in later paragraphs.

Suppose a constraint function is given by

$$c(\underline{x}) \leq \alpha \quad ,$$

and we wish to minimize Eq. 4 subject to Eq. 3 and this scalar constraint. The constant-gain feedback solution of the unconstrained

---

Ref. 8. G. N. Saridis, "On the Exact and Approximate Solutions of the Otpimal Control Problem with Bounded State Variables," Ph.D. dissertation, Purdue University, Lafayette, IN, August 1965.

problem may be found from the well known steady-state Ricatti equation (Ref. 9). Consequently, the strategy is to implement the linear regulator while continuously monitoring $c(\underline{x})$. Whenever the optimal unconstrained trajectories are found to be approaching the constraint boundary $c(\underline{x}) = \alpha$, a nonlinear control is introduced to cause the system to follow the boundary. The controller is switched back to its linear mode when the linear regulator would cause the state of the system to remain in the allowable region (i.e., $c(\underline{x}) \leq \alpha$). These points may be illustrated with the diagram shown in Fig. 5. The state space is divided into an allowable region and a region in which the constraint is violated. For an initial condition in the allowable region the system follows the optimal unconstrained trajectory until it reaches the constraint boundary. At this point the control is switched in order to cause the system to follow the boundary of the constraint region (i.e., the optimal constrained trajectory). When the linear regulator would cause the system to move off the constraint boundary into the allowable region a switch is made back to the optimal unconstrained trajectory. The linear regulator then drives the system along the unconstrained path to the desired final condition.

The control that keeps the system on the boundary is determined by requiring the time derivative of $c(\underline{x})$ to be 0 when $c(x)$ is equal to α. Thus

$$\dot{c}(x) = (\nabla c')\dot{\underline{x}} = 0 \ ,$$

where ∇ is the gradient operator and the prime (') represents the transpose. Substituting for $\dot{\underline{x}}$ from Eq. 3 we have

$$(\nabla c') \ (A\underline{x} + bu_B) = 0$$

or

$$u_B = - \ (\nabla c'b)^{-1} \ \nabla c'A\underline{x} \ , \qquad (7)$$

where u_B is the control required to ensure that $c(\underline{x})$ remains constant. It is important to note that u_B only keeps the system on the boundary but does not necessarily drive the system to the boundary. We may have $\dot{c}$ equal 0 for any value of c, but we would like to have $\dot{c}$ equal to 0 when c equals α; therefore we implement u_B only when c equals α. If the optimal unconstrained trajectories tend to exceed the boundary, then

---

Ref. 9. A. Bryson and Y. Ho, Applied Optimal Control, John Wiley & Sons, New York, 1975.

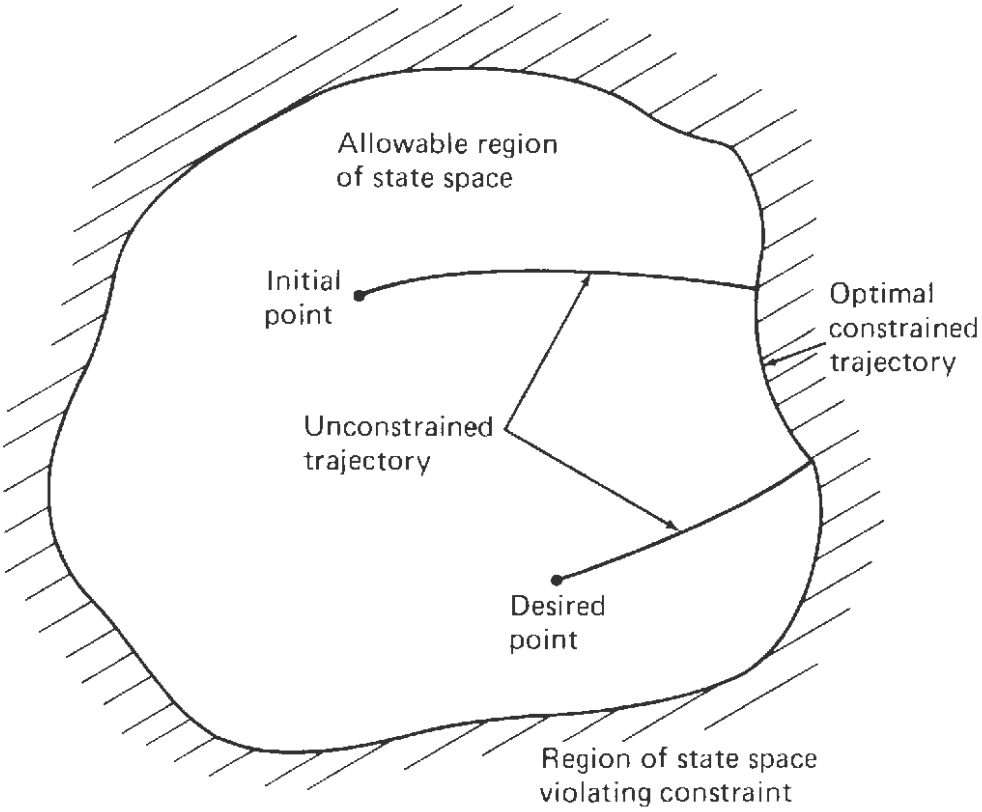

Fig. 5 Optimal Trajectory with State Constraints

$$\dot{c} > 0$$

or

$$\nabla c'[A\underline{x} + bu_R] > 0 \quad ,$$

where u_R is the linear regulator control. If the regulator is driving the system away from the boundary into the allowable region, then

$$\dot{c} < 0$$

or

$$\nabla c'[A\underline{x} + bu_R] < 0 \quad .$$

In accordance with Ref. 7, we may now establish a nonlinear controller as follows:

$$\bar{u}(\underline{x}) = [1 - W(\underline{x})]u_R + W(\underline{x})\, u_B \ ,$$

where u_R is the unconstrained linear regulator control, u_B is the optimal control law on the boundary, $c(\underline{x}) = \alpha$, and $W(\underline{x})$ is a scalar weighting function given by

$$W(\underline{x}) = \begin{cases} 0 & c(\underline{x}) \leq \delta \\ & \text{or} \\ & \delta < c(\underline{x}) \leq \alpha, \ \nabla c'[A\underline{x} + bu_R] \leq 0 \\ \dfrac{c(x) - \delta}{\alpha - \delta} & \delta < c(\underline{x}) \leq \alpha, \ \nabla c'[A\underline{x} + bu_R] > 0 \\ \text{Undefined} & c > \alpha \end{cases} , \qquad (8)$$

where δ is a constant ($\delta \leq \alpha$). The parameter δ is introduced to alleviate the problem of switching from the linear mode ($\bar{u} = u_R$) to the nonlinear mode ($\bar{u} = u_B$). It provides a smooth and gradual switch by means of the weighting function $W(\underline{x})$. For our specific problem, δ will be selected from a stability analysis in Section 6 in conjunction with a physical interpretation to be presented in the next section.

In summary, the control $\bar{u}$ assumes the linear mode ($\bar{u} = u_R$) for all states such that $c(\underline{x}) \leq \delta \leq \alpha$ or for all states such that the optimal constrained trajectory is directed away from $c(x) = \alpha$. The control $\bar{u}$ assumes the nonlinear mode when the optimal unconstrained trajectories tend to exceed the boundary $c(\underline{x}) = \alpha$.

APPLICATION OF THE STATE-CONSTRAINED CONTROLLER TO THE VEHICLE-FOLLOWING PROBLEM

We now return to the specific problem of vehicle-follower control by application of the technique discussed above. Initially, a triple-integration vehicle plant will be assumed. In addition, since the behavior of the preceding vehicle is unknown, it is necessary to consider the preceding vehicle jerk as an additional input to the system. As a result, the uncoupled system to be controlled is given by

$$\begin{bmatrix} \dot{S} \\ \dot{V}_T \\ \dot{A}_T \\ \dot{V}_P \\ \dot{A}_P \end{bmatrix} = \begin{bmatrix} 0 & -1 & 0 & 1 & 0 \\ 0 & 0 & 1 & 0 & 0 \\ 0 & 0 & 0 & 0 & 0 \\ 0 & 0 & 0 & 0 & 1 \\ 0 & 0 & 0 & 0 & 0 \end{bmatrix} \begin{bmatrix} S \\ V_T \\ A_T \\ V_P \\ A_P \end{bmatrix} + \begin{bmatrix} 0 \\ 0 \\ 1 \\ 0 \\ 0 \end{bmatrix} J_T + \begin{bmatrix} 0 \\ 0 \\ 0 \\ 0 \\ 1 \end{bmatrix} J_P \qquad (9)$$

$$\dot{\underline{x}} = A\underline{x} + bJ_T + dJ_P \ .$$

The system is subject to the constraint of Eq. 6:

$$\underline{g}(\underline{x}) \leq \underline{\alpha} \ , \qquad (10)$$

where $\underline{g}$ and $\underline{\alpha}$ are 3×1 vectors. The control input J_T, which keeps the system on the constraint boundary, is given by Eq. 7 with an additional term due to the preceding vehicle jerk. Therefore, for the ith constraint function of Eq. 10 we have

$$(J_T)_i = -(\nabla g'_i b)^{-1} \nabla g'_i [A\underline{x} + dJ_P], \text{ where } i = 1, 2, 3, 4, 5. \qquad (11)$$

The term dJ_P will be eliminated in Section 5 by deriving several suboptimal controls. The first four controls as given by Eq. 11 correspond to the four distinct forms of the kinematic constraint function. The fifth control corresponds to the acceleration limit where $g_5(x) = |A_T| \leq A_s$. The jerk limit, $|J_T| \leq J_s$, may be satisfied with a saturation limiter at the jerk input. It is desirable that only one constraint boundary be encountered at a time. That is, if the system follows one constraint element of Eq. 10 it does not violate any other constraints. This will be true for the four kinematic constraint functions since only one can be valid for any particular set of vehicle states. Similarly, the vehicle can be on either the jerk limit or the acceleration limit, but not both. The only case of concern is that the control required to keep the vehicle on the kinematic boundary may exceed jerk or acceleration limits. However, since the formulation of the kinematic constraint function explicitly includes the jerk and acceleration capabilities of the vehicle it is reasonable to expect that the limits will not be violated.

The overall control strategy is depicted by the system block diagram shown in Fig. 6. The constant feedback gains (k_1, k_2, k_3, and k_4) represent the optimal solution to the unconstrained problem that was studied in Ref. 6. The block denoted by NL is the nonlinear transition mechanism discussed below. When the system is operating in its linear mode, NL = 1.

The block denoted NL in Fig. 6 constitutes the transition controller shown in Fig. 7. The general technique of Saridis discussed previously is applied twice in the transition mechanism; the first application results in the kinematic boundary control and the second results in a block labeled "acceleration boundary controller." Although the principal element of the system is the kinematic boundary control we begin by discussing the acceleration boundary controller, since this is a simpler application of the general technique. The input to this control element is the jerk command J_L (Fig. 7).

The acceleration boundary controller functions to maintain vehicle acceleration between -2.6 and $+2.6$ m/s^2. We know the jerk command should be 0 with an A_T of either $+2.6$ or -2.6 m/s^2. Thus, when $J_L > 0$ the system is approaching the upper bound of $A_T = 2.6$ m/s^2 and when $J_L < 0$ the system is approaching $A_T = -2.6$ m/s^2. Consequently, for the upper limit case we select a δ_2 such that when $A_T > \delta_2$ we gradually reduce J_T (through the weighting function $W_2(\underline{x})$) until $J_T = 0$ when $A_T = 2.6$ m/s^2. Thus, the system will remain on the limit (2.6 m/s^2) until $J_L < 0$; we may then set $W_2(\underline{x}) = 0$. Similarly, whenever $A_T < -\delta_2$ and the system is approaching the negative acceleration limit ($J_L < 0$) the weighting function

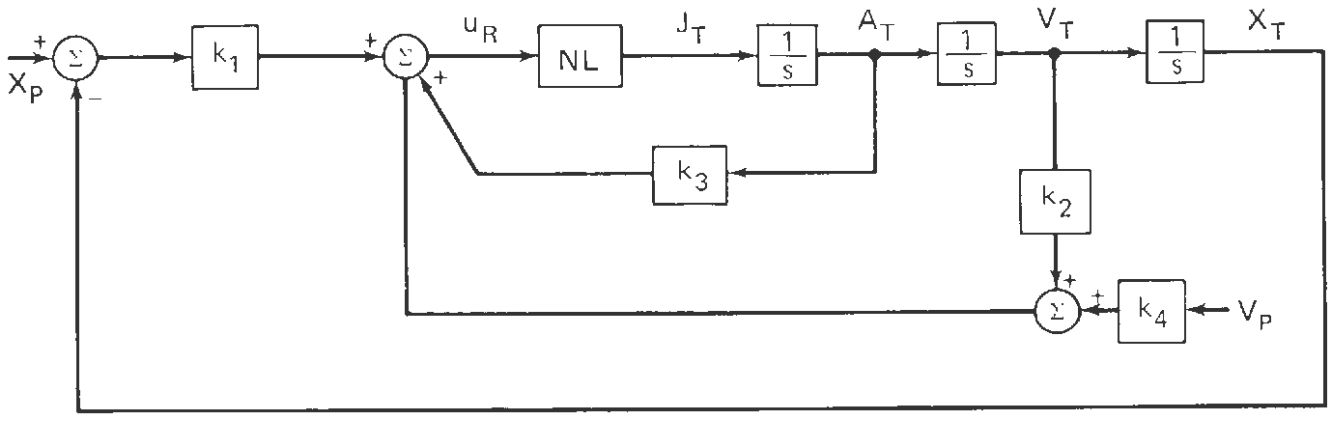

Fig. 6 System Block Diagram

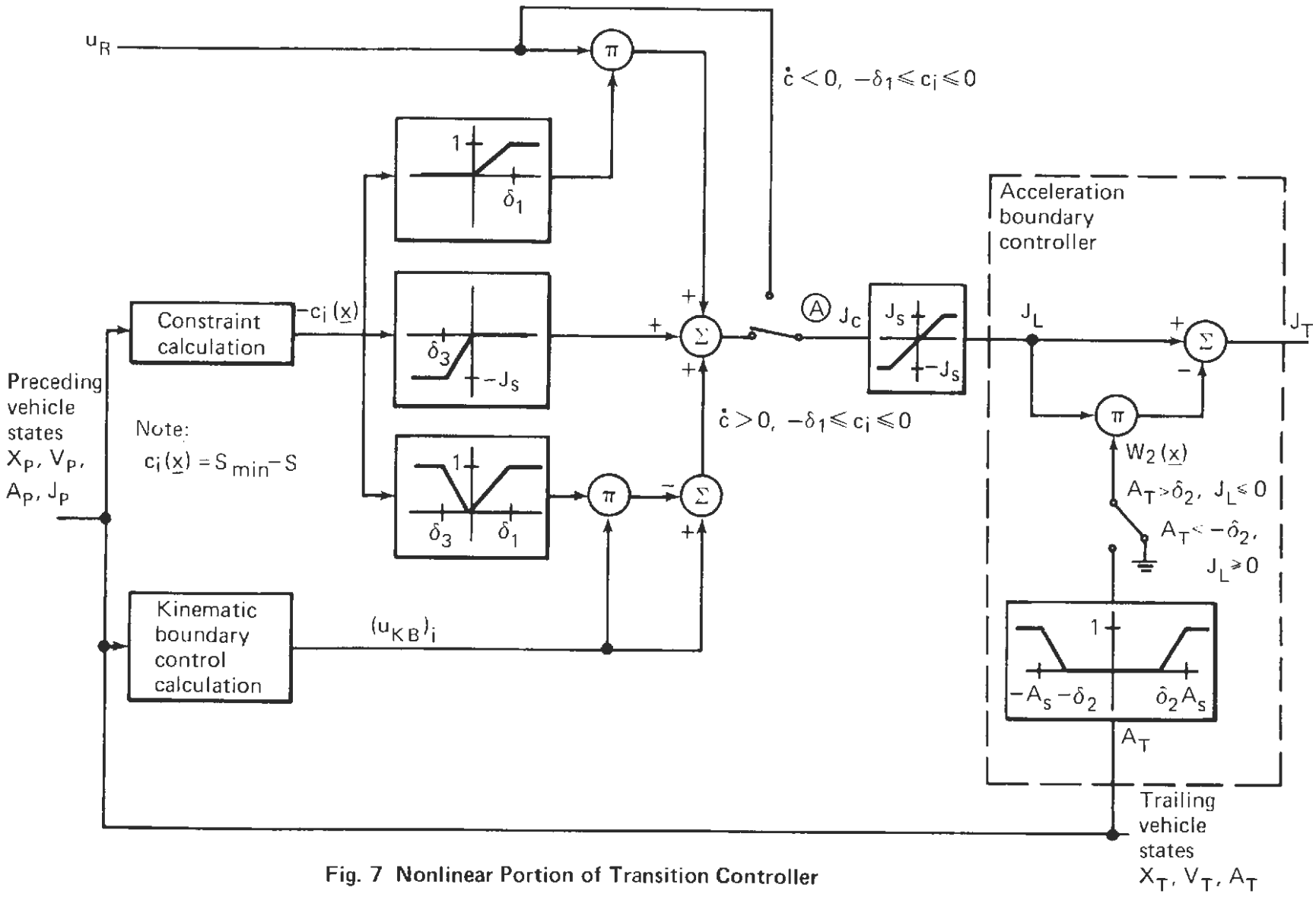

Fig. 7 Nonlinear Portion of Transition Controller

$W_2(\underline{x})$ is again introduced until $J_T = 0$ when $A_T = -2.6$ m/s^2. The switch in Fig. 7 indicates setting $W_2(x) = 0$ under the conditions noted. The acceleration boundary controller described above is therefore a form of Eq. 8 and may be summarized as follows:

$$J_T = J_L(1 - W_2(\underline{x}))$$

$$W_2(\underline{x}) = \begin{cases} 0 & |A_T| < \delta_2 \\ & \text{or } A_T > \delta_2,\ J_L \leq 0 \\ & \text{or } A_T < -\delta_2,\ J_L \geq 0 \\ \dfrac{|A_T| - \delta_2}{A_s - \delta_2} & \text{otherwise} \end{cases} .$$

Note that for $\delta_2 = A_s$ the acceleration boundary controller becomes the usual constrained-range integration process. We introduce δ_2 only to make the limiting process more gradual.

The saturation limiter preceding the acceleration boundary controller assures that the vehicle will remain within jerk limits, since

$$|J_T| = |J_L\ (1 - W_2(\underline{x}))| \leq |J_L| \leq J_s .$$

The remaining portion of Fig. 7 comprises the kinematic boundary control. As discussed earlier, we introduce the control $(u_{KB})_i$ (the subscript denotes kinematic boundary) whenever the constraint function, $c_i(\underline{x})$, approaches 0. The kinematic boundary control will maintain $c_i(\underline{x})$ at 0 until it is appropriate to switch back to the linear regulator. However, in a real system, perturbations may cause $c_i(\underline{x})$ to exceed 0. It will be shown that the controller of Fig. 7 handles this situation in addition to the control strategy outlined earlier.

As shown in Fig. 7, the kinematic constraint function, $c_i(\underline{x})$, is continuously calculated from Eqs. 1 and 2 and the relations listed in Appendix A. Note the output of the constraint calculation in Fig. 7 is the negative of the kinematic constraint, $-c_i(\underline{x})$, with i = 1, 2, 3, and 4 (recall the kinematic constraint consists of four different functions of the vehicle states and

applicable at any given time according to the values of A_T, V_T, A_P, and V_P). The appropriate values of $c_i(\underline{x})$ and $(u_{KB})_i$ (as calculated from Eq. 11) for a given set of vehicle states are then used as shown in Fig. 7. The result of the constraint calculation, $-c_i(\underline{x})$, is an input to three nonlinearities and drives the operation of the controller as follows. If $-c_i(\underline{x}) \geq \delta_1$ we are in a kinematically safe condition and the outputs of the top and bottom nonlinearities are equal to 1 while the center nonlinearity has an output of 0. Hence, the boundary control $(u_{KB})_i$ is multiplied by 0 and cancels itself at the summing junction. The linear regulator output, u_R, is also multiplied by 1 and becomes the jerk command, J_c. If $c_i(\underline{x}) = 0$ the output of all three nonlinearities is 0. As a result, the output of the summing junction at J_c is $(u_{KB})_i$, the control required to maintain $c_i(\underline{x})$ at 0. For $0 < -c_i(\underline{x}) \leq \delta_1$, we have a combination of the linear regulator control u_R and the kinematic boundary control $(u_{KB})_i$, given by the equation

$$J_c = \left(1 - \frac{\delta_1 + c_i(\underline{x})}{\delta_1} \right) u_R + \left(\frac{\delta_1 + c_i(\underline{x})}{\delta_1} \right) (u_{KB})_i \quad .$$

When $-c_i(\underline{x}) \leq 0$ we are in a kinematically unsafe condition. Consequently, a braking action will occur due to the following operation of the controller. When $-c_i(\underline{x}) \leq \delta_3$ the linear regulator command is multiplied by 0 while the kinematic boundary control is multiplied by 1, cancelling itself at the summing junction. Thus, the only output at J_c is due to the center nonlinearity, which provides a value $-J_s$, the negative jerk limit. For values of the constraint $\delta_3 \leq -c_i(\underline{x}) \leq 0$, the jerk command is given by a linear combination of $-J_s$ and the boundary control $(u_{KB})_i$:

$$J_c = \left(1 + \frac{c_i(\underline{x})}{\delta_3} \right) (u_{KB})_i + J_s \frac{c_i(\underline{x})}{\delta_3} \quad .$$

In summary, whenever vehicle spacing is greater than the kinematically required spacing by at least a distance δ_1 we use the linear regulator jerk command (Fig. 8a). When vehicle spacing equals the kinematically required spacing we implement the control $(u_{KB})_i$ that maintains this condition (Fig. 8b). Finally, if vehicle spacing is less than the kinematically required spacing by a distance δ_3, we apply the full negative jerk command (Fig. 8c).

To this point we have assumed switch A is in the position as shown in Fig. 7. This is true because, for large initial conditions such as in the case of overtaking, the regulator command will

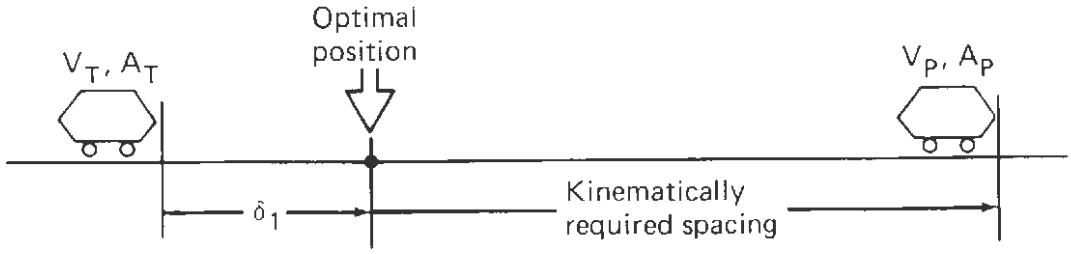

a. Linear regulator input

b. Kinematic boundary control input, $(u_{KB})_i$

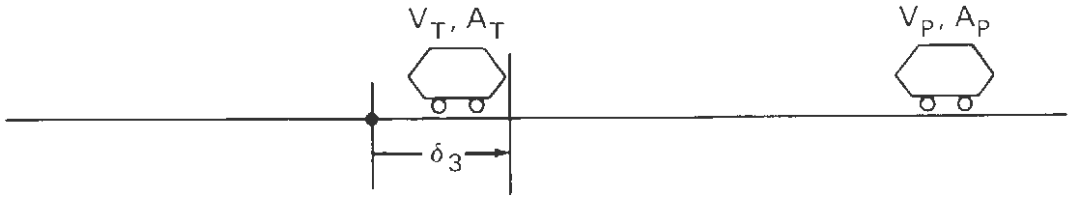

c. Negative jerk limit input, $-J_s$

Fig. 8 Controller Commands

be large and therefore tend to cause the vehicle to violate the kinematic constraint. In accordance with the control strategy presented earlier and Eq. 8 with $\dot{c} > 0$, and when $-\delta_1 \leq c_i(\underline{x}) \leq 0$, switch A will then switch to the position shown in Fig. 5. When the linear regulator would cause the system to move off the boundary into the allowable region (i.e., $\dot{c} < 0$, $-\delta \leq c_i \leq 0$) then a switch is made back to the linear regulator.

The final point to examine is how initially to switch on the regulator. We will not consider the mechanism that switches the vehicle from an open-loop velocity command to a closed-loop jerk command. However, we will require that the controller provide a

0 jerk command at the switching time in order to reduce any undesirable transients. In addition, a reasonable choice for the switch time is when $-c_i(\underline{x}) = \delta_1$. That is, when the vehicle approaches the kinematic boundary we switch from a velocity-command mode to a regulation mode. Note from Fig. 7 that if we were to simply switch in the controller as shown, a jerk command ($J_c = u_R$) would result. Therefore, we would like to modify u_R during this initial switch-on phase in order to produce $J_c = u_R = 0$ when $-c_i(\underline{x}) = \delta_1$, but then gradually increase u_R to its full value. For example, we may use a value u'_R given by

$$u'_R = \left(1 - \sqrt{-c_i(\underline{x})/\delta_1}\right) u_R \ .$$

Thus, when $-c_i(\underline{x}) = \delta_1$, then $u'_R = 0$. As $-c_i(\underline{x})$ decreases to 0, u'_R increases to u_R. When $c_i(\underline{x})$ is near 0 we set u'_R equal to u_R for the remainder of the transition and in the subsequent regulation mode.

KINEMATIC BOUNDARY CONTROL AND MODIFICATION OF KINEMATIC CONSTRAINT

As we have seen in the previous section, the control that keeps the vehicle on the kinematic boundary forms the principal portion of the transition controller. This control is obtained from Eq. 11:

$$(u_{KB})_i = -(c'_i b)^{-1} \ c'_i[A\underline{x} + dJ_p], \ i = 1, 2, 3, 4,$$

where, from Eqs. 1 and 2,

$$c_i(\underline{x}) = d_r^T - d_r^P - V_{min}(t_r^T - t_r^P) + hV_{min} - S, \ i = 1, 2, 3, 4. \quad (12)$$

As shown in Appendix A the distance and time functions d_r^T and t_r^T as well as d_r^P and t_r^P depend on one of two possible maneuvers, thus yielding four constraint functions and four corresponding controls.

Equation 11 may be explicitly written in terms of the partial derivatives comprising the gradient of $c(\underline{x})$ as follows. First, the gradient is given by:

$$\nabla c' = \left[-1 \left(\frac{\partial c}{\partial V_T}\right)_j \left(\frac{\partial c}{\partial A_T}\right)_j \left(\frac{\partial c}{\partial V_P}\right)_k \left(\frac{\partial c}{\partial A_P}\right)_k \right] \quad , \quad \begin{matrix} j = 1,2 \\ k = 1,2, \end{matrix}$$

where j and k denote one of the two maneuvers. Using Eqs. 9 and 12 and substituting into Eq. 11, we have

$$u_{KB} = - \frac{\left(\frac{\partial c}{\partial V_T}\right)_j A_T + \left(\frac{\partial c}{\partial V_P}\right)_k A_P + \left(\frac{\partial c}{\partial A_P}\right)_k J_P - (V_P - V_T)}{\left(\frac{\partial c}{\partial A_T}\right)_j} \quad \begin{matrix} j = 1, 2 \\ k = 1, 2, \end{matrix} \tag{13}$$

where

$$\left(\frac{\partial c}{\partial V_T}\right)_j = \left(\frac{\partial d_r^T}{\partial V_T}\right)_j - V_{min} \left(\frac{\partial t_r^T}{\partial V_T}\right)_j \quad , \qquad j = 1, 2, \tag{13a}$$

$$\left(\frac{\partial c}{\partial V_P}\right)_k = - \left(\frac{\partial d_r^T}{\partial V_P}\right)_k + V_{min} \left(\frac{\partial t_r^T}{\partial V_P}\right)_k \quad , \qquad k = 1, 2, \tag{13b}$$

$$\left(\frac{\partial c}{\partial A_P}\right)_k = - \left(\frac{\partial d_r^P}{\partial A_P}\right)_k + V_{min} \left(\frac{\partial t_r^P}{\partial A_P}\right)_k \quad , \qquad k = 1, 2, \text{ and} \tag{13c}$$

$$\left(\frac{\partial c}{\partial A_T}\right)_j = \left(\frac{\partial d_r^T}{\partial A_T}\right)_j - V_{min} \left(\frac{\partial t_r^T}{\partial A_T}\right)_j \quad , \qquad j = 1, 2. \tag{13d}$$

The expressions for $\frac{\partial d_r^T}{\partial V_T}$, $\frac{\partial d_r^T}{\partial A_T}$, $\frac{\partial t_r^T}{\partial V_T}$, $\frac{\partial t_r^T}{\partial A_T}$, $\frac{\partial d_r^P}{\partial V_P}$, $\frac{\partial d_r^P}{\partial A_P}$, $\frac{\partial t_r^P}{\partial V_P}$, and $\frac{\partial t_r^P}{\partial A_P}$ are given in Appendix B. In Section 5, it will be shown how the above control law may be simplified to one expression to produce a suboptimal control.

Inspection of Eq. 13 reveals that it is necessary that

$$\left(\frac{\partial c}{\partial A_T}\right)_j \neq 0 \quad , \qquad j = 1, 2, \tag{14}$$

if the system is to be controllable on the boundary. If we substitute the appropriate expressions for Maneuver 2 given in Appendix B into Eq. 13d and set $V_T = V_{min}$ and $A_T = 0$, the result in the condition of Eq. 14 is violated. This singularity at V_{min} may be removed through simple modification of the control law. The violation of Eq. 14 occurs when $V_T = V_{min}$ and a cancellation results in Eq. 13d. Thus, if we vary V_{min} as a function of V_T so that V_T never equals V_{min}, the cancellation will not occur. This may be accomplished with a function of the form

$$V'_{min} = \begin{cases} V_{min} & V_T \geq V_1 \\ V_2 - (V_2 - V_{min}) \left[\dfrac{V_T - V_{min}}{V_1 - V_{min}} \right]^{\frac{1}{2}} & , \quad V_T < V_1 \ , \end{cases}$$

where V_1 is selected to be slightly greater than V_{min}, and V_2 is slightly less than V_{min}. Consequently, for V_T greater than some selected velocity, V_1, the V_{min} used in calculating the kinematic boundary control (Eq. 13) is the actual minimum line speed. When V_T approaches the minimum line speed we use a new value, V'_{min}, for purposes of control calculation. Hence, for $V_T \leq V_1$, V'_{min} is given by the above equation until at $V_T = V_{min}$ we have $V'_{min} = V_2$. For $V_{min} = 10$ m/s, the values used for V_1 and V_2 are 10.5 m/s and 9 m/s, respectively. For the suboptimal controls discussed in Section 5 the condition of Eq. 14 holds for all values of V_T and therefore it is unnecessary to use the above modification.

As was indicated in the discussion of the kinematic boundary controller, we switch to the linear regulator whenever it tends to drive the system off the kinematic boundary into an acceptable region. From Eq. 12 we see that this will occur whenever the preceding vehicle does not decelerate to minimum line speed but rather remains at some velocity V_P that is greater than V_{min}. As a result, switching the regulator on will cause a transient and may even produce limit cycling. Hence, it would be desirable to modify the kinematic constraint (Eq. 12) such that the kinematic boundary will coincide with the nominal operating headway. That is, when the kinematic constraint (Eq. 12) so that the kinematic boundary will coincide with the nominal operating headway. That is, when

spacing as required by the constraint function is the desired headway, hV_T. This is easily accomplished by replacing hV_{min} with hV_T in Eq. 12, so we now have

$$c_i(\underline{x}) = d_r^T - d_r^P - V_{min}\,(t_r^T - t_r^P) + hV_T - S, \quad i = 1, 2, 3, 4. \tag{15}$$

This is acceptable, since $hV_T \geq hV_{min}$; therefore the spacing when $c_i(\underline{x}) = 0$ is greater than the spacing required by our original constraint. Also note an additional term, hA_T, that will result in the numerator of Eq. 13. Since the nominal operating headway is now on the kinematic boundary, the kinematic boundary control will act to maintain the desired headway and hence obviate the linear regulator shown in Fig. 6. The input u_R to the transition controller may be replaced with a positive jerk command of 2.6 m/s^3. Therefore, u_R will be present to drive the system to the kinematic boundary whenever $c_i(\underline{x}) < 0$. The controller then takes the basic structure shown in Fig. 9. The details of switching from velocity-command to regulation mode have been left out of the diagram. In addition, we have selected $\delta_1 = \delta_3 = \Delta$ while the acceleration limiter is shown as a constrained range integration. Also note that the ratio J_s/Δ is, in effect, a controller gain that affects system response and stability. This aspect will be discussed in Section 6.

The kinematic constraint ($\varepsilon = -c(\underline{x})$) is calculated as a function of preceding and trailing vehicle states (ε denotes error between spacing and kinematically required spacing). Similarly, the kinematic boundary control $(u_{KB})_i$ (i.e., the jerk required to keep ε constant) is calculated as a function of preceding and trailing vehicle states. When $\varepsilon > \Delta$ (or when $c(\underline{x}) < -\Delta$), the vehicle is in a kinematically safe condition and the full positive jerk capability of the vehicle is commanded to the propulsion system. At the same time the boundary control is multiplied by 1 and thus cancels itself out at the summing junction. When $\varepsilon = 0$, the commanded jerk input is the kinematic boundary control, $(u_{KB})_i$. When $\varepsilon < -\Delta$ (or when $c(\underline{x}) > \Delta$) the vehicle is in a kinematically unsafe condition and the full negative jerk limit is commanded to the propulsion system. Again, when $c(\underline{x}) > \Delta$ the boundary control is multiplied by 1 and cancels itself at the summing junction.

In summary, ε drives the system to the kinematic spacing and $(u_{KB})_i$ keeps the system at this spacing. The jerk limiters and deceleration limiters following the summing junction are not necessary in the optimal case since the control that keeps the vehicle on the boundary will not exceed limits. However, the suboptimal controls to be presented require these limiters particularly when switching occurs.

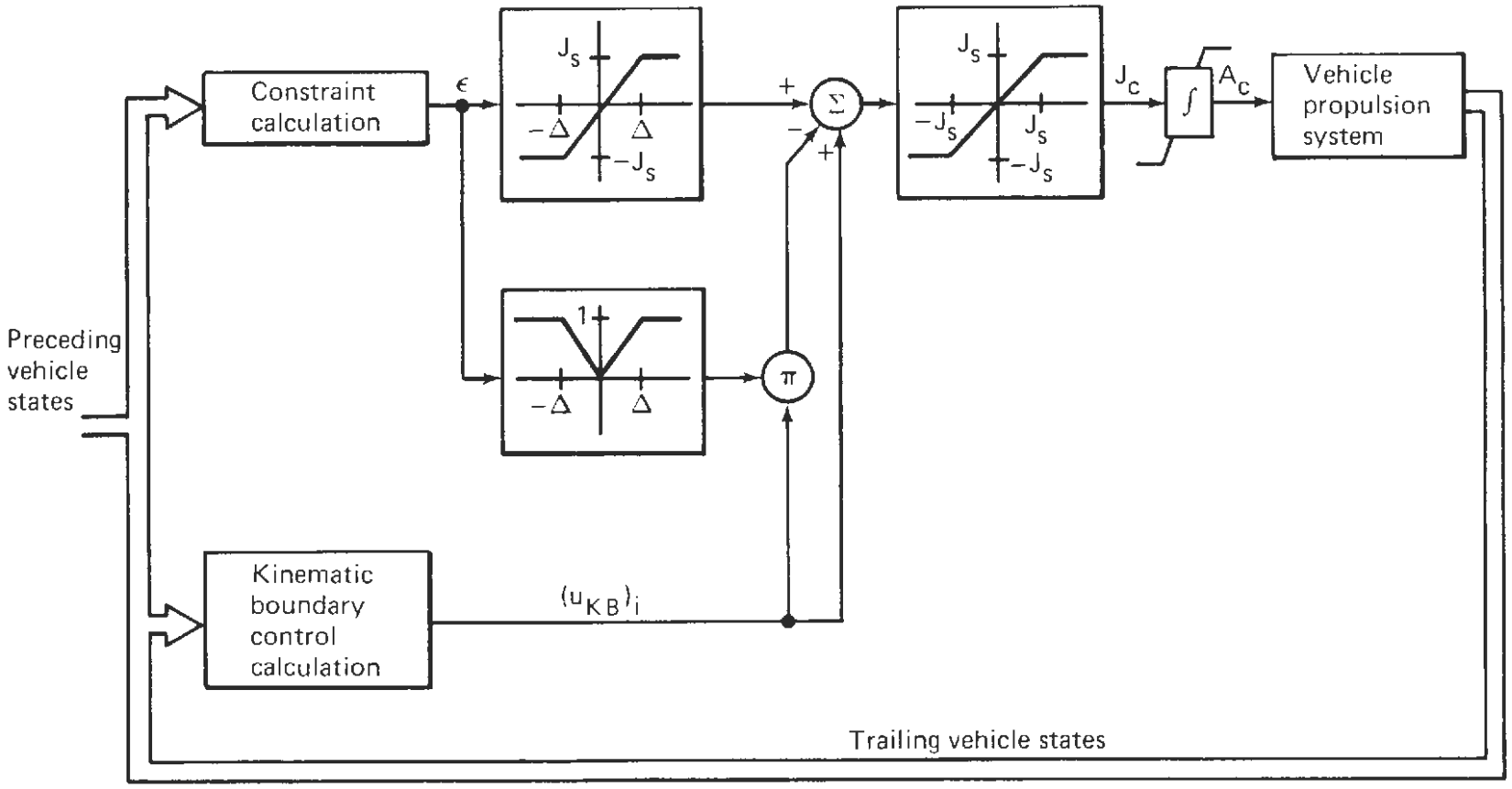

Fig. 9 Controller Structure

We will now compare the vehicle responses in an overtaking situation using the original constraint equation (Eq. 12) and the modified kinematic constraint. The trailing vehicle is traveling at 20 m/s while the preceding vehicle has a speed of 10 m/s and the initial spacing is set at 100 m. The resulting response for a desired headway of 0.5 s using the optimal control is shown in Fig. 10. The spacing plot shows the actual vehicle spacing and the spacing as required by the kinematic constraint (i.e., the spacing required to prevent collision in the event of a minimum time maneuver by the preceding vehicle; see Section 3). In Fig. 10 the preceding vehicle is traveling at minimum line speed and therefore it is assumed that it will not decelerate. Thus, the trailing vehicle may precisely follow the on-limits trapezoidal deceleration profile to achieve the desired spacing. That is, it can wait until the last possible moment before reacting to the presence of the preceding vehicle. The modified optimal control response is shown in Fig. 11; note that the maintained spacing is slightly larger than the required spacing.

The comparison of headways for the two control strategies is shown in Fig. 12. Here, headway is defined as spacing divided by trailing vehicle velocity; vehicle acceleration is not included in this definition. The apparently small degradation in performance as shown by Fig. 12 justified the adoption of Eq. 15 as the kinematic constraint throughout the remainder of this report.
The headway comparison is shown in Fig. 15. The overshoot in the optimal response is somewhat more accentuated with a 3-s headway than with 0.5-s headway. However, the vehicle is decelerating at this point and therefore the loss of headway is not as serious as it appears (recall that the headway calculation only involves velocity). On the other hand, the modified optimal control will always keep the vehicle above the desired headway (in the overtaking situation) since we have included the term hV_T rather than hV_{min} in the constraint function. Hence, the vehicle will maintain a spacing of at least hV_T.

Although the control strategy described in this section will be called the optimal control, it is optimal only on the constraint boundary. However, since we have further constrained the vehicle to operate in a velocity-command mode until the boundary is reached, the overall control law should provide a good approximation to the optimal. That is, the control which takes the vehicle from $-c(\underline{x}) = \delta_1$ to $c(\underline{x}) = 0$ is the approximation suggested by Saridis. Thereafter, the control on the kinematic boundary is the optimal constrained trajectory.

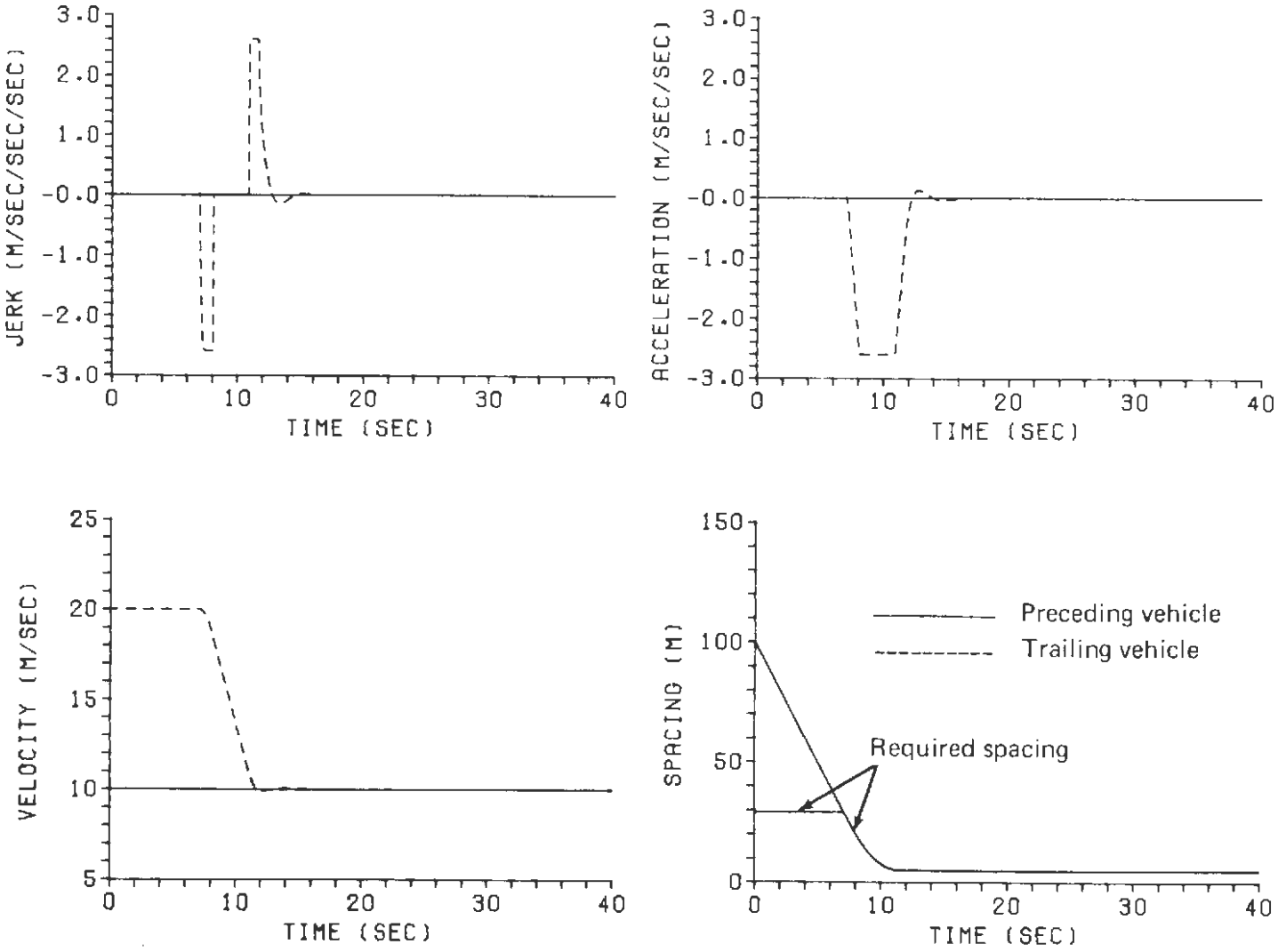

Fig.10 Overtaking Maneuver Using the Optimal Control with h=0.5 s

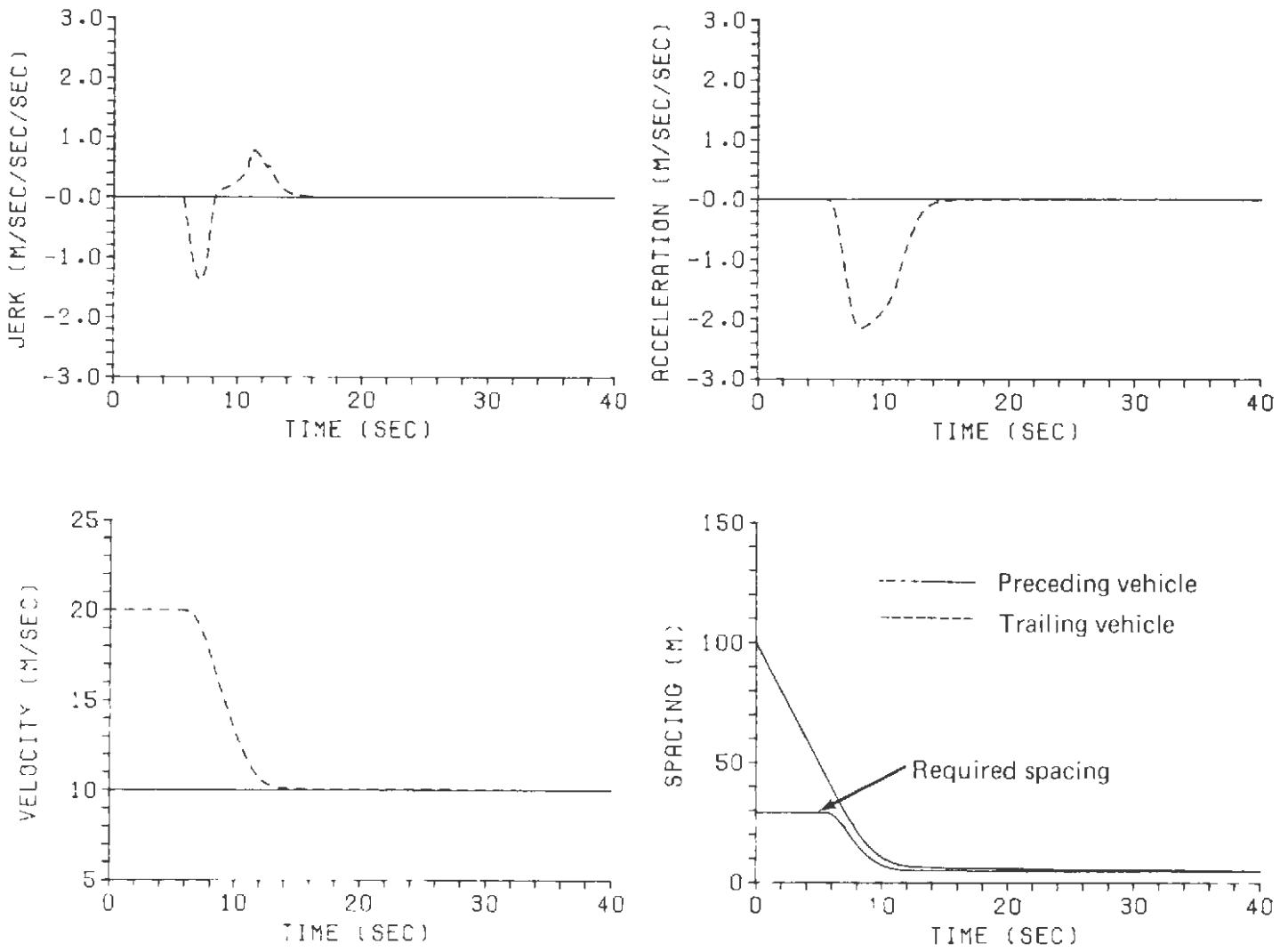

Fig. 11 State Profiles for Case 1 Using the Modified Optimal Control with h = 0.5 s

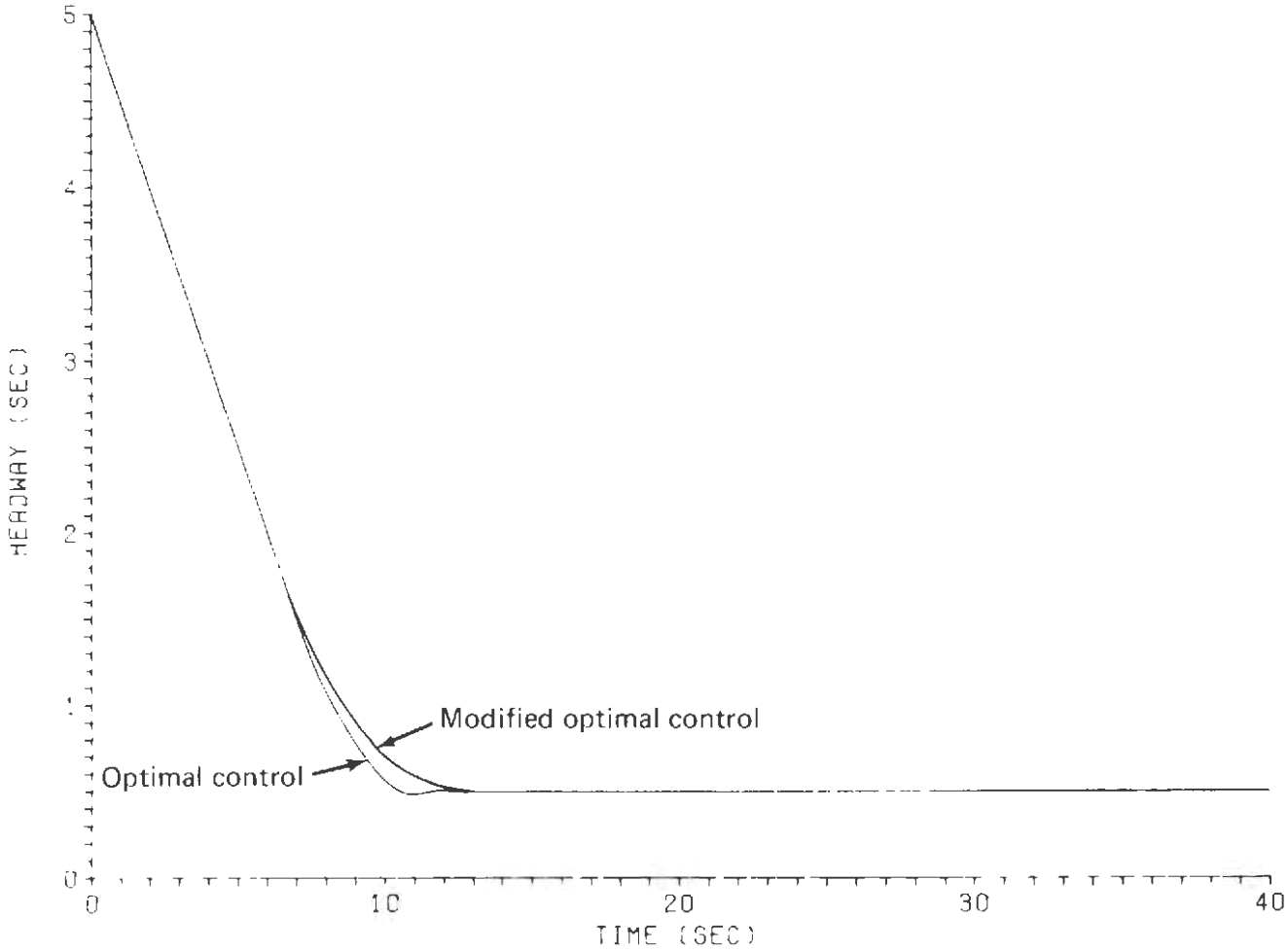

Fig. 12 Comparison Between Optimal and Modified Optimal Control Headway Profiles

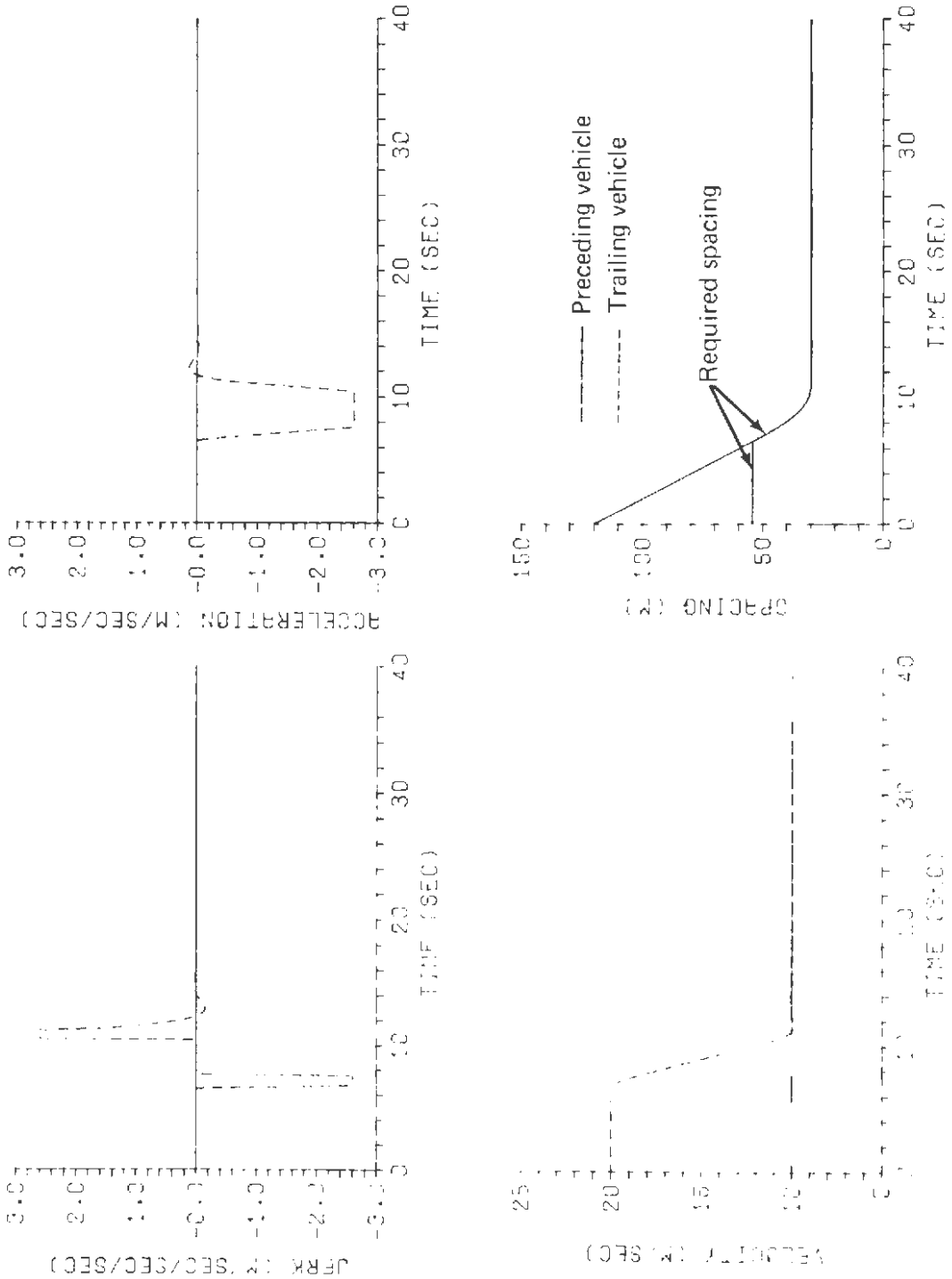

Fig. 13 Overtaking Maneuver Using the Optimal Control with h=3 s

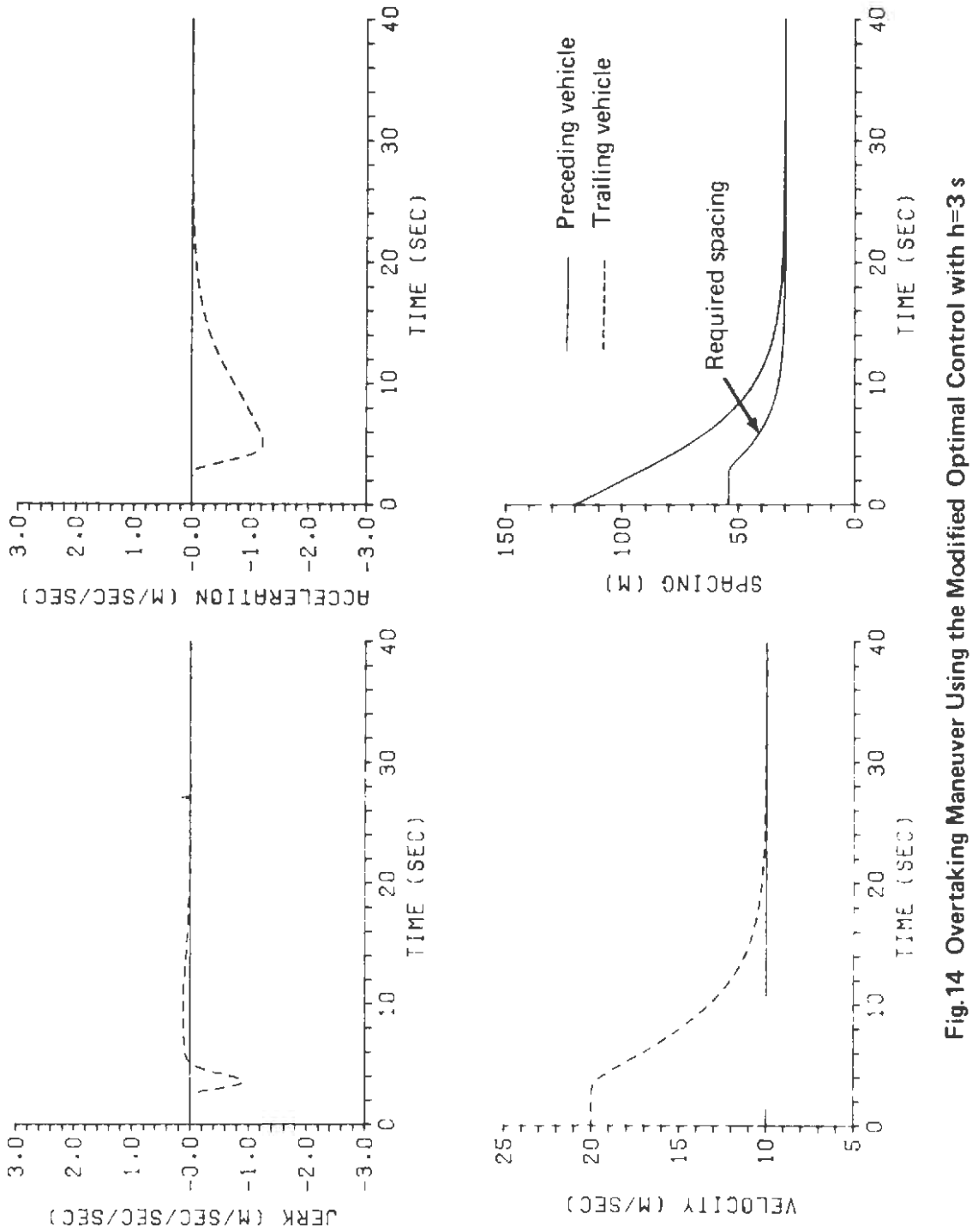

Fig.14 Overtaking Maneuver Using the Modified Optimal Control with h=3 s

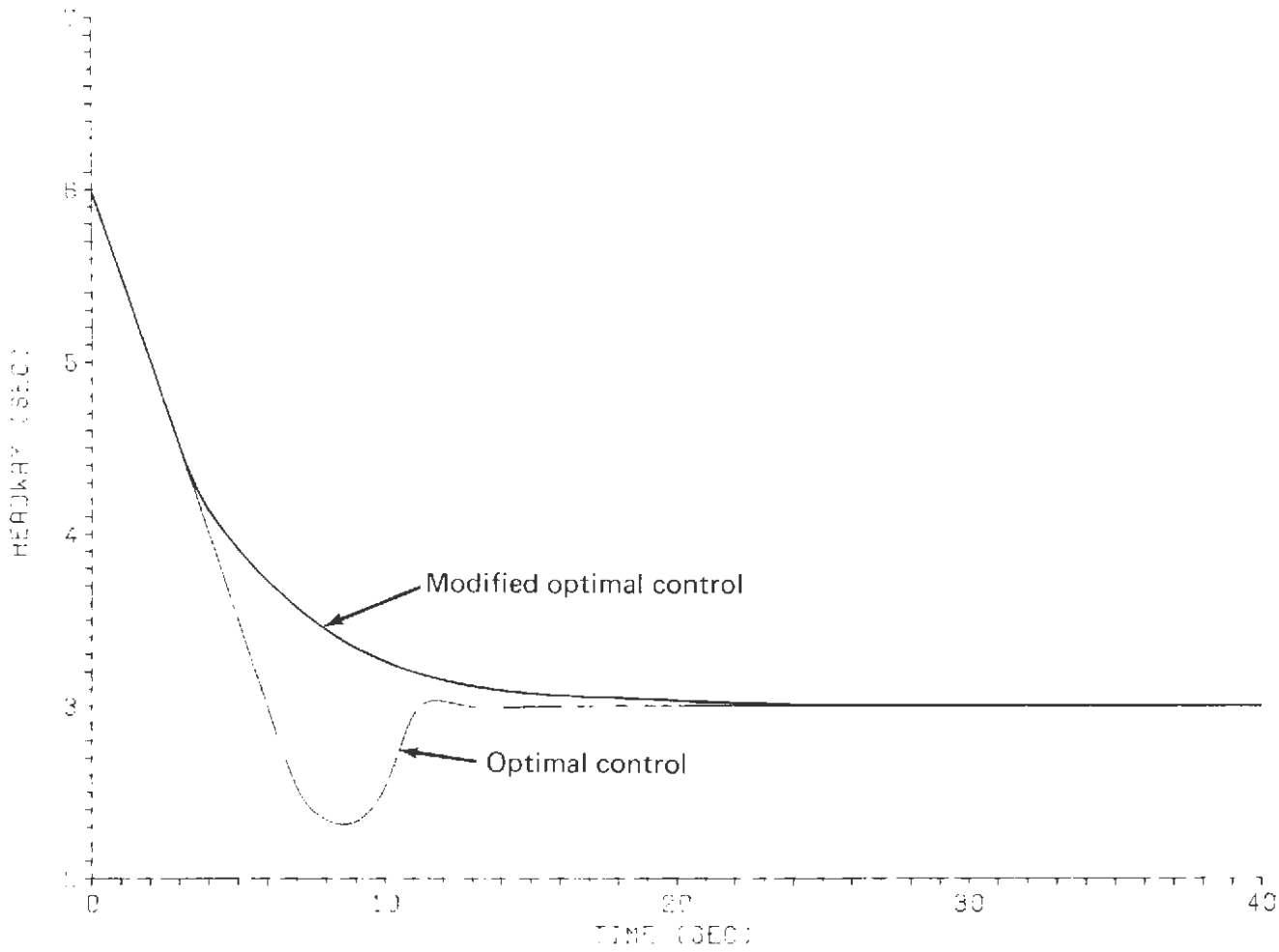

Fig. 15 Comparison between Optimal and Modified Optimal Control Headway Profiles with h=3 s

5. SUBOPTIMAL VEHICLE CONTROL

In this section we will investigate several suboptimal control strategies that lead to considerable simplification of the controller described in Section 4. All of the suboptimal controllers presented are derived to simplify the kinematic constraint so that the resulting control will always keep the vehicle outside the actual kinematic boundary but will require less computation and information. In all cases we will use the kinematic constraint described at the end of Section 4, with desired final spacing of hV_T rather than hV_{min}. Consequently, the kinematic boundary controller will act as a regulator at nominal headway with the regulator of Fig. 5 replaced by a constant jerk command of $+2.6\ m/s^3$ (Fig. 9). This allows simplification of the controller without degradation in performance as shown by the examples in Section 4.

SUBOPTIMAL CONTROL I

The first simplification of the kinematic constraint assumes that the preceding vehicle will always decelerate to the negative acceleration limit even if the vehicle is traveling at minimum line speed. As a result, although the actual minimum line speed remains the same, for purposes of control calculation we adopt a new minimum line speed that is less than the actual. Consequently, we need only consider Maneuver 1 in the kinematic constraint vector

$$\begin{bmatrix} c(\underline{x}) \\ |A| \\ |J| \end{bmatrix} \leq \begin{bmatrix} 0 \\ A_s \\ J_s \end{bmatrix} ,$$

where $c(\underline{x}) = d_r^T - d_r^P - V_{min}\ (t_r^T - t_r^P) + hV_T - S$, and d_r^T, d_r^P, t_r^T, t_r^P are given in Appendix A for Maneuver 1. If we assume that a vehicle traveling at 10 m/s will decelerate at the jerk limit to a -2.6 m/s acceleration, the largest final velocity it can have is 7.4 m/s. As a result, consistent with our assumption for Maneuver 1 we may set $V_{min} = 7.4$ m/s in the constraint equation although

our minimum line speed is still 10 m/s. The control u_{KB} is given in Eq. 13 with j, k = 1 (i.e., using the partial derivatives for Maneuver 1 given in Appendix B).

The computational requirements are considerably less than those for the optimal but we still require measurements of all vehicle states (i.e., V_T, A_T, V_P, A_P, J_P, and S). Also note that the above control is identical to the optimal control for velocities greater than 12.6 m/s (i.e., velocities for which Maneuver 1 is applicable in the optimal control).

SUBOPTIMAL CONTROL II

The remaining suboptimal strategies are obtained from simplification of the kinematic constraint for suboptimal control I with the aim of only requiring error states (i.e., spacing and its derivatives). First, we will examine the kinematic constraint in Section 4. In terms of vehicle states it is given by:

$$\begin{aligned} c(\underline{x}) = {} & 0.007\ (A_t^4 - A_P^4) + 0.05\ (A_T^3 - A_P^3) + 0.1\ (A_T^2 - A_P^2) \\ & + 0.074\ (A_T^2\ V_T - A_P^2\ V_P) + 0.38\ (A_T\ T_T - A_P\ V_P) + 0.5\ (V_T - V_P) \\ & + 0.19\ (V_T^2 - V_P^2) - 10\ [0.38\ (A_T - A_P) + 0.074\ (A_T^2 - A_P^2) \\ & + 0.38\ (V_T - V_P)] + hV_T - S\ , \end{aligned} \tag{16}$$

where we have used $A_S = 2.6\ m/s^2$, $J_S = 2.6\ m/s^3$, and $V_{min} = 10\ m/s$.

If we drop all acceleration terms in the above constraint, the kinematic constraint becomes

$$c(\underline{x}) = -\ 3.3\ (V_T - V_P) + 0.19\ (V_T^2 - V_P^2) + hV_T - S\ . \tag{17}$$

There is no guarantee that Eq. 17 satisfies the kinematic constraint. However, the additional simplifications to be shown below and a comparison with the original constraint in the next section will justify its use.

The second term in Eq. 17 may be factored to yield

$$c(\underline{x}) = -\ 3.3\ (V_T - V_P) + 0.19\ (V_T - V_P)\ (V_T + V_P) + hV_T - S\ .$$

Since we are interested in error states, the sum term $V_T + V_P$ may be eliminated by substituting $V_T + V_{max}$ (where $V_{max} = 25$ m/s) to obtain

$$c(\underline{x}) = 1.4\ (V_T - V_P) + 0.19\ V_T\ (V_T - V_P) + hV_T - S\ .$$

This is permissible since $V_T \leq V_{max}$ and the new required spacing is greater than that required by Eq. 17. In order to formulate a jerk-command input from the above constraint it is necessary that $\dot{c}(\underline{x})$ contain a trailing-vehicle jerk term or, equivalently, that $c(\underline{x})$ include an acceleration term. Thus, we simply add a constant times A_T to yield

$$c(\underline{x}) = 1.4\ (V_T - V_P) + 0.19\ (V_T - V_P) + kA_T + hV_T - S\ , \qquad (18)$$

where k will be determined in Section 6.

The corresponding control that keeps $c(\underline{x}) = 0$ is then given by

$$u_{KB} = -\frac{1}{k}\left[-1.4\ A_E - 0.19\ (V_E\ A_T + V_T) + hA_T - V_E\right]\ ,$$

where $A_E = A_P - A_T$ and

$V_E = V_P - V_T$.

Note that J_P no longer appears in the expression for u_{KB} since $\partial c/\partial A_P = 0$ in Eq. 13.

SUBOPTIMAL CONTROL III

Equation 18 may be further simplified by substituting the value of V_{max} for V_T in the second term. Again, this is valid since $V_T \leq V_{max}$ and therefore our new minimum spacing is greater than that required by Eq. 18. As a result, we have

$$c(\underline{x}) = 6\ (V_T - V_P) + kA_T + hV_T - S\ , \qquad (19)$$

and the corresponding control is given by

$$u_{KB} = -\frac{1}{k}\left(-6\,A_E + hA_T - V_E\right) . \tag{20}$$

Consequently, the control (Eq. 20), which keeps the vehicle on the kinematic boundary defined by Eq. 19, becomes a linear time-invariant feedback controller (assuming the vehicle is within jerk and acceleration limits). The transfer function (Eq. 20) is

$$G(s) = \frac{X_T(s)}{X_P(s)} = \frac{6s + 1}{ks^2 + (6 + h)\,s + 1} \tag{21}$$

with a natural frequency of

$$\omega_n = \sqrt{\frac{1}{k}} ,$$

and damping

$$\xi = \frac{6 + h}{2\sqrt{k}} .$$

We may now calculate k based on string-stability requirements. The magnitude of the transfer is given by

$$\begin{aligned} |G(j\omega)|^2 &= \left|\frac{6\,j\omega + 1}{(1 - k\omega^2) + j\,(6 + h)\,\omega}\right|^2 \\ &= \frac{1 + 36\,\omega^2}{1 + 36\,\omega^2 + 12\,h\omega^2 + h^2\omega^2 - 2\,k\omega^2 + k^2\omega^4} \end{aligned} \tag{22}$$

From Eq. 22 the magnitude of the transfer will always be less than 1 if

$$k^2\omega^4 - (2k - 12h - h^2)\,\omega^2 \geq 0 ,$$

which reduces to the requirement

$$-2k + 12h + h^2 \geq 0 \ ,$$

or

$$k \leq 6h + \frac{h^2}{2} \quad . \tag{23}$$

It is desirable to have k as large as possible to reduce bandwidth and decrease the time in which a transition will occur. For a headway of 0.5 s, a value of $k = 2.0$ has been selected for both suboptimal controls II and III. Although there is no strict justification for $k = 2.0$ in suboptimal control II, it seems a reasonable choice since the string stability requirement will still hold for $10 \leq V_T \leq 25$ in the second term coefficient of Eq. 18. For example, if $V_T = 10$ is substituted, Eq. 18 becomes

$$c(\underline{x}) = 3.3\ (V_T - V_P) + 2.0\ A_T + 0.5\ V_T - S \ ,$$

and the corresponding control meets the above string-stability magnitude criterion. Block diagrams for suboptimal controls II and III with desired headway equal to 0.5 s are shown in Figs. 16 and 17, respectively. Note that the acceleration and jerk limiters are not shown.

For a desired headway equal to 3 s the same logic as above may be followed to select a value of k. From Eq. 23 the string-stability requirement will be met at $h = 3$ s for any value of k not exceeding 22.5.

The major simplification in obtaining suboptimal controls II and III was to eliminate the acceleration terms in the constraint function for suboptimal control I. Therefore, the validity of suboptimal controls II and III needs to be established, since we have not yet noted the effect of removing these terms. Consequently, the kinematic constraint functions derived for suboptimal controls II and III were tested against the actual kinematic constraint for all possible combinations of preceding and trailing vehicle states within the designated limits. As might be expected, the actual constraint is violated for small velocity errors and large negative acceleration errors, since suboptimal controls II and III do not include acceleration error in the constraint functions. The only concern in violating the kinematic constraint is that the suboptimal controller may be turned on too

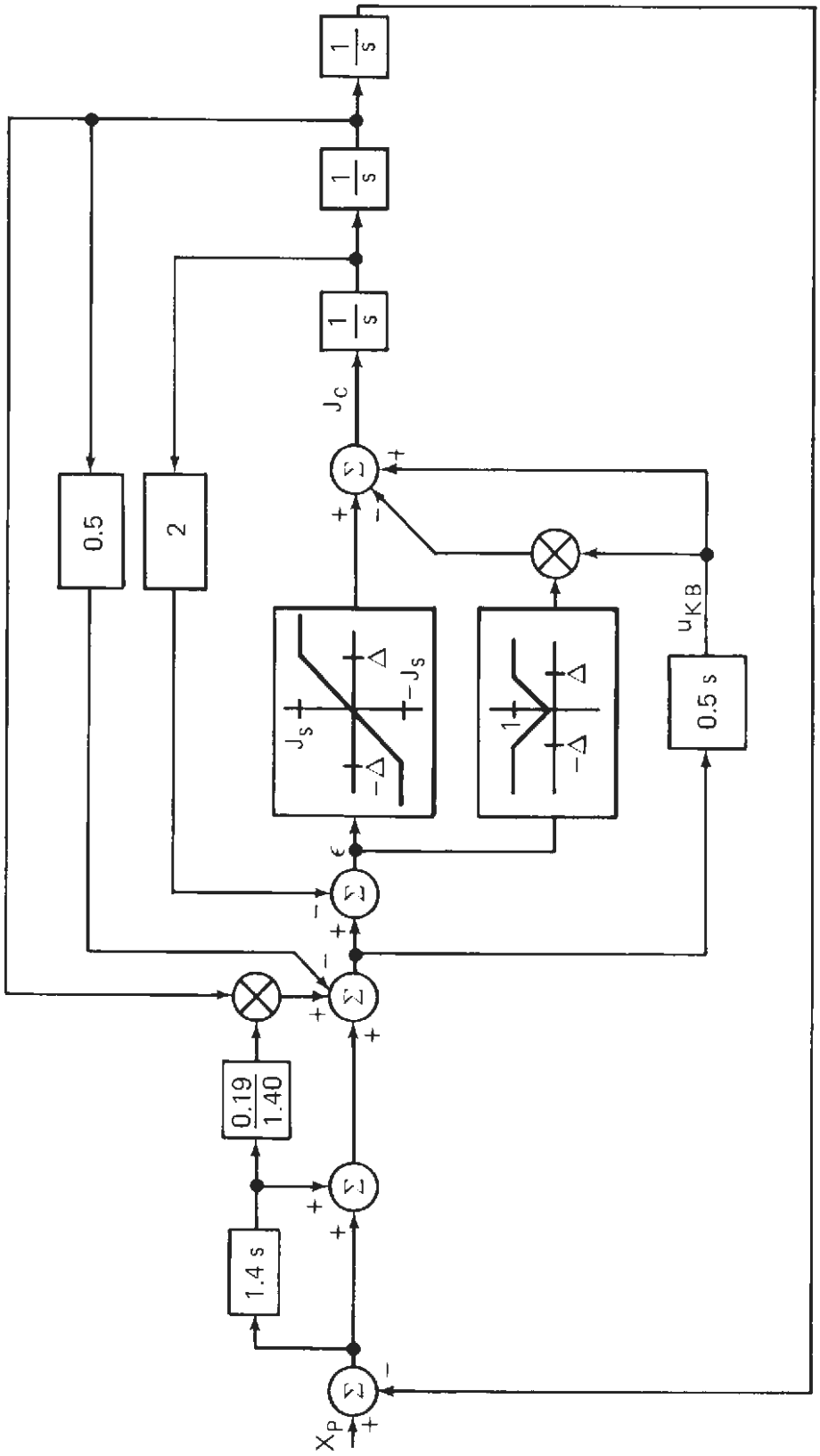

Fig. 16 Suboptimal Control II

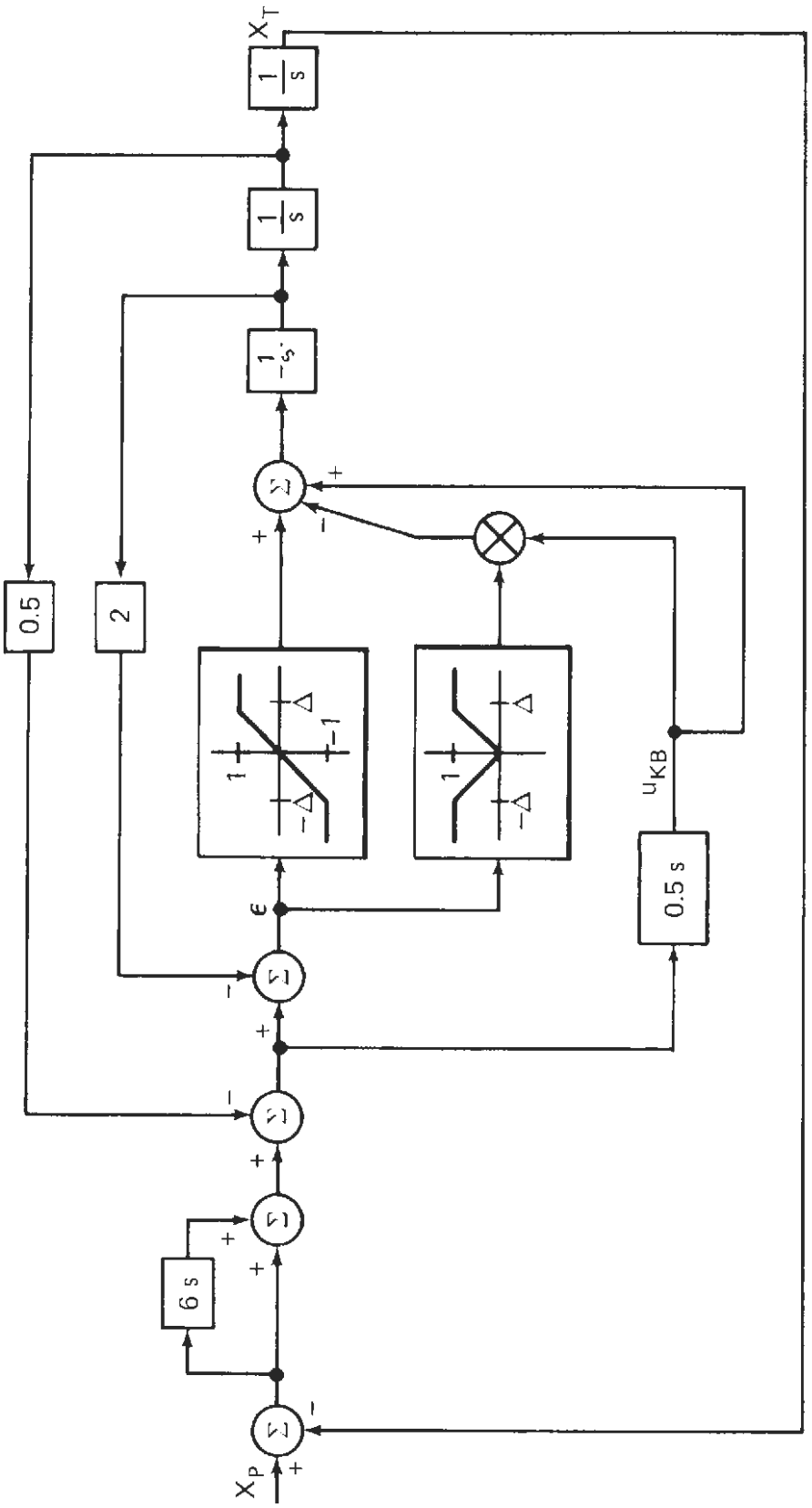

Fig. 17 Suboptimal Control III

late and collision is then unavoidable. If the suboptimal controller is invoked outside the boundary, preceding-vehicle velocity changes will be followed and the danger of collision is not present. If we are to assume an overtaking situation with the trailing vehicle initially in velocity command mode with zero acceleration, it is assured the transition controller will be switched on outside the actual kinematic boundary using suboptimal controls II and III. Therefore, the approximations are justified for this case.

6. DESCRIBING FUNCTION STABILITY ANALYSIS

Experimental evidence to be shown in Section 7 indicates there is no closed-loop stability problem with the nonlinear controller. This section will present analytic verification of stability for the suboptimal controllers, which are simple enough to allow a describing function analysis. We begin by deriving the describing function for the basic dual-input controller nonlinearity. The derivation is greatly simplified through removal of jerk and acceleration limiters. Hence, this removal represents a further approximation in the analysis, but we retain the basic nonlinear feature of the controller. The dual-input static nonlinearity of the controller is then transformed into a single-input dynamic nonlinearity. As a result, the nonlinear and linear parts of the feedback loop may be separated. Consequently, the describing function (frequency dependent) may be plotted separately from the plot of the linear transfer on a Nichol's chart. The presence of limit cycles is then determined at intersection points of the linear and nonlinear characteristics.

The selection of the parameter Δ is shown ot be aided by the describing function analysis and is discussed later. It is pointed out that certain system considerations beyond closed-loop stability are involved in the selection of Δ. Consequently, at a headway of 0.5 s it is deduced that a value of Δ of approximately 1 should prove satisfactory. The subsequent stability analysis demonstrates that a value of $\Delta = 1$ provides sufficient stability.

In discussion of suboptimal control III, the describing function in conjunction with the Nichol's chart is used to verify the stability of suboptimal control III where the controller gains are selected for a 0.5-s headway. A small-signal linear analysis provides additional verification of stability.

The stability of suboptimal control II is then studied in a similar manner. However, there is an additional nonlinearity in the form of a multiplier. The describing function of this nonlinearity is derived, and thus only the first harmonic of the multiplier output is considered.

DESCRIBING FUNCTION DERIVATION

The closed-loop stability of suboptimal controls II and III will be studied with the use of describing functions. Suboptimal

control III is shown in Fig. 17 where the jerk and acceleration limiters have been removed to simplify the analysis. The nonlinear portion of the system is redrawn in Fig. 18 with the nonlinearities in parallel, thus illustrating the describing function derivation to be described below. Suboptimal control II, which will be discussed later, contains the same basic nonlinearity. A sinusoidal signal with a particular amplitude and phase will be assumed at each input to the nonlinearity. The output, Y, will be periodic and a function of the input amplitudes, X_1 and X_2, and the relative phase, θ. The describing function of the nonlinearity is determined by the first term of the Fourier series of the output. That is, since Y is periodic it may be expressed as a Fourier series given by

$$Y(t) = a_0 + \int_{n=1}^{\infty} (a_n \cos n\omega t + b_n \sin n\omega t)$$

where

$$a_0 = \frac{1}{T} \int_0^T Y(t)\, dt \tag{24a}$$

$$a_n = \frac{2}{T} \int_0^T Y(t) \cos n\omega t\, dt \tag{24b}$$

$$b_b = \frac{2}{T} \int_0^T Y(t) \sin n\omega t\, dt \tag{24c}$$

From Fig. 18, when $X_1 \leq \Delta$, the output is given by

$$Y(t) = \begin{cases} \frac{J_s}{\Delta} X_1 \sin \Psi - \frac{X_1 X_2}{\Delta} \sin \Psi \sin (\Psi + \theta) \\ \qquad + X_2 \sin (\psi + \theta), \quad \sin \psi \geq 0 & (25a) \\ \frac{J_s}{\Delta} X_1 \sin \psi + \frac{X_1 X_2}{\Delta} \sin \psi \sin (\psi + \theta) \\ \qquad + X_2 \sin (\psi + \theta), \quad \sin \psi < 0 & (25b) \end{cases}$$

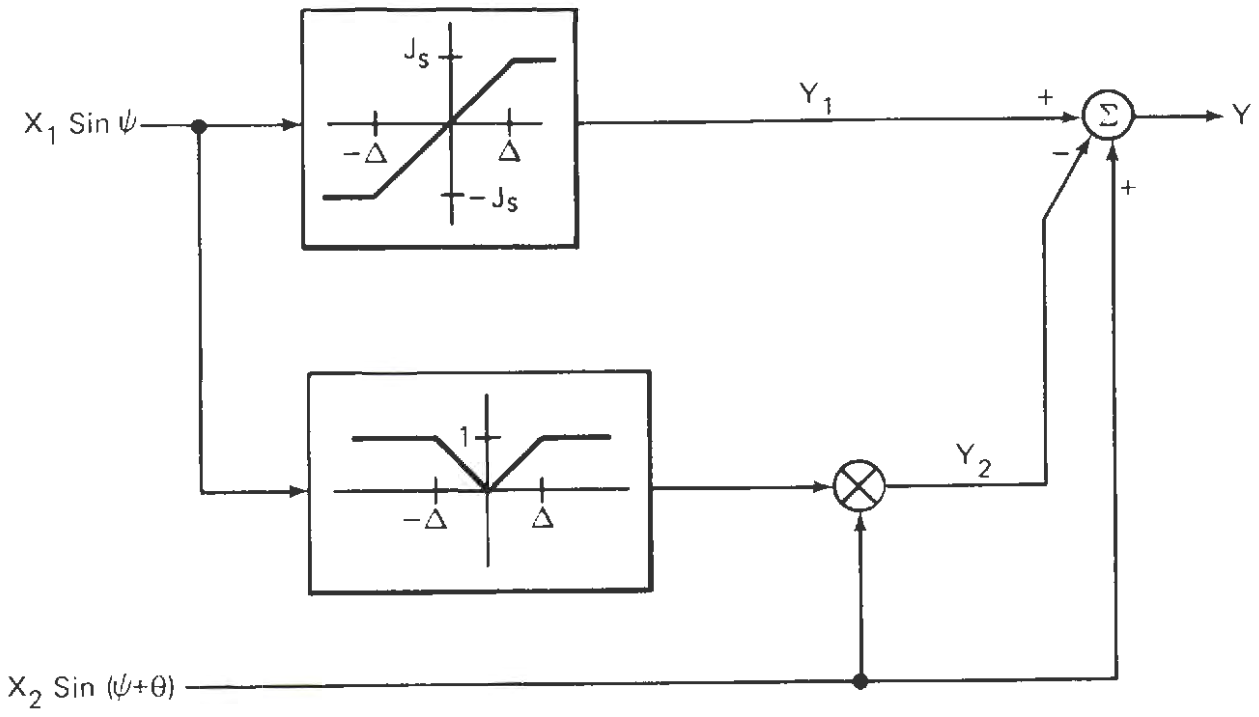

Fig. 18 Nonlinear Portion of System

When $X_1 > \Delta$ the output is given by

$$Y(t) = \begin{cases} \dfrac{J_s}{\Delta} X_1 \sin\psi - \dfrac{X_1 X_2}{\Delta} \sin\psi \sin(\psi+\theta) \\ \qquad + X_2 \sin(\psi+\theta), \\ \qquad 0 \le \psi \le \psi_1, \quad \pi - \psi_1 \le \psi \le \pi & (26a) \\ \dfrac{J_s}{\Delta} X_1 \sin\psi + \dfrac{X_1 X_2}{\Delta} \sin\psi \sin(\psi+\theta) \\ \qquad + X_2 \sin(\psi+\theta), \\ \qquad \pi < \psi < \pi + \psi_1, \quad 2\pi - \psi_1 \le \psi \le 2\pi & (26b) \\ J_s \qquad \psi_1 \le \psi \le \pi - \psi_1 & (26c) \\ -J_s \qquad \pi + \psi_1 \le \psi \le 2\pi - \psi_1 , & (26d) \end{cases}$$

where

$$\psi_1 = \sin^{-1} \frac{\Delta}{X_1} \quad .$$

Substituting Eqs. 25 and 26 into Eq. 24 with n = 1 we obtain the first harmonic of the output, given by

$$[Y(t)]_{n=1} = \begin{cases} \left(\frac{X_1 J_s}{\Delta} + X_2 \cos\theta - M_1 \right) \sin \omega t \\ \qquad + (X_2 \sin\theta - N_1) \cos \omega t \qquad X_1 \leq \Delta \qquad (27a) \\ (M_0 - M_2) \sin \omega t - N_2 \cos \omega t \qquad X_1 > \Delta \ , \qquad (27b) \end{cases}$$

where

$$M_0 = \frac{2 J_s X_1}{\pi \Delta} \left\{ \psi_1 + \frac{\Delta}{X_1} \left[1 - \left(\frac{\Delta}{X_1} \right)^2 \right]^{\frac{1}{2}} \right\} \qquad (28a)$$

$$M_1 = \frac{8 X_1 X_2 \cos\theta}{3\pi\Delta} \qquad (28b)$$

$$N_1 = \frac{4 X_1 X_2 \sin\theta}{3\pi\Delta} \qquad (28c)$$

$$M_2 = \frac{X_2 \cos\theta}{\pi} (-2\psi_1 + \sin 2\psi_1) + \frac{4 X_1 X_2}{3\pi\Delta} \cos\theta \left\{ 2 - \cos\psi_1 \left[\left(\frac{\Delta}{X_1} \right)^2 + 2 \right] \right\} \qquad (28d)$$

$$N_2 = \frac{4 X_1 X_2}{3\pi\Delta} \sin\theta \, (1 - \cos^3 \psi_1) - \frac{X_2 \sin\theta}{\pi} (2\psi_1 + \sin 2\psi_1) \ . \qquad (28e)$$

We may now form the describing function as the gain and phase of the output relative to the input, $X_1 \sin \psi$. First, the gain is given by

$$|N(X_1,X_2,\theta)| = \frac{1}{X_1}\left[\left(\frac{X_1 J_s}{\Delta} + X_2 \cos\theta - M_1\right)^2 + (X_2 \sin\theta - N_1)^2\right]^{\frac{1}{2}} \qquad X_1 \geq \Delta \quad (29a)$$

$$|N(X_1,X_2,\theta)| = \frac{1}{X_1}\left[(M_0 - M_2)^2 + N_2^2\right]^{\frac{1}{2}} \qquad X_1 > \Delta \ . \quad (29b)$$

The phase is given by

$$\text{Arg}\,[N(X_1,X_2,\theta)] = \tan^{-1}\left[(X_2 \sin\theta - N_1)\Big/\left(\frac{X_1 J_s}{\Delta} + X_2 \cos\theta - M_1\right)\right] \qquad X_1 \leq \Delta \quad (30a)$$

$$\text{Arg}\,[N(X_1,X_2\theta)] = \tan^{-1}\,[-N_2/(M_0 - M_2)] \qquad X_1 > \Delta. \quad (30b)$$

We will next consider how the describing function may be used to provide a closed-loop stability analysis of the system.

DESCRIBING FUNCTION CHARACTERISTICS

First note that the nonlinearity of Fig. 18 may be drawn as a single-input dynamic nonlinearity, as shown in Fig. 19. The transfer function G(s) is selected so that the output becomes $X_2 \sin(\psi + \theta)$, the second input to the static nonlinearity of Fig. 18. Consequently, the resulting closed loop may be easily separated into linear and nonlinear parts. Thus, we may determine gain and phase only due to the linear portion of the loop. Similarly, the gain and phase of the nonlinear portion is determined from the describing function as given by Eqs. 29 and 30. To investigate stability, the magnitude-phase plot will be used as follows. A sustained oscillation or limit cycle will exist whenever the characteristic equation of the closed-loop transfer function equals 0, or

$$L(j\omega)\, N(A,\omega) = -1 \ ,$$

where $L(j\omega)$ is the transfer function of the linear portion. This is equivalent to

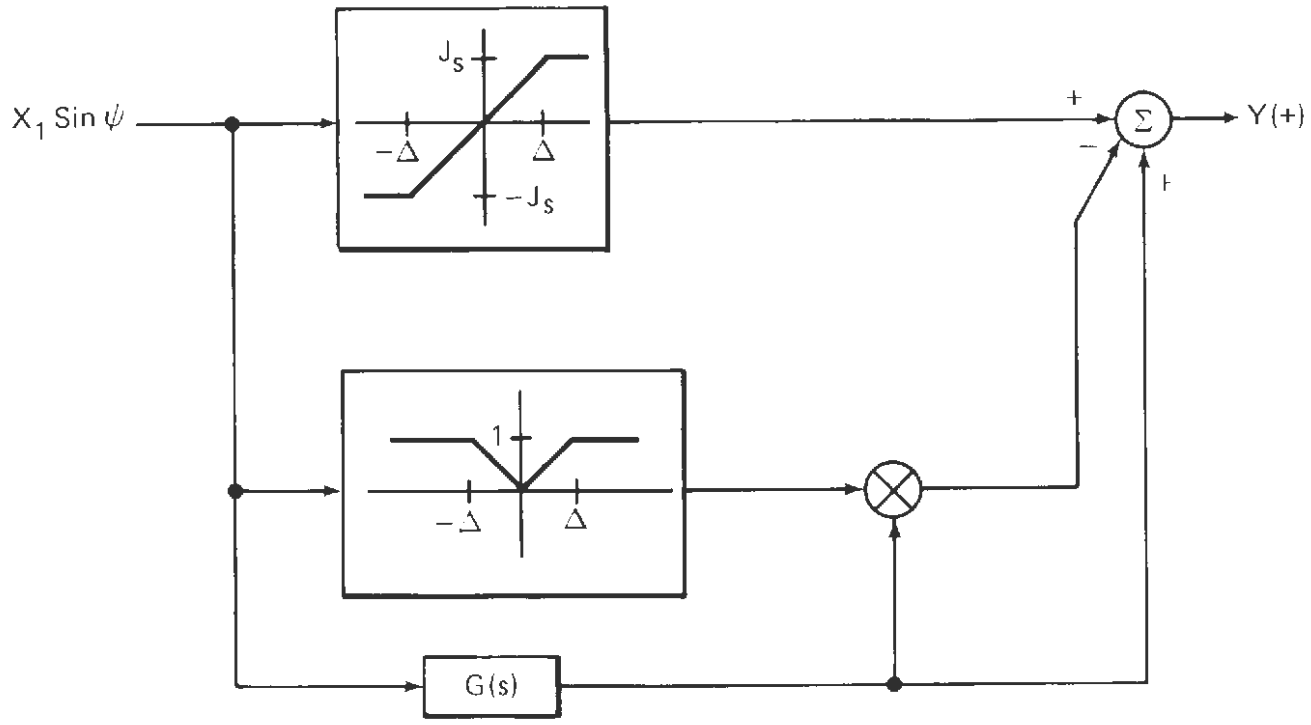

Fig.19 Single-Input Dynamic Nonlinearity

$$L(j\omega) = -\frac{1}{N(A,\omega)} \quad .$$

Thus, we may separately plot the left- and right-hand sides of the above equation. The curve $-1/N(A,\omega)$ then acts as the $-1 + j0$ point of a linear stability analysis plot. If an intersection of the two plots occurs at a particular frequency, a limit cycle will exist. The stability of the limit cycle is determined by considering a perturbation in the amplitude of the limit cycle as follows. If an increase in amplitude causes a further increase in amplitude, the limit cycle is unstable. That is, if an increase in amplitude along $-1/N(A,\omega)$ falls in a region to the right of the $L(j\omega)$ characteristic, the limit cycle is unstable. If an increase in amplitude falls to the left of the linear characteristic, the limit cycle is stable.

Before proceeding with stability analysis, some comments on the selection of the value of Δ will be noted in the following discussion.

SELECTION OF Δ

The primary purpose of the stability analysis is to determine the stability of the closed-loop system as a function of the

parameter Δ. Hence, we may select a value for Δ that yields a system with sufficient stability margin. However, a more direct way to select Δ is to consider the physical constraints in the problem.

Recall that ε is defined as the difference between the actual spacing and the kinematically required spacing. Thus, Δ is a measure of the deviation allowed from the desired spacing before full braking (or full acceleration) is applied. Suppose the desired headway is 0.5 s. Assuming a vehicle length of 3 m, the separation between vehicles at a minimum line velocity of 10 m/s is then 2 m. Consequently, it is readily apparent that we would like Δ to be smaller than 2 m, but at the same time a very small value of Δ would not be desirable since this would imply the necessity of a high sampling rate and possible noise problems. Hence, an intermediate value of $\Delta = 1$ should prove satisfactory. In fact, experimental evidence has indicated that a value of $\Delta = 1$ provides good performance.

The stability analysis in the following discussion is intended to verify closed-loop stability using the value of $\Delta = 1$. Moreover, from a stability viewpoint it will be shown we have a great deal of freedom in choosing Δ. For the 3-s headway case a value of $\Delta = 15$ is selected.

SUBOPTIMAL CONTROL III

To investigate the closed-loop stability of suboptimal control III, we will first separate the diagram of Fig. 17 into nonlinear and linear parts. This is most easily accomplished by breaking the loop at the jerk mode (the point at the output of the nonlinearity summing junction). The loop can then be drawn as in Fig. 20, where G(s) of Fig. 19 is given by

$$G(s) = \frac{1}{2} \frac{6.5\ s^2 + s}{2\ s^2 + 6.5\ s + 1} .$$

The technique outlined in the description of the nonlinear portion of the system will now be used to determine limit cycles as a function of Δ, the value of ε at which saturation occurs (as shown in Fig. 9). The magnitude phase plot for suboptimal control III is shown in Fig. 21 with $\Delta = 10$. The plot of the nonlinear portion is shown for amplitudes of the input up to A = 100 and for frequencies of 0.5, 1.5, 2.5, 3.5, and 4.5 rad/s. The

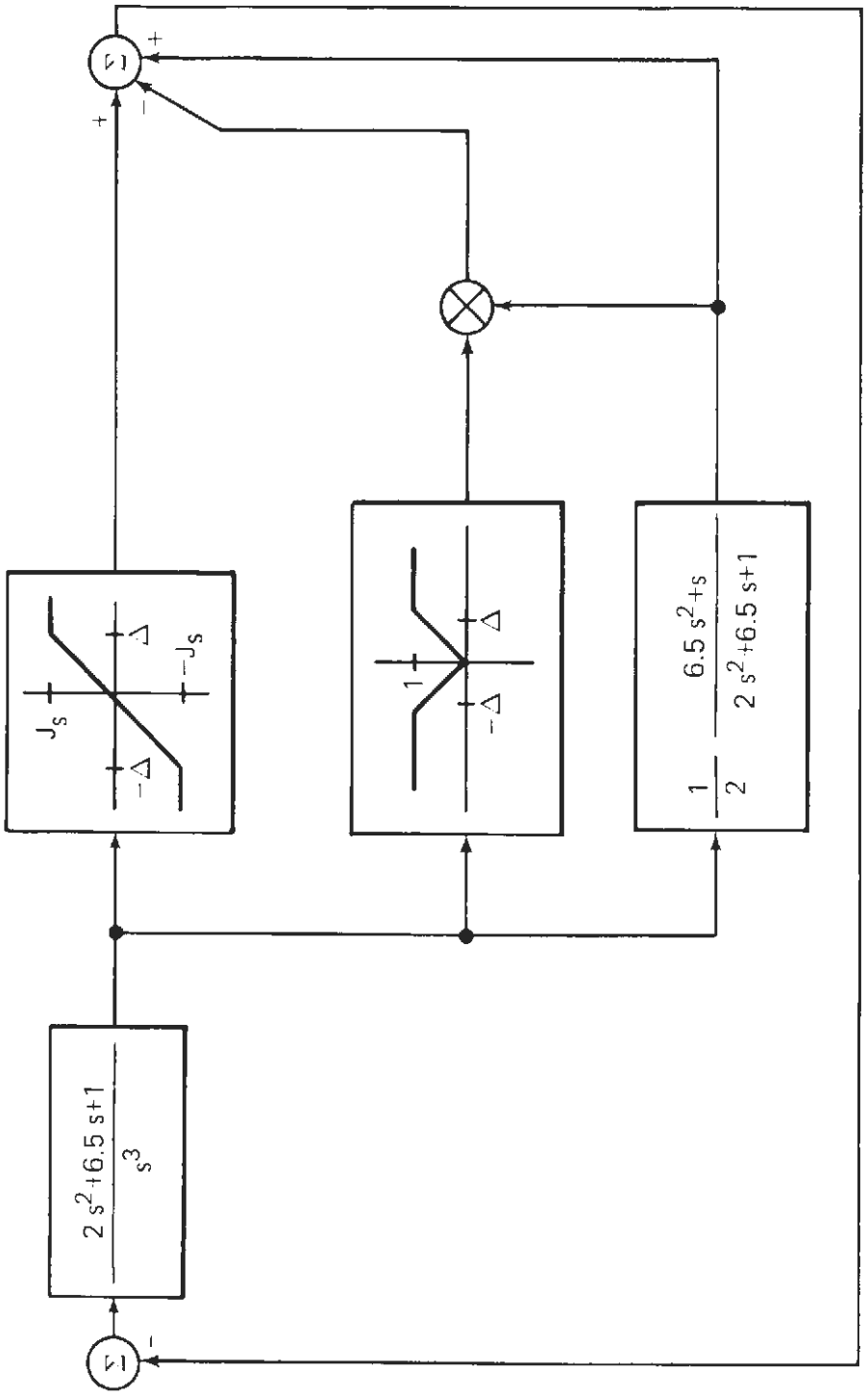

Fig. 20 Suboptimal Control III Stability Loop

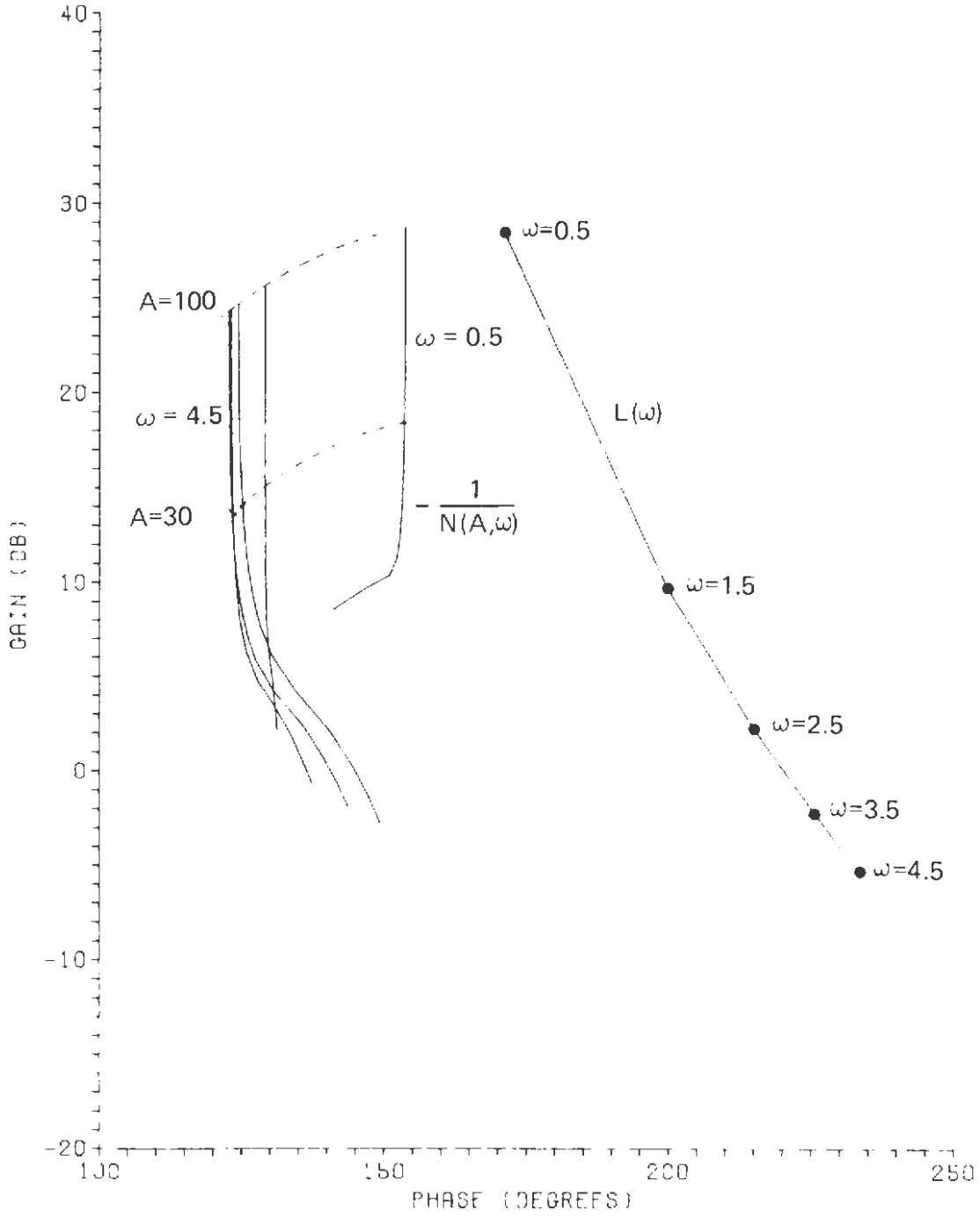

Fig. 21 Magnitude Phase Plot for Suboptimal Control III, Δ=10

linear characteristic, $L(\omega)$, is shown for a frequency range of 0.5 to 4.5 rad/s. Extrapolating the curves shows that an unstable limit cycle will occur at a frequency less than 0.5 rad/s and an amplitude somewhat greater than A = 100. However, in view of the jerk and acceleration limits in the system, the advent of such amplitudes is impossible. Oscillations with amplitude less than the limit cycle amplitude will decay to 0. Therefore it is concluded that the system is stable with a good margin.

The magnitude phase plot with $\Delta = 1$ is shown in Fig. 22. Again, the plot shows that an unstable limit cycle will occur at approximately 0.7 rad/s and an amplitude greater than A = 25. This is still well beyond the jerk and acceleration limits imposed on the system. Therefore, the selection of $\Delta = 1$ provides sufficient stability. Additional verification will be shown by the (approximate) linear analysis in the following paragraphs.

The magnitude phase plot with $\Delta = 0.1$ is shown in Fig. 23. As the plot shows, the effect of the nonlinearity is essentially that of a relay, which is the result when $\Delta = 0$. With $\Delta = 0$, the loop of Fig. 20 then becomes the linear portion followed by a nonlinearity with describing function

$$N(A,\omega) = \frac{4J_s}{\pi A} \quad .$$

The frequency and amplitude of the limit cycle can be determined analytically by first determining at what frequency the phase shift of the linear portion is 180°. Hence.

$$L(\omega) = \frac{2(j\omega)^2 + 6.5(j\omega) + 1}{(j\omega)^3}$$

$$= -\frac{6.5}{\omega^2} + j\frac{1 - 2^2}{\omega^3} \quad .$$

Solving $1 - 2\omega^2 = 0$ yields $\omega = 0.7$ rad/s. The amplitude of the limit cycle is determined by setting the open-loop gain equal to 1 and solving for A:

$$\frac{4J_s}{\pi A}\ \frac{6.5}{(0.7)^2} = 1 \ .$$

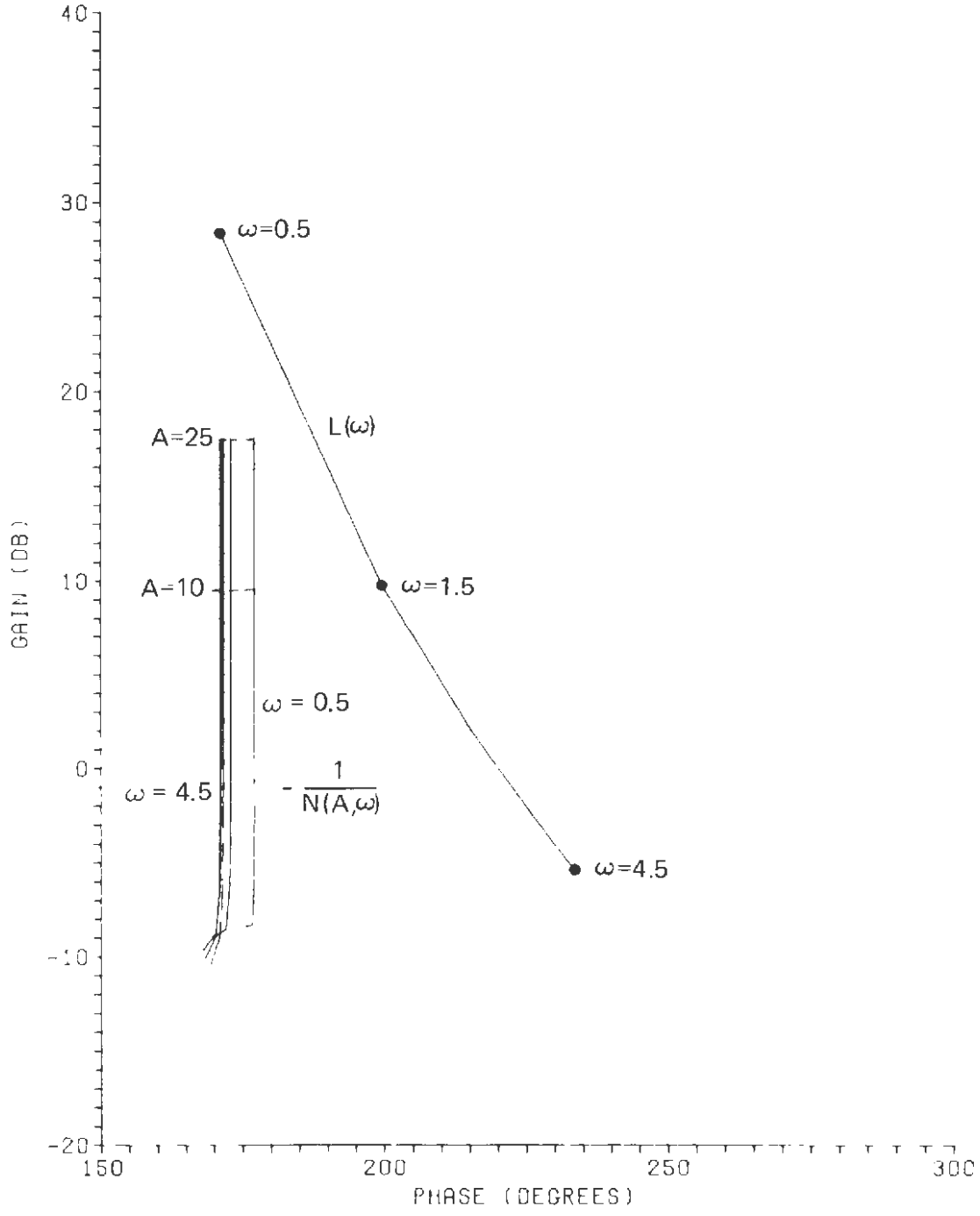

Fig. 22 Magnitude Phase Plot for Suboptimal Control III, Δ=1

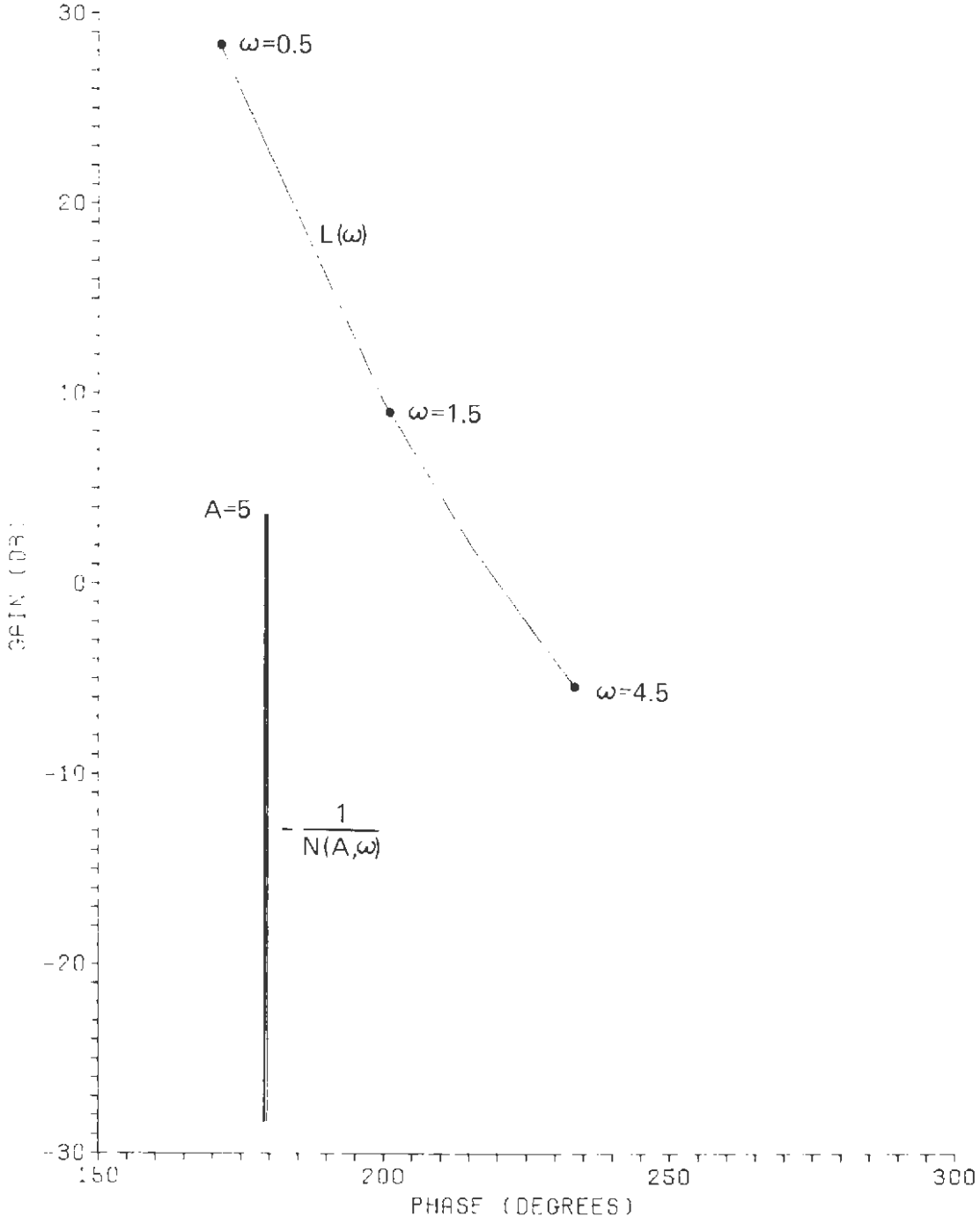

Fig. 23 Magnitude Phase Plot for Suboptimal Control III, Δ=0.1

With $J_s = 2.6$, $A = 44$. Consequently, the worst-case or limiting condition of $\Delta = 0$ produces a limit cycle at 0.7 rad/s with an amplitude of $A = 44$. The system will be stable with any positive value of Δ for signals well beyond the jerk and acceleration bounds of the system. Thus, we are free to select a value of Δ based on system considerations such as headway and sampling rate.

Linear Analysis

A small-signal linear analysis of suboptimal control III may be accomplished by considering small perturbations in ϵ about $\epsilon = 0$. Consequently, the output of the multiplier in Fig. 20 is approximately 0. Letting $K = J_s/\Delta$, the resulting open-loop transfer, $G(s)$, for $\epsilon \ll \Delta$ is then

$$G(s) = K \frac{2s^2 + 6.5s + 1}{s^3} + \frac{1}{2}\frac{6.5s + 1}{s^2}$$

$$= \frac{(3.25 + 2K)s^2 + (6.5K + 0.5)s + K}{s^3} .$$

By the Routh Criterion, a system with the above open-loop transfer will be closed-loop stable if

$$K > 0$$

and

$$K < (3.25 + 2K)(6.5K + 0.5) .$$

Since the first inequality implies the second, the system will be stable when $K > 0$. The cutoff frequency for the open-loop transfer with $K = 2.6$ is found to be approximately 8.6 rad/s. The resulting phase margin is approximately 76°. Hence, for small signals the system has sufficient stability margin.

STABILITY ANALYSIS OF SUBOPTIMAL CONTROL II

The closed-loop stability of suboptimal control II may be determined in a manner similar to suboptimal control III. However, there is an additional nonlinearity (multiplier), as shown by the

block diagram in Fig. 16. As in the case of suboptimal control III, the loop will be broken following the nonlinearity summing junction at J_c in Fig. 16. The describing functions for the transfer from J_c to ε and from J_c to u_{KB} will now be derived.

First, an input given by A sin ωt will be assumed at J_c. Consequently, the signal at ε is

$$\varepsilon = \left(- \frac{A}{\omega^3} + \frac{2\ A}{\omega} \right) \cos\ \omega t + \left(\frac{0.5\ A}{\omega^2} + \frac{1.4\ A}{\omega^2} \right) \sin\ \omega t$$

$$- \frac{0.19\ A^2}{\omega^4} \sin^2\ \omega t\ , \qquad (31)$$

and the signal at u_{KB} is

$$u_{KB} = \frac{A}{2\ \omega^2} \sin\ \omega t + \frac{0.7\ A}{\omega} \cos\ \omega t - \frac{0.19\ A^2}{\omega^3} \sin\ \omega t \cos\ \omega t\ . \qquad (32)$$

Substituting Eq. 31 into Eqs. 24b and 24c, the describing function is given by

$$N_\varepsilon(A,\omega) = \frac{1}{A} (b_1 + j a_1)$$

$$= \frac{1.9}{\omega^2} + j\ \frac{2\omega^2 - 1}{\omega^3}\ . \qquad (33)$$

Substituting Eq. 32 into Eqs. 24b and 24c, the describing function for u_{KB} is given by

$$N_{u_{KB}}(A,\omega) = \frac{1}{2\ \omega^2} + j\ \frac{0.7}{\omega}\ . \qquad (34)$$

As a result, we may determine G(s) in the dynamic nonlinearity (Fig. 19) by dividing Eq. 34 by Eq. 33 to yield

$$G(s) = \frac{0.7\ s^2 + 0.5\ s}{2\ s^2 + 1.9\ s + 1} \quad . \tag{35}$$

The system may now be separated into nonlinear (describing function) and linear parts to produce the loop shown in Fig. 24, which may be used for purposes of stability analysis.

The magnitude-phase plots for values of Δ of 10, 1, and 0.1 are shown in Figs. 25, 26, and 27, respectively. The plot with $\Delta = 10$ indicates an unstable limit cycle at approximately $A = 32$ and $\omega = 0.5$ rad/s. The plots for $\Delta = 1$ and $\Delta = 0.1$ are nearly identical with unstable limit cycles indicated at approximately $A = 15$ and $\omega = 0.7$ rad/s. Consequently, stability is not as sensitive to Δ, as in the case of suboptimal control III. Again, signals within the jerk and acceleration limits of the system will decay to 0. As in suboptimal control III, the amplitude and frequency of the limit cycle for the condition $\Delta = 0$ may be analytically determined. The frequency at which the phase of the linear portion is 180° is given by

$$\mathrm{Im}[G(\omega)] = 1 - 2\ \omega^2 = 0$$

or

$$\omega = 0.7 \text{ rad/s} \ .$$

The amplitude of the limit cycle is then found from

$$\frac{4J_s}{\pi A}\ \frac{1.9}{\omega^2} = 1$$

or

$$A = 12.8 \ .$$

Although $\Delta = 0$ would provide a stable system, a bang-bang jerk command is undesirable in terms of passenger comfort. Thus, a selection of $\Delta = 1$ should prove satisfactory.

It has been shown that suboptimal controls II and III are closed-loop stable in the range of jerk and acceleration limited signals that would be expected in a vehicle-following system. The

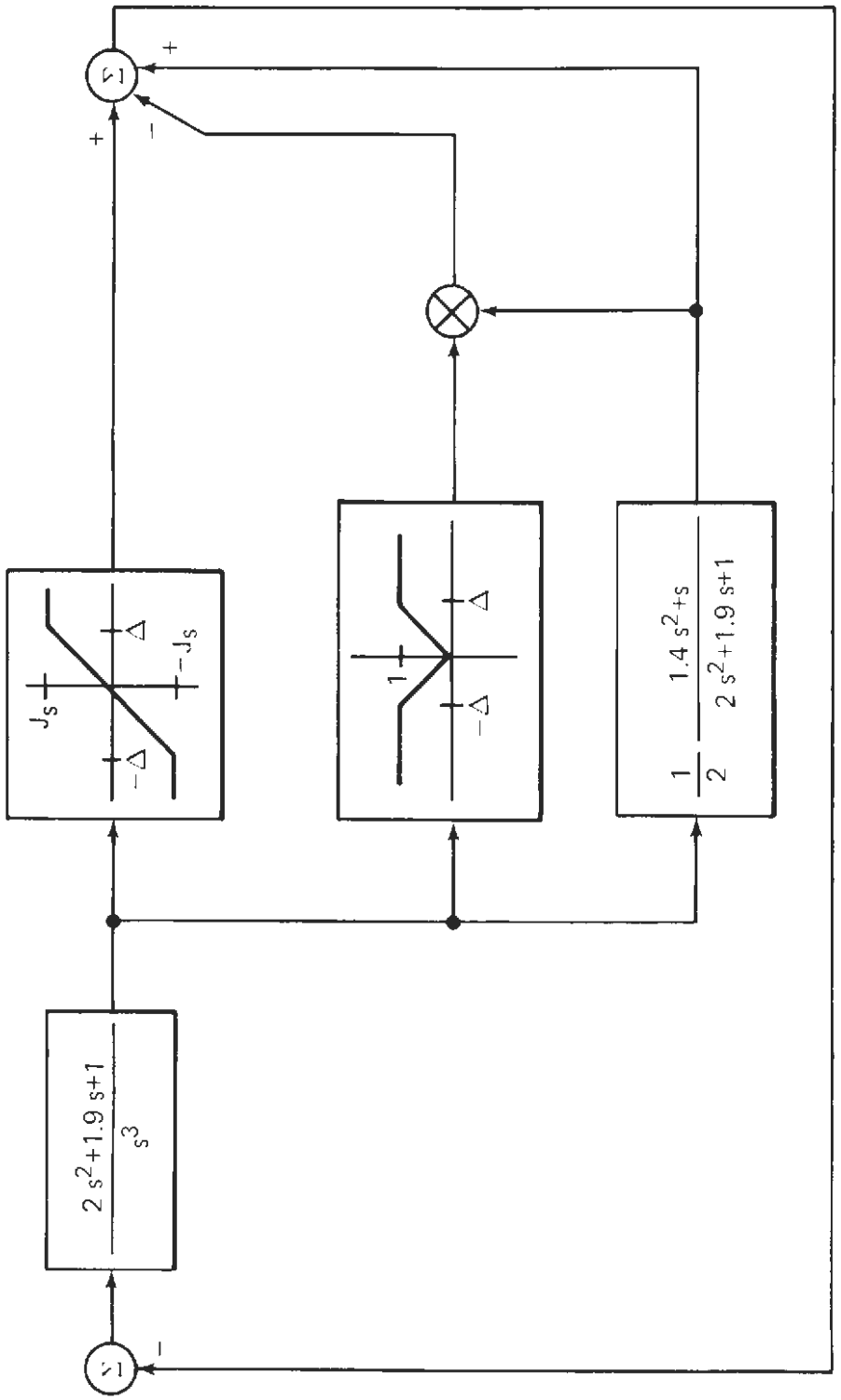

Fig. 24 Suboptimal Control II Stability Loop

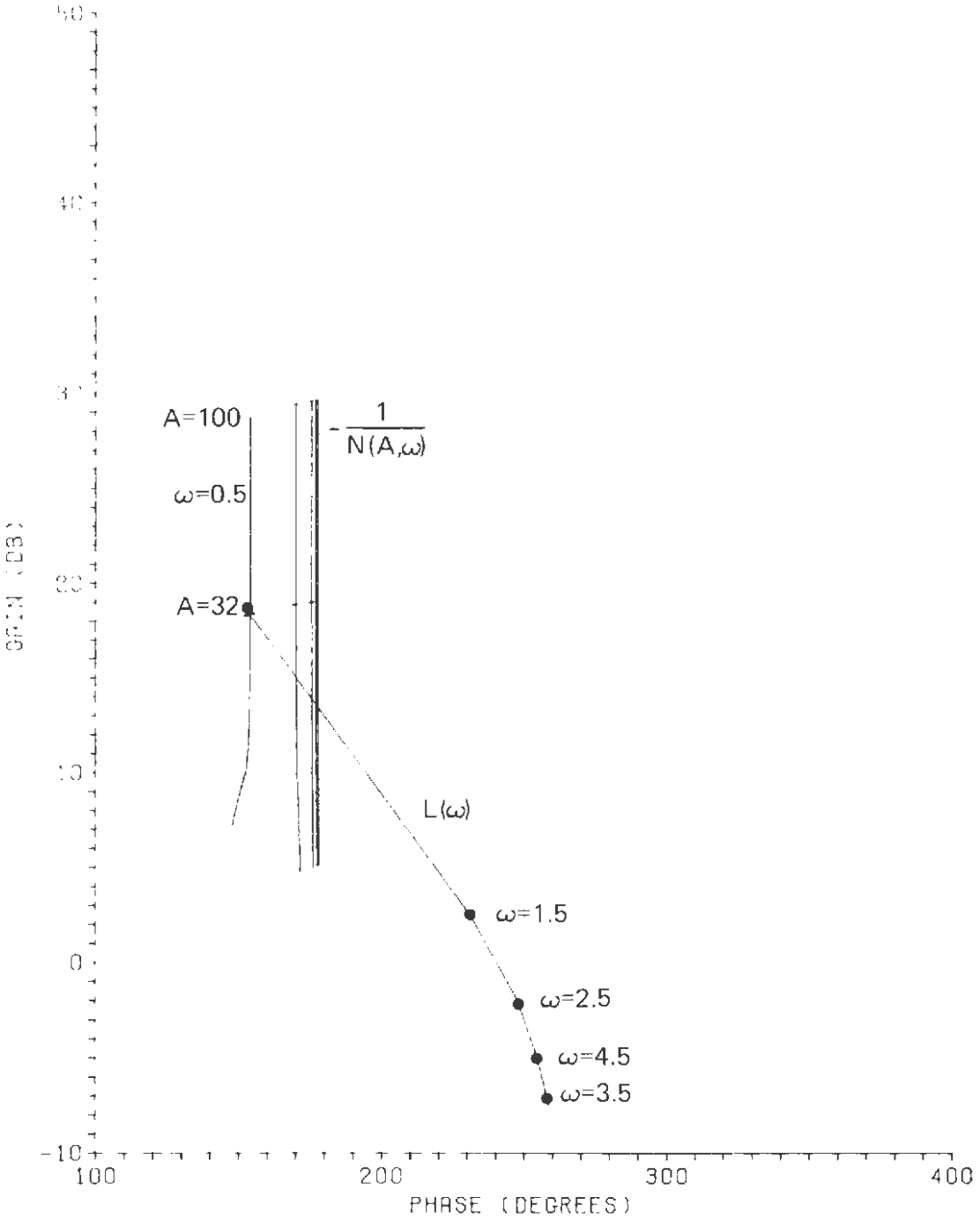

Fig. 25 Magnitude Phase Plot of Suboptimal Control II, Δ=10

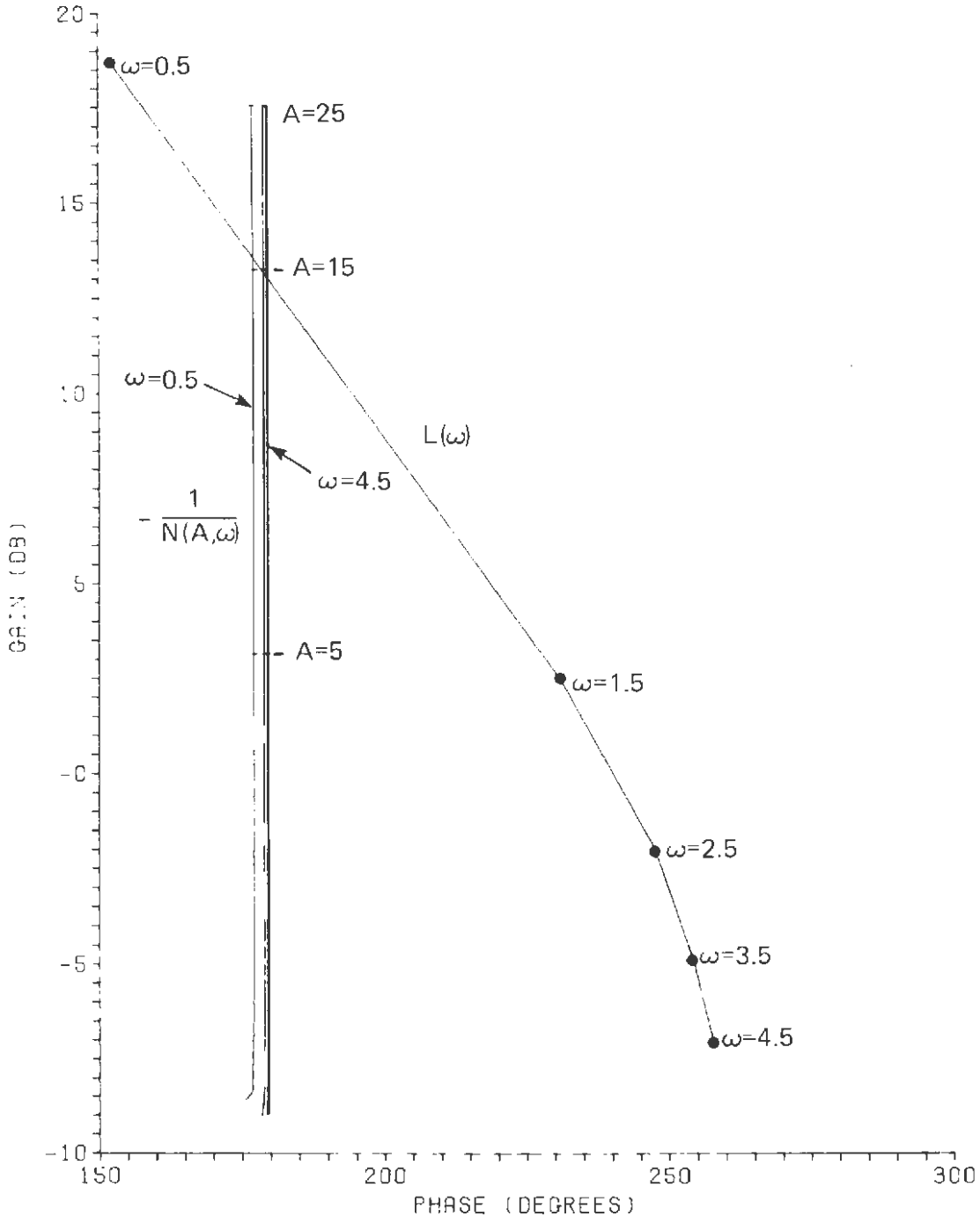

Fig. 26 Magnitude Phase Plot for Suboptimal Control II, Δ=1

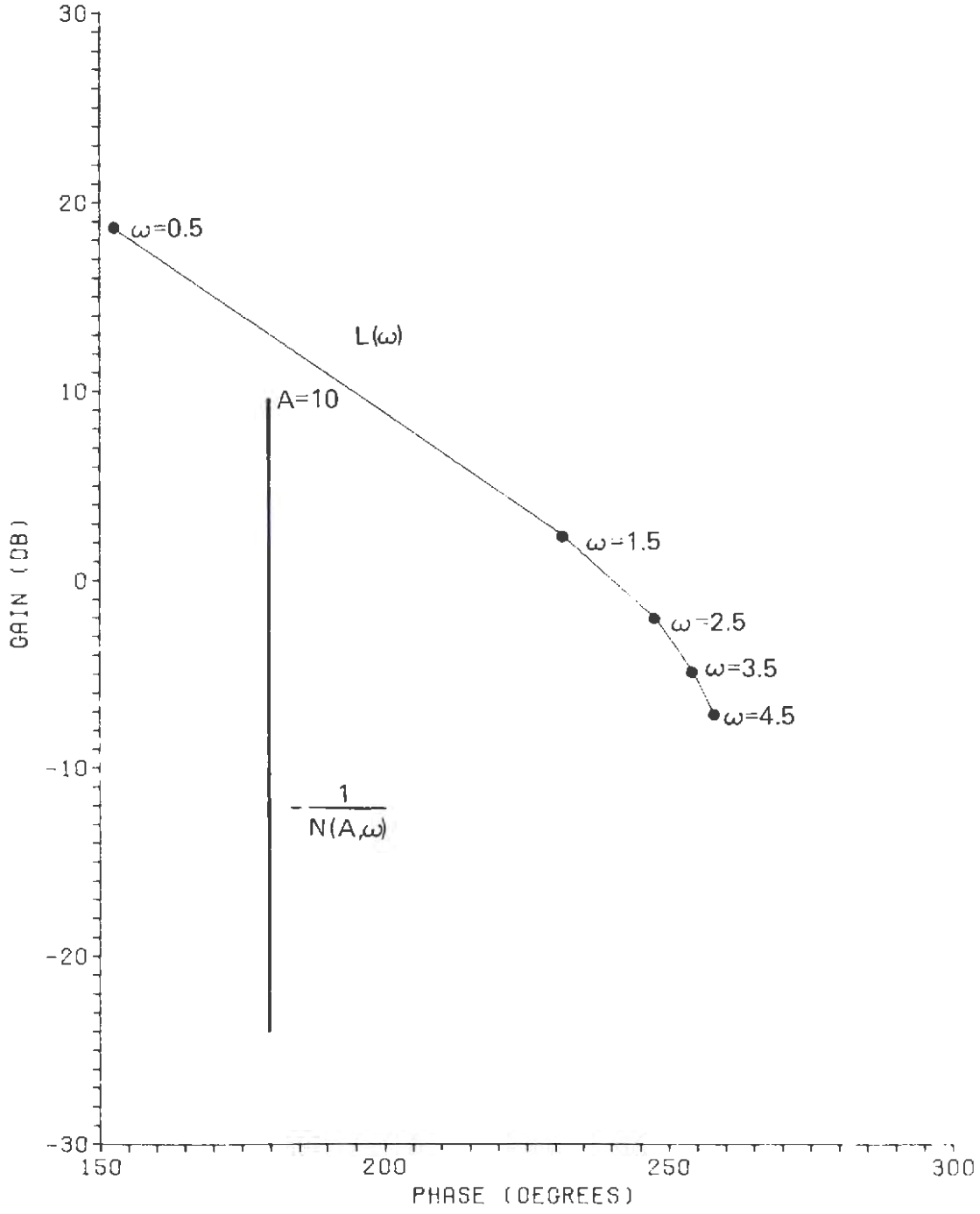

Fig. 27 Magnitude Phase Plot for Suboptimal Control II, Δ=0.1

analysis does not include the presence of the jerk and acceleration limiters; however, the design of the controller is based upon an explicit consideration of the jerk and acceleration capabilities of the vehicle. Thus, in normal operation, commanded jerk inputs should not exceed the jerk limit and the resulting acceleration should not exceed the acceleration limit. Hence, the analysis in conjunction with previous experimental evidence indicates a stable controller. In addition, the analysis has indicated that for any positive value of Δ the system will be stable. Therefore, we are free to choose a value of Δ based on other system considerations.

7. COMPARISON OF SUBOPTIMAL CONTROLS

A number of test cases have been simulated to demonstrate the performance of the optimal control (where "optimal" henceforth refers to the modified optimal of Section 4) and various suboptimal controls discussed in previous sections. In this section, the suboptimal controls are (a) evaluated in terms of the headway profile for some typical maneuvers where the desired headway is 0.5 s, (b) shown to operate satisfactorily as a regulator at nominal headway (for desired headways of 3 and 0.5 s), and (c) implemented in a five-vehicle string and show good performance (again for desired headways of 3 and 0.5 s).

The procedure in obtaining the suboptimal controls and the differences between them are summarized in Fig. 28 for convenience.

EVALUATION OF SUBOPTIMAL CONTROLS

Three test cases are presented for the optimal control and suboptimal controls I, II, and III. The first case involves a simple transition where a trailing vehicle traveling at 20 m/s encounters a preceding vehicle 100 m ahead with a speed of 10 m/s. The resulting response for a desired headway of 0.5 s using the modified optimal control is shown in Fig. 29. In the jerk, acceleration, and velocity curves the solid line denotes the preceding vehicle while the dashed line indicates the trailing vehicle. The plot of spacing shows both vehicle spacing and the spacing as required by the original kinematic constraint (Eq. 12). The response curves for suboptimal controls I, II, and III are shown in Figs. 30, 31, and 32, respectively. A comparison of the headway profiles for each control law is shown in Fig. 33. As expected, it takes progressively longer to complete the transition as the control law becomes simpler.

The second example is a similar overtaking situation with the trailing vehicle at 25 m/s, the preceding vehicle at 15 m/s, and an initial spacing of 100 m. At 10 s into the transition the preceding vehicle decelerates on limits to 10 m/s. The resulting responses of the optimal control and suboptimal controls I, II, and III are shown in Figs. 34, 35, 36, and 37, respectively. The comparison of headway profiles is shown in Fig. 38.

Finally, the last case has both the trailing and preceding vehicles at a velocity of 25 m/s with an initial spacing of 50 m.

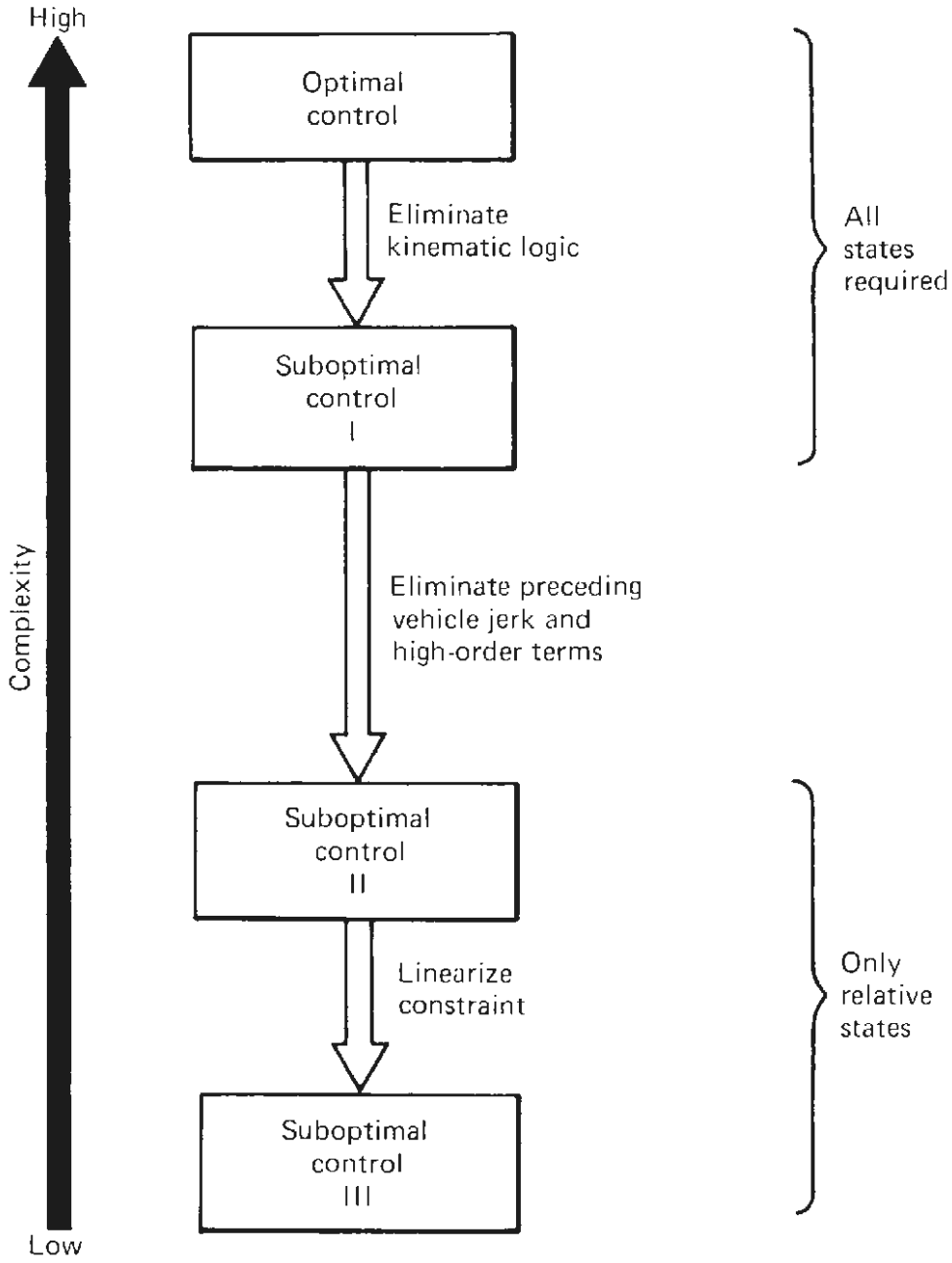

Fig. 28 Controller Complexity

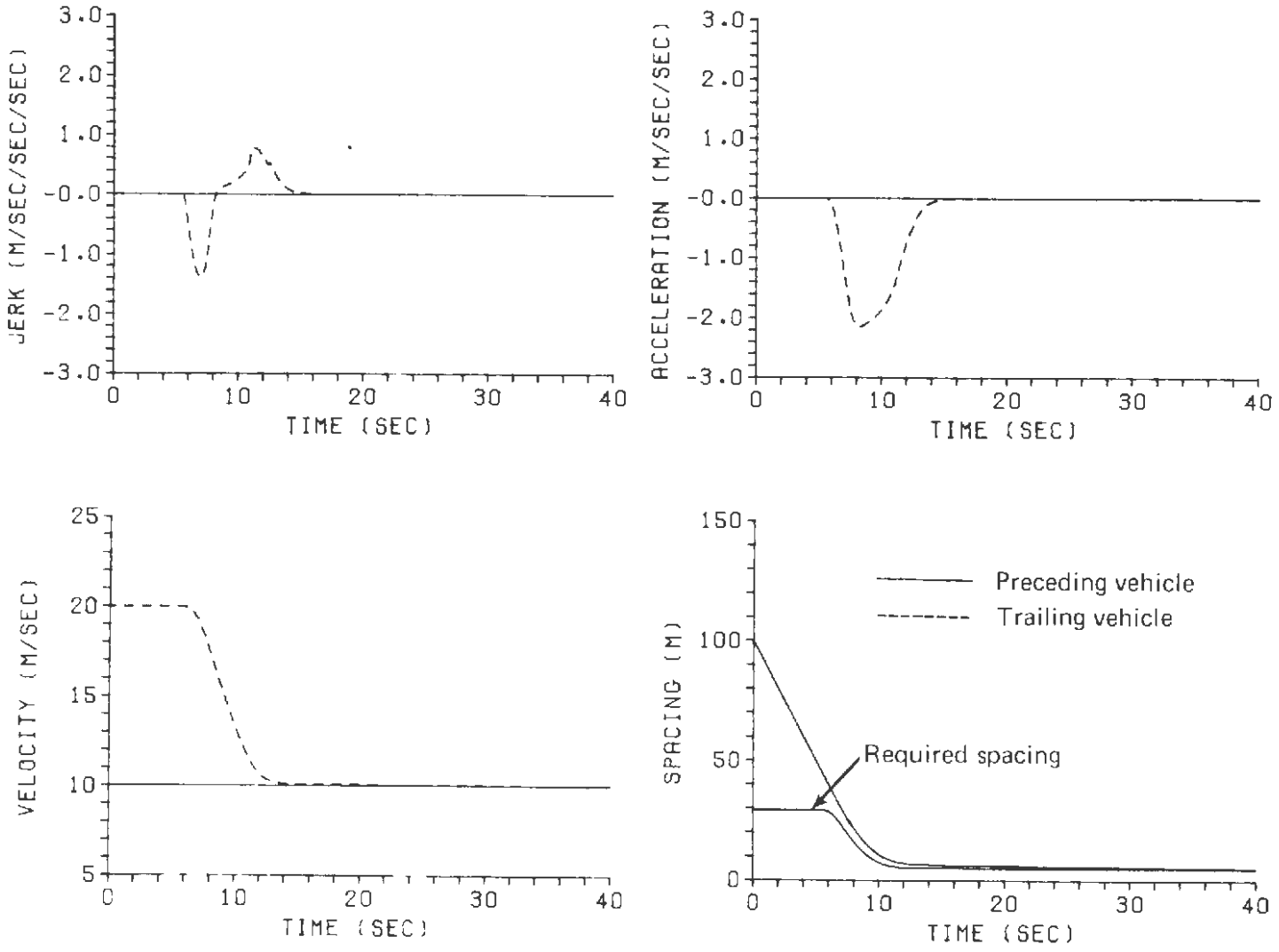

Fig. 29 State Profiles for Case 1 Using Optimal Control

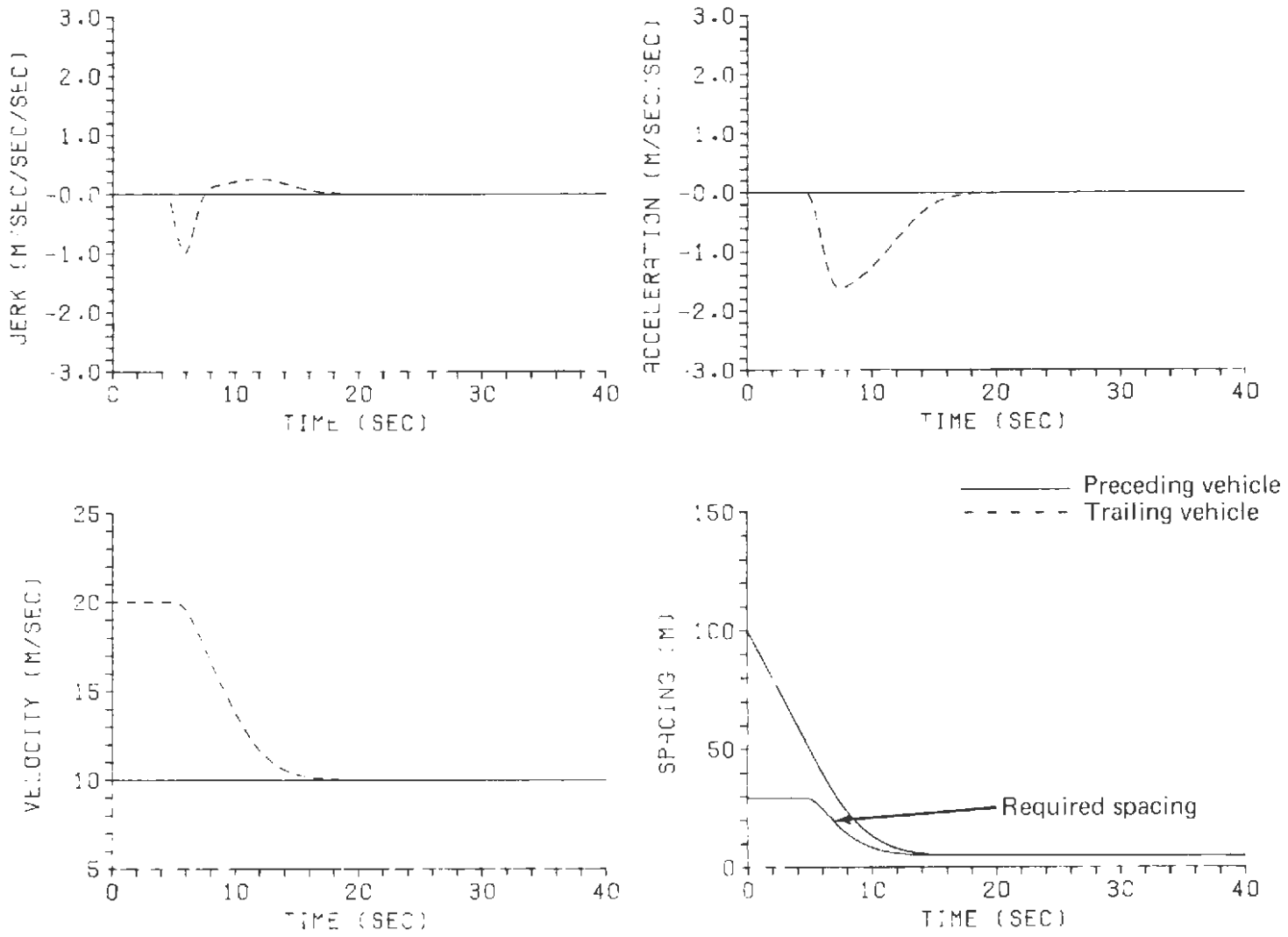

Fig. 30 State Profiles for Case 1 Using Suboptimal Control I

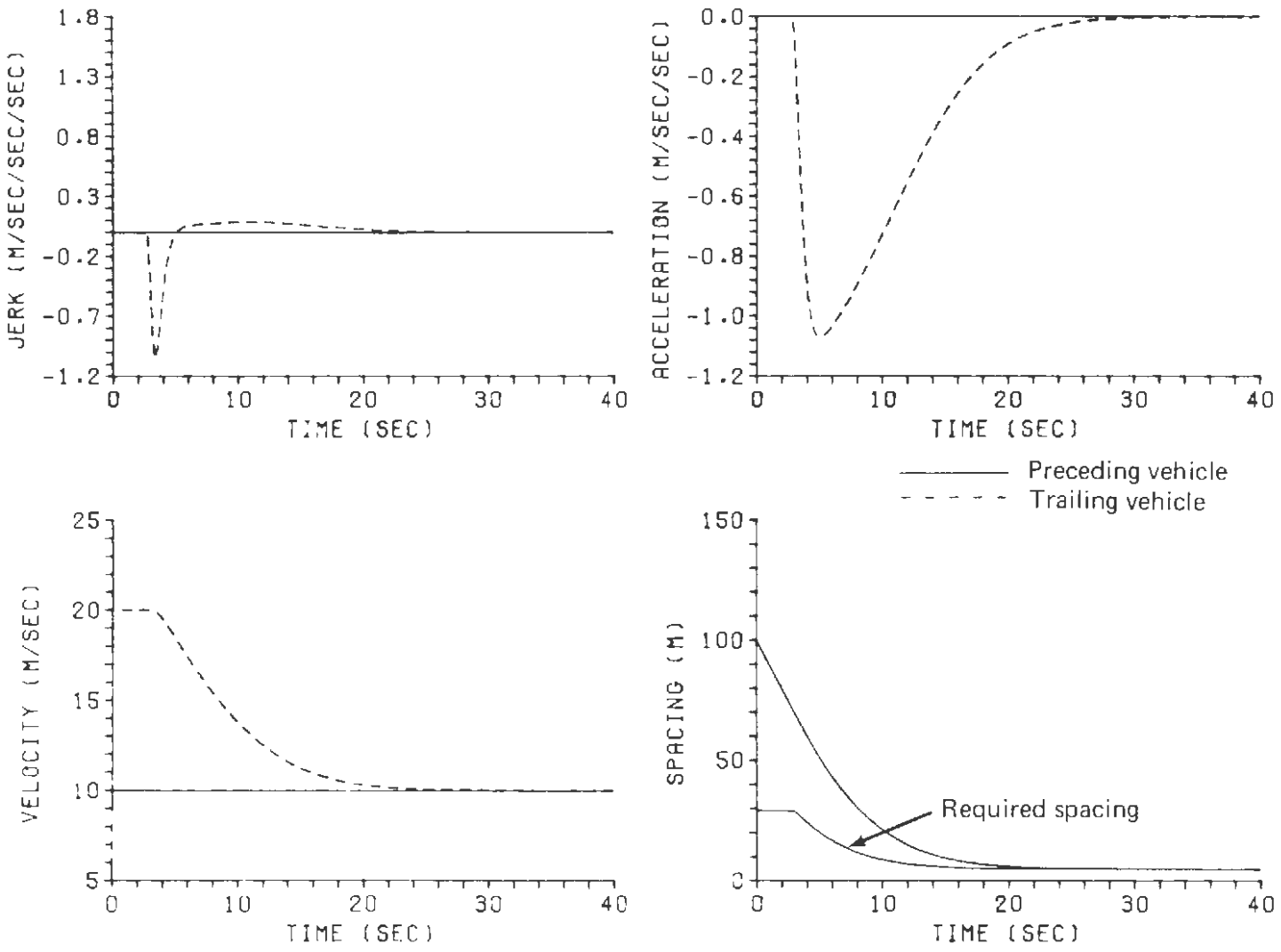

Fig. 31 State Profiles for Case 1 Using Suboptimal Control II

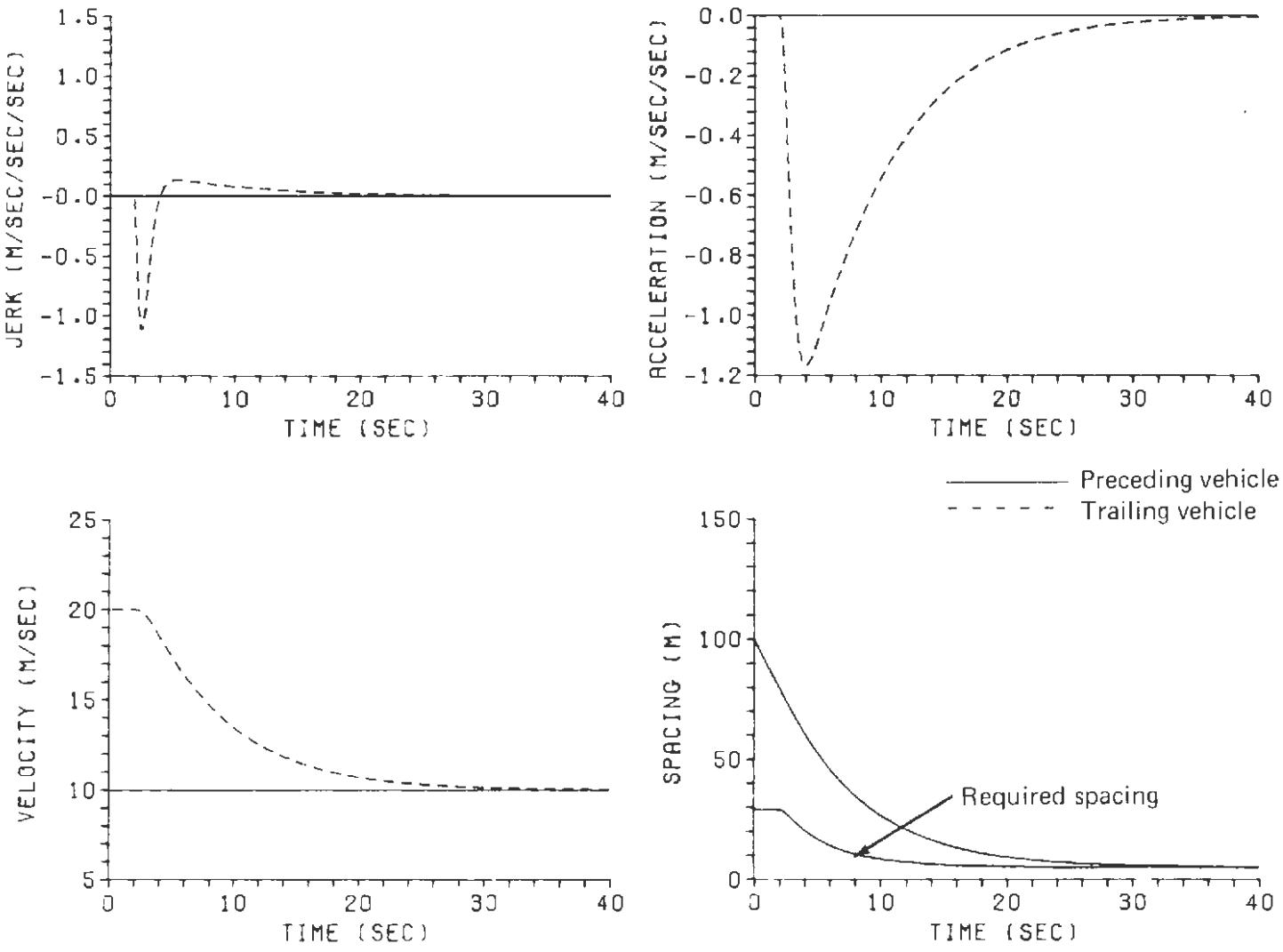

Fig. 32 State Profiles for Case 1 Using Suboptimal Control III

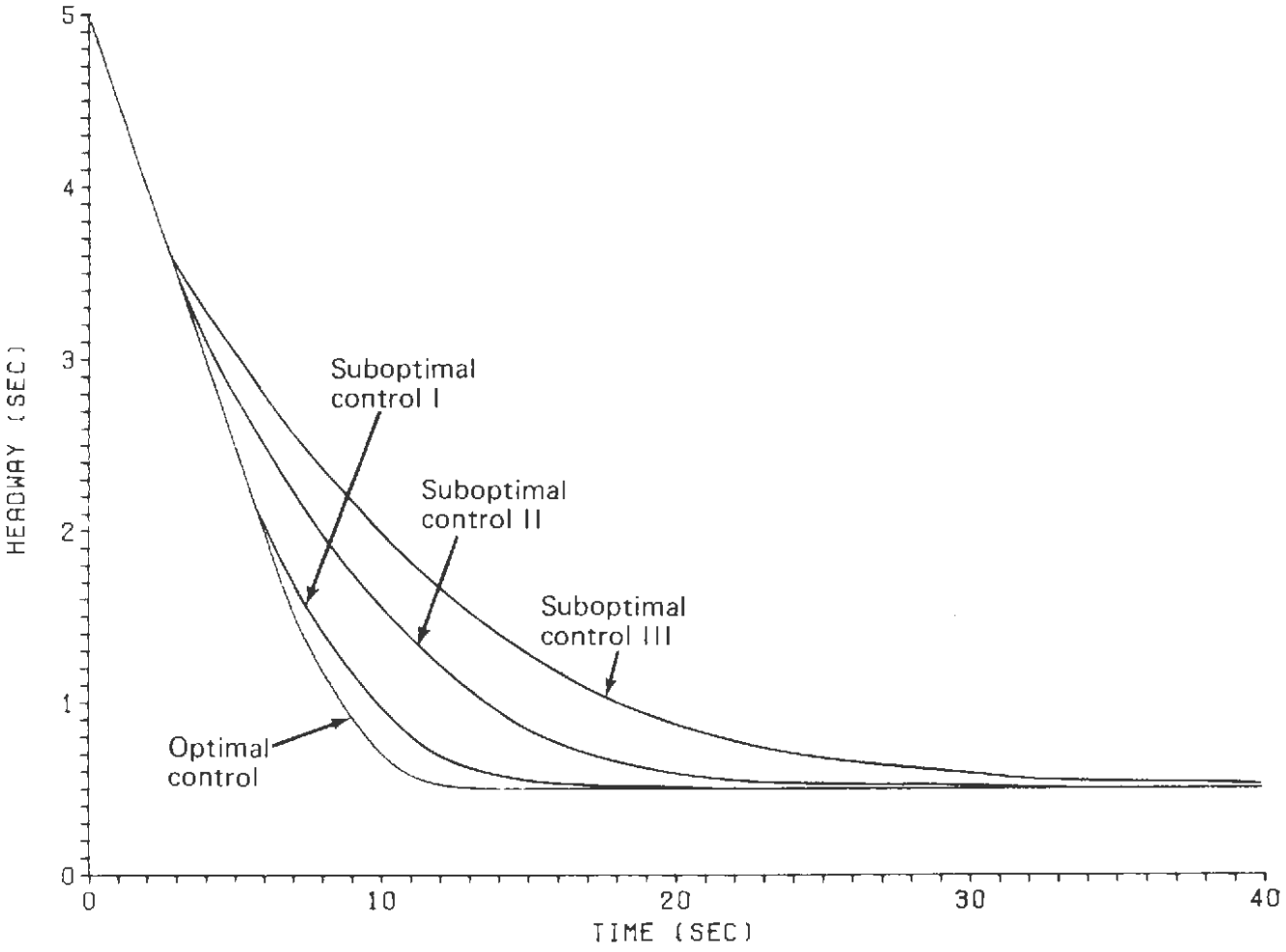

Fig. 33 Headway Comparison for Case I

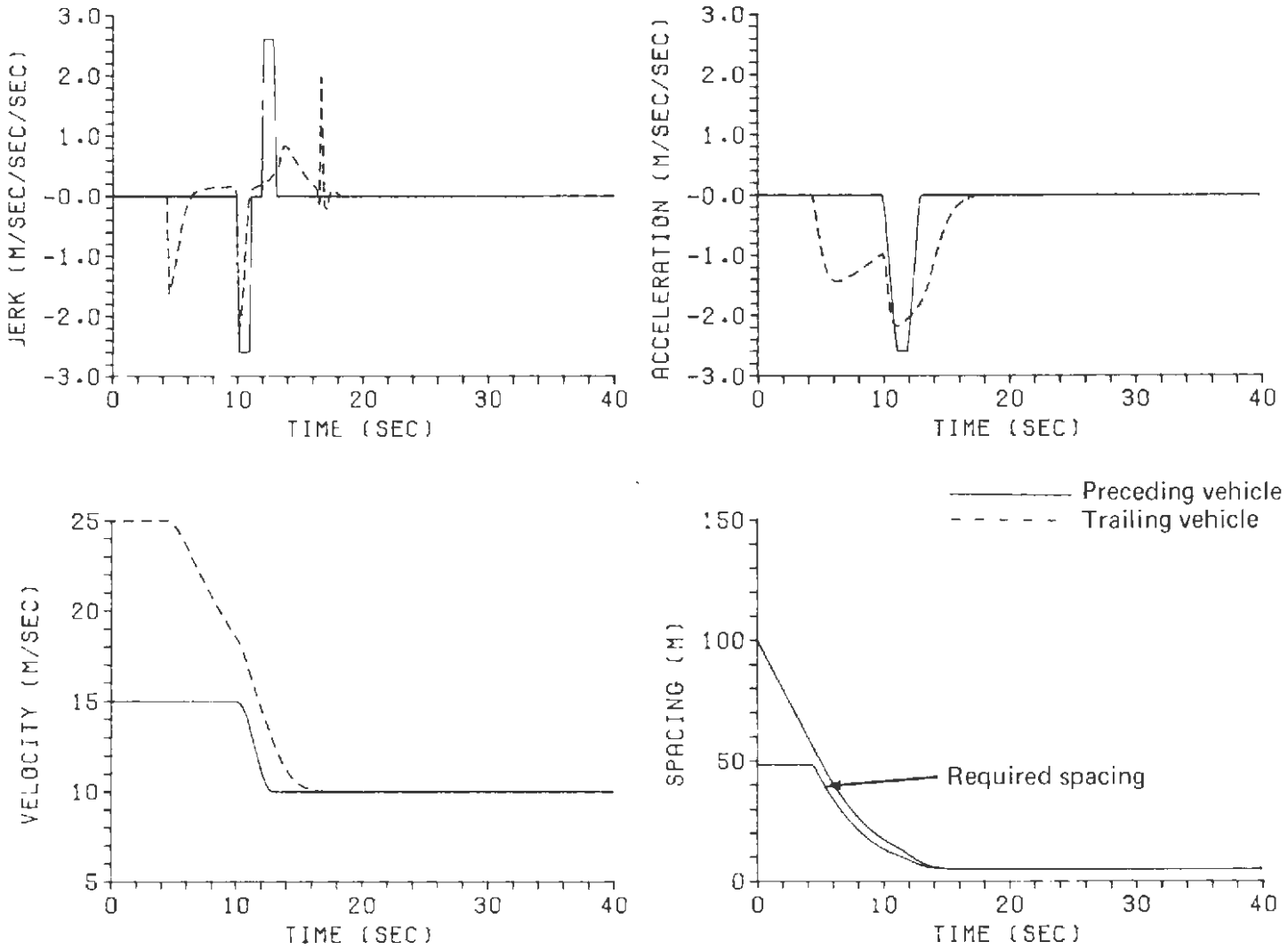

Fig. 34 State Profiles for Case 2 Using Optimal Control

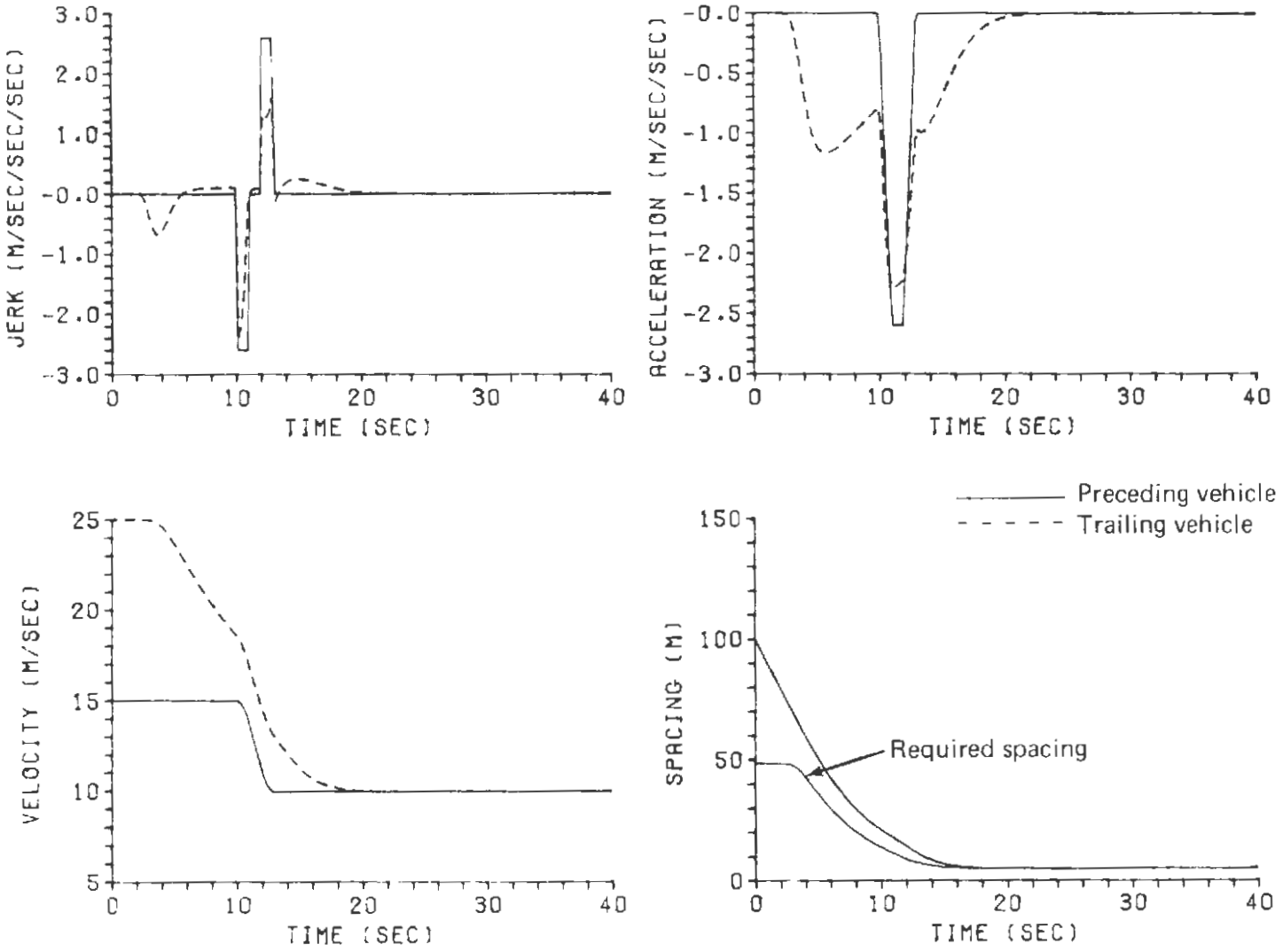

Fig. 35 State Profiles for Case 2 Using Suboptimal Control I

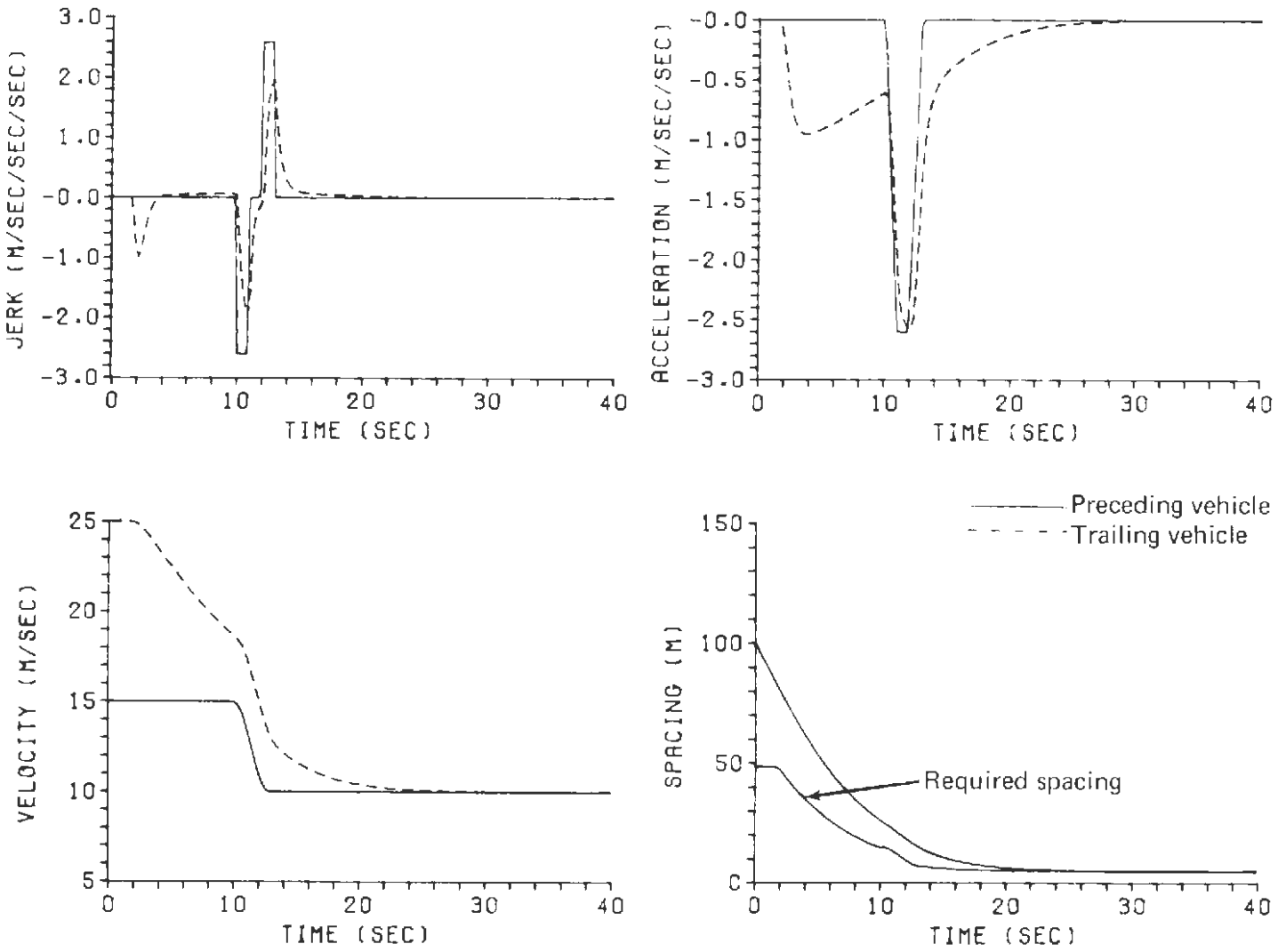

Fig. 36 State Profiles for Case 2 Using Suboptimal Control II

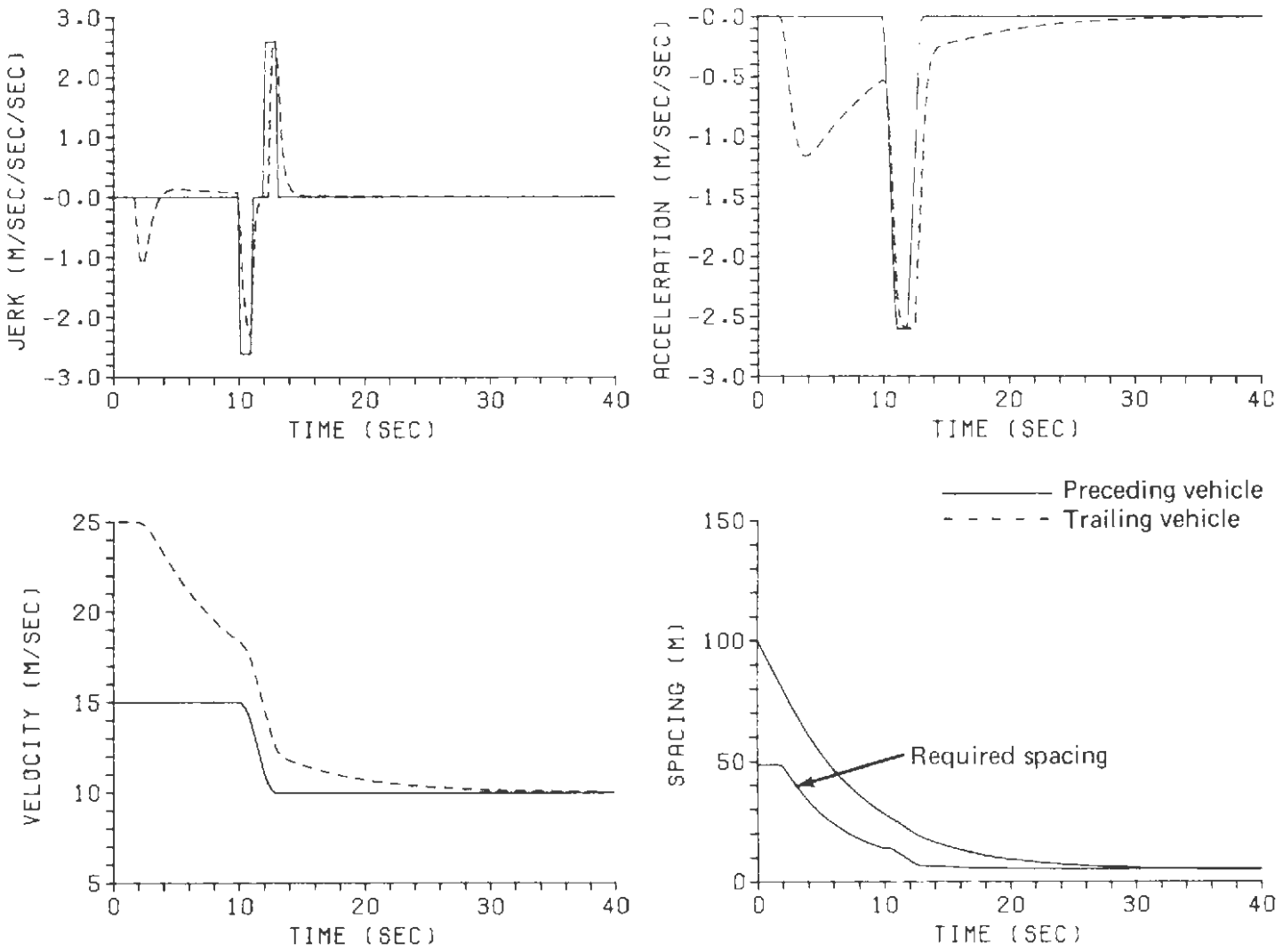

Fig. 37 State Profiles for Case 2 Using Suboptimal Control III

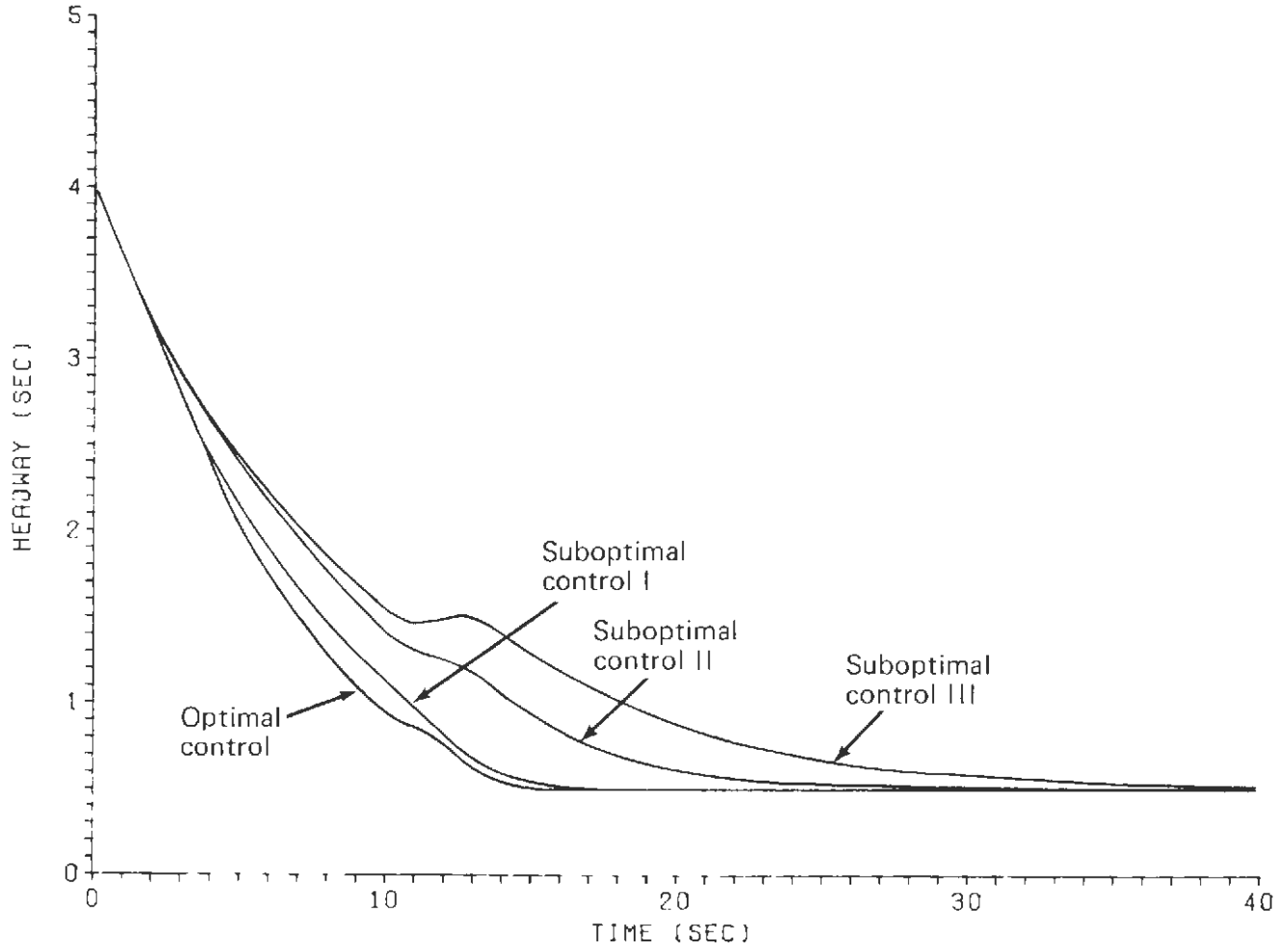

Fig. 38 Headway Comparison for Case 2

The preceding vehicle decelerates on limits to 10 m/s; the ensuing mode transitions are shown in Figs. 39, 40, 41, and 42 for the optimal control and suboptimal controls I, II, and III, respectively. The headway comparison is shown in Fig. 43.

Table 1 summarizes the results of the above test cases in terms of the time required to attain 50% (0.75 s) and 10% (0.55 s) of the desired headway (h = 0.5 s) for each of the control laws discussed. Suboptimal control III requires approximately three times the amount of time for the optimal control to reach a headway of 0.55 s for a typical maneuver. However, there is a significant difference between the times required to attain 0.55-s and 0.75-s headways for suboptimal control III. Consequently, the relative performance of suboptimal control III appears more satisfactory in terms of nulling large initial headway errors rather than the total time to acquire the desired headway. On the other hand, with a relatively small increase in complexity, suboptimal control II performs significantly better. Compared to the optimal control the time required to attain a 0.55-s headway is approximately twice as long for suboptimal control II. In addition, since the error states is the only informational requirement, suboptimal control II seems a good choice among the control laws that have been considered.

TRANSITION CONTROLLER AS A REGULATOR

At the end of Section 5 the kinematic constraint was reformulated such that the kinematic boundary coincides with the desired operating headway. As a result the control that keeps the vehicle on the kinematic boundary will act to maintain the desired headway in steady state (i.e., $V_T = V_P$, and $A_T = A_P = 0$). An example demonstrates this fact in Figs. 44, 45, and 46 using suboptimal controls I, II, and III, respectively, with a desired headway of 0.5 s. Each vehicle is initially traveling at 10 m/s with a headway of 0.5 s. The preceding vehicle accelerates on limits to 25 m/s and then immediately decelerates back to 10 m/s. As shown in Figs. 44, 45, and 46, each control law performs satisfactorily in following lead-vehicle maneuvers. Note the drop in required spacing as the preceding vehicle accelerates. This is a result of the preceding vehicle velocity becoming greater than the trailing vehicle velocity. Consequently, the distance required for the preceding vehicle to decelerate to minimum line speed becomes greater than the distance required for a trailing vehicle to decelerate to minimum line speed. The required spacing due purely to kinematics will become negative and therefore tend to cancel the residual desired spacing term, hV_T, in the kinematic constraint function. The trailing vehicle will respond by accelerating until the spacing as required by kinematics is 0 and the residual desired spacing is acquired.

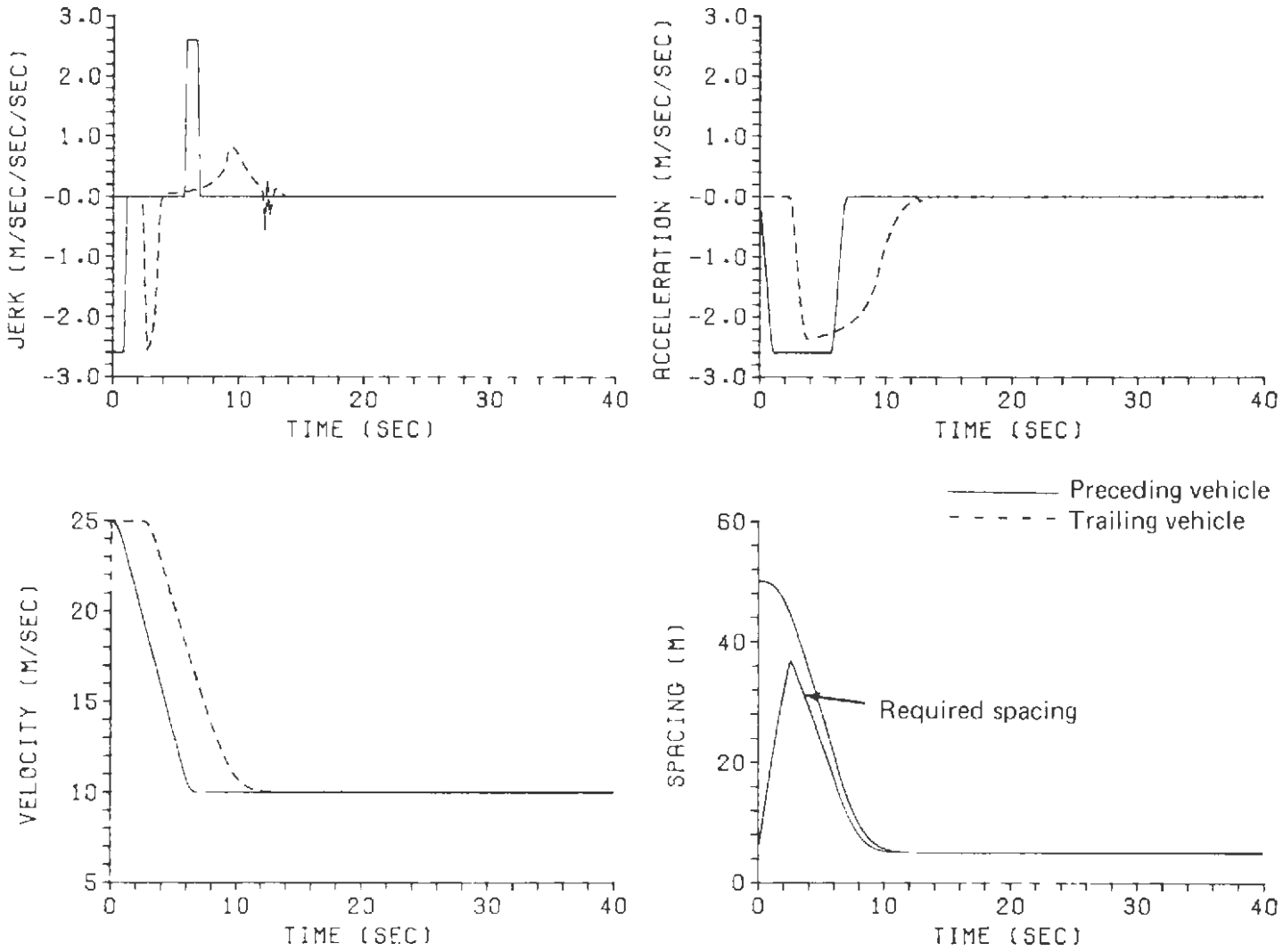

Fig. 39 State Profiles for Case 3 Using Optimal Control

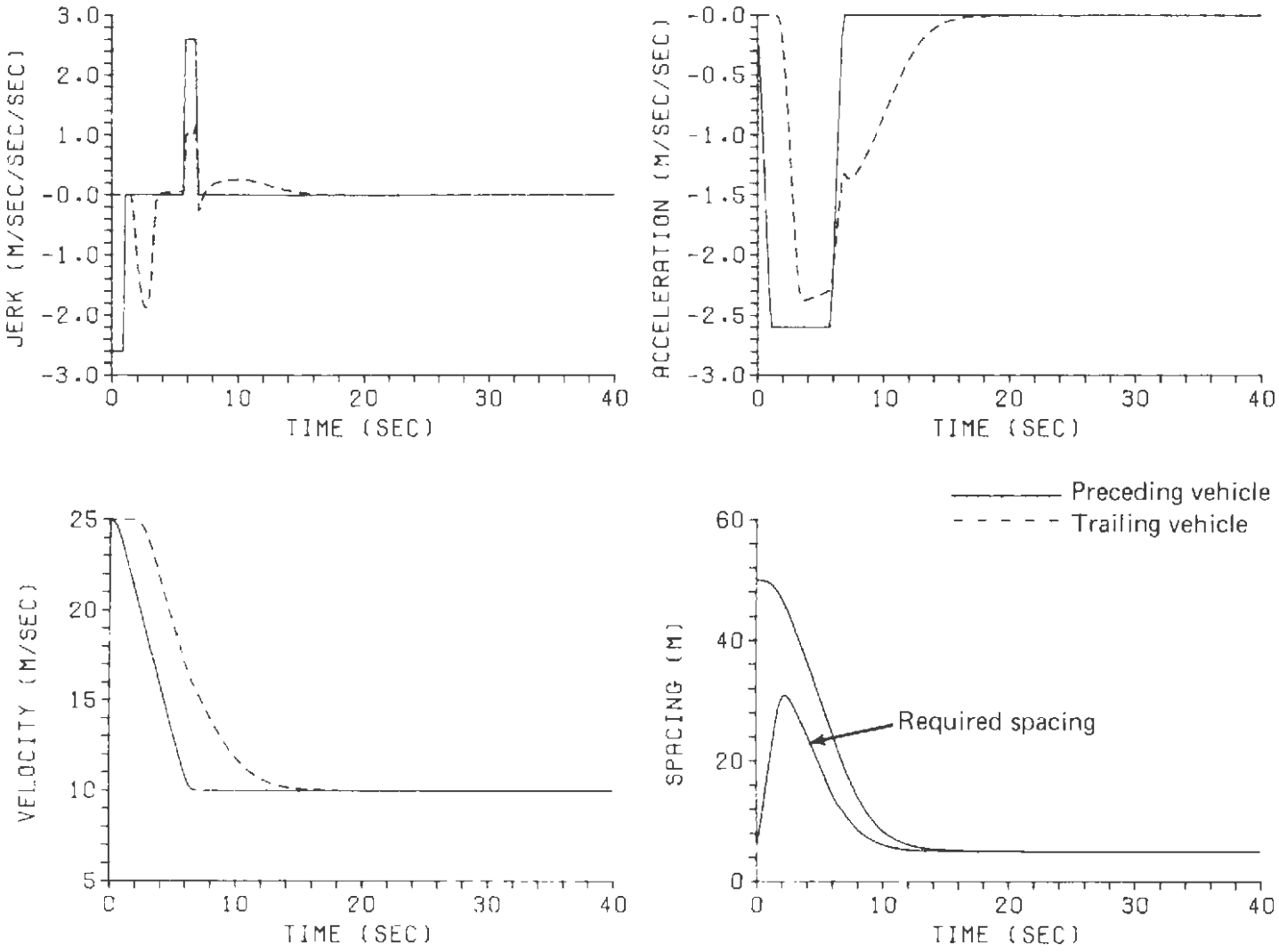

Fig. 40 State Profiles for Case 3 Using Suboptimal Control I

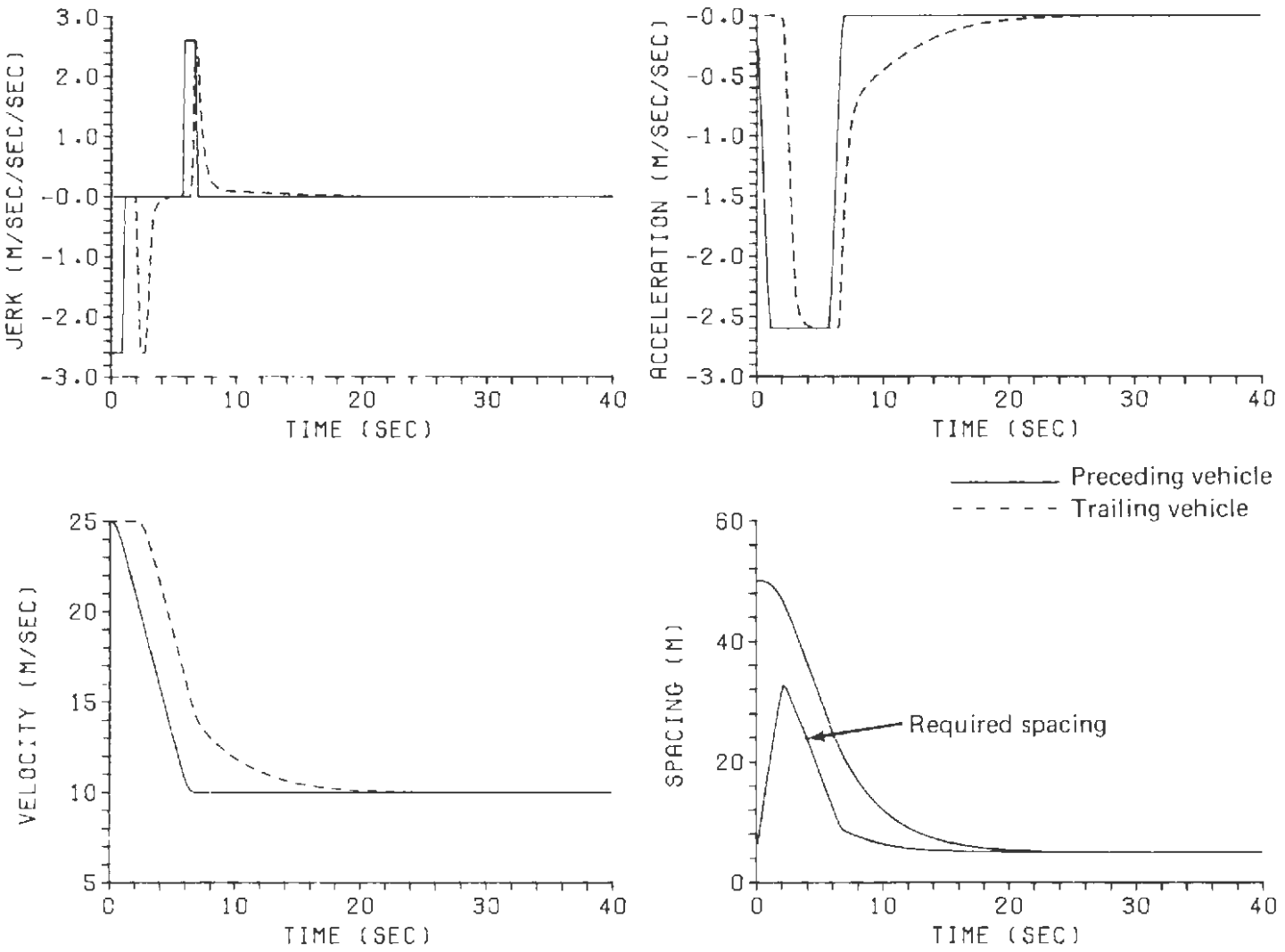

Fig. 41 State Profiles for Case 3 Using Suboptimal Control II

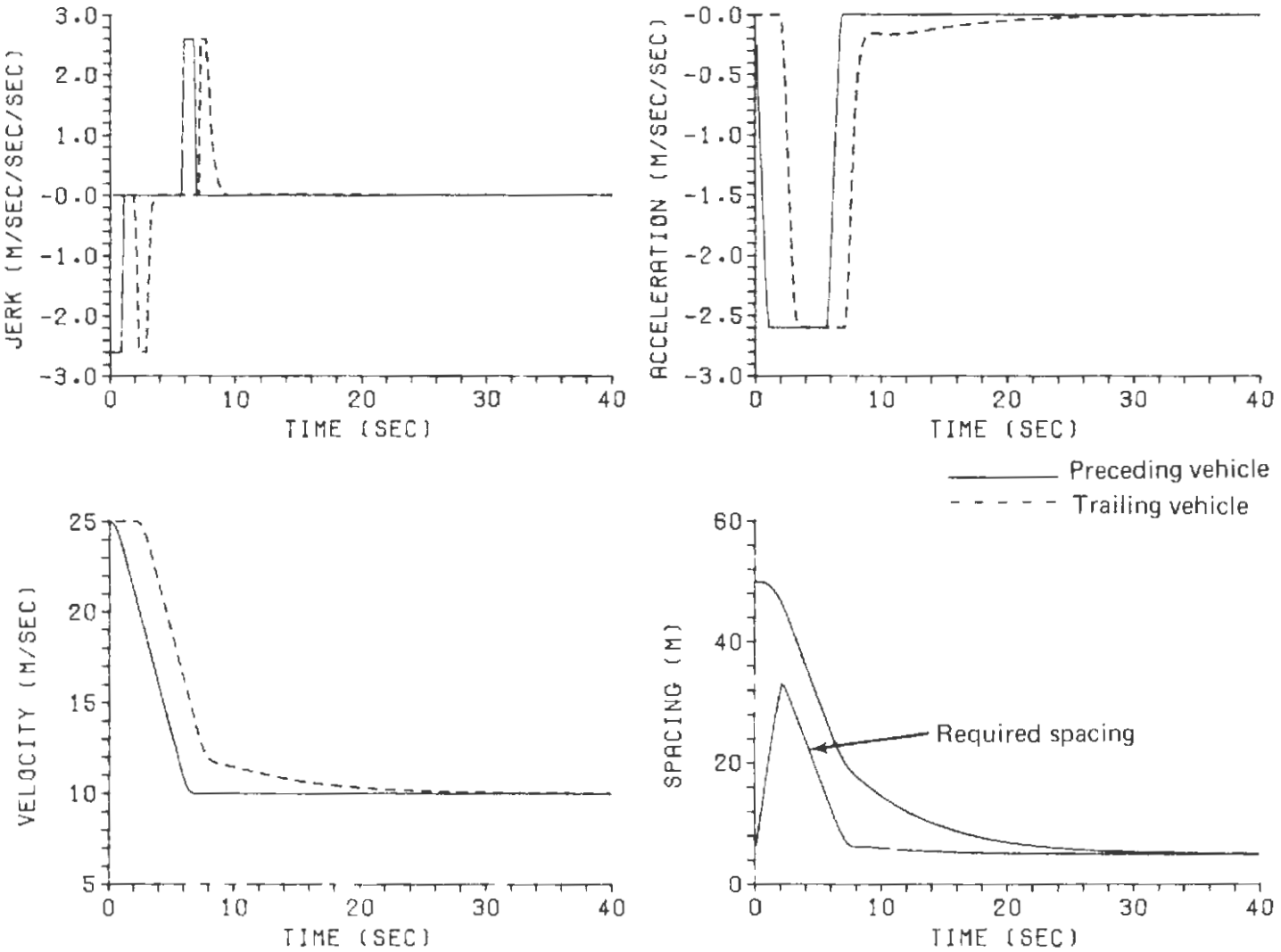

Fig. 42 State Profiles for Case 3 Using Suboptimal Control III

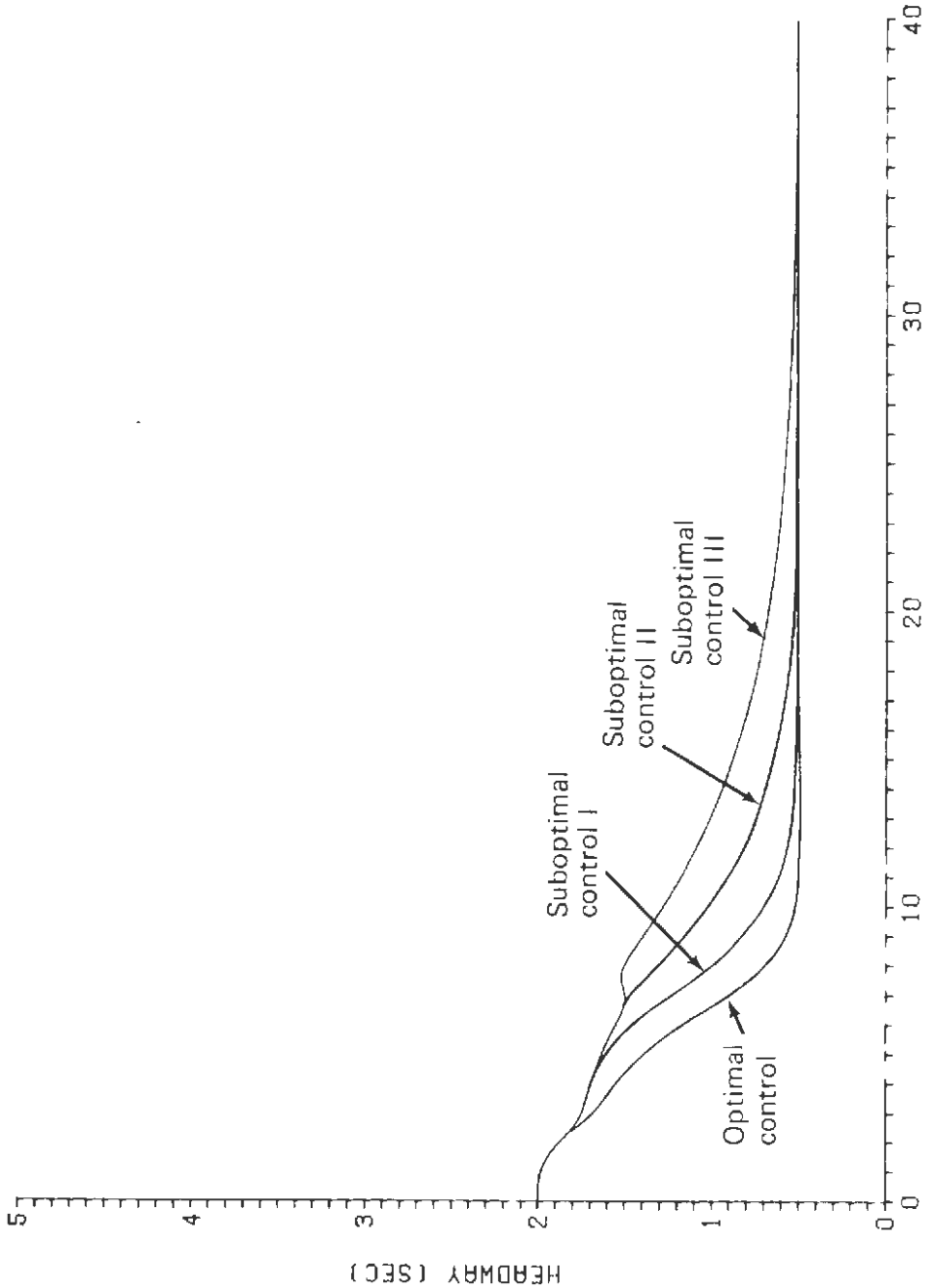

Fig. 43 Headway Comparison for Case 3

Table 1

Comparison of Times to Attain 50 and 10% of a Desired Final Headway (0.5 s) for Various Control Laws

	Case 1		Case 2		Case 3	
Percent of desired headway (%)	50	10	50	10	50	10
Headway (s)	(0.75)	(0.55)	(0.75)	(0.55)	(0.75)	(0.55)
Optimal Control (s)	9.7	11.4	12.2	13.9	7.8	9.5
Suboptimal Control I (s)	11.5	15.0	13.7	16.5	9.7	12.5
Suboptimal Control II (s)	16.2	21.5	17.1	22.5	12.9	18.5
Suboptimal Control III (s)	22.7	32.5	22.7	32.5	17.7	27.5

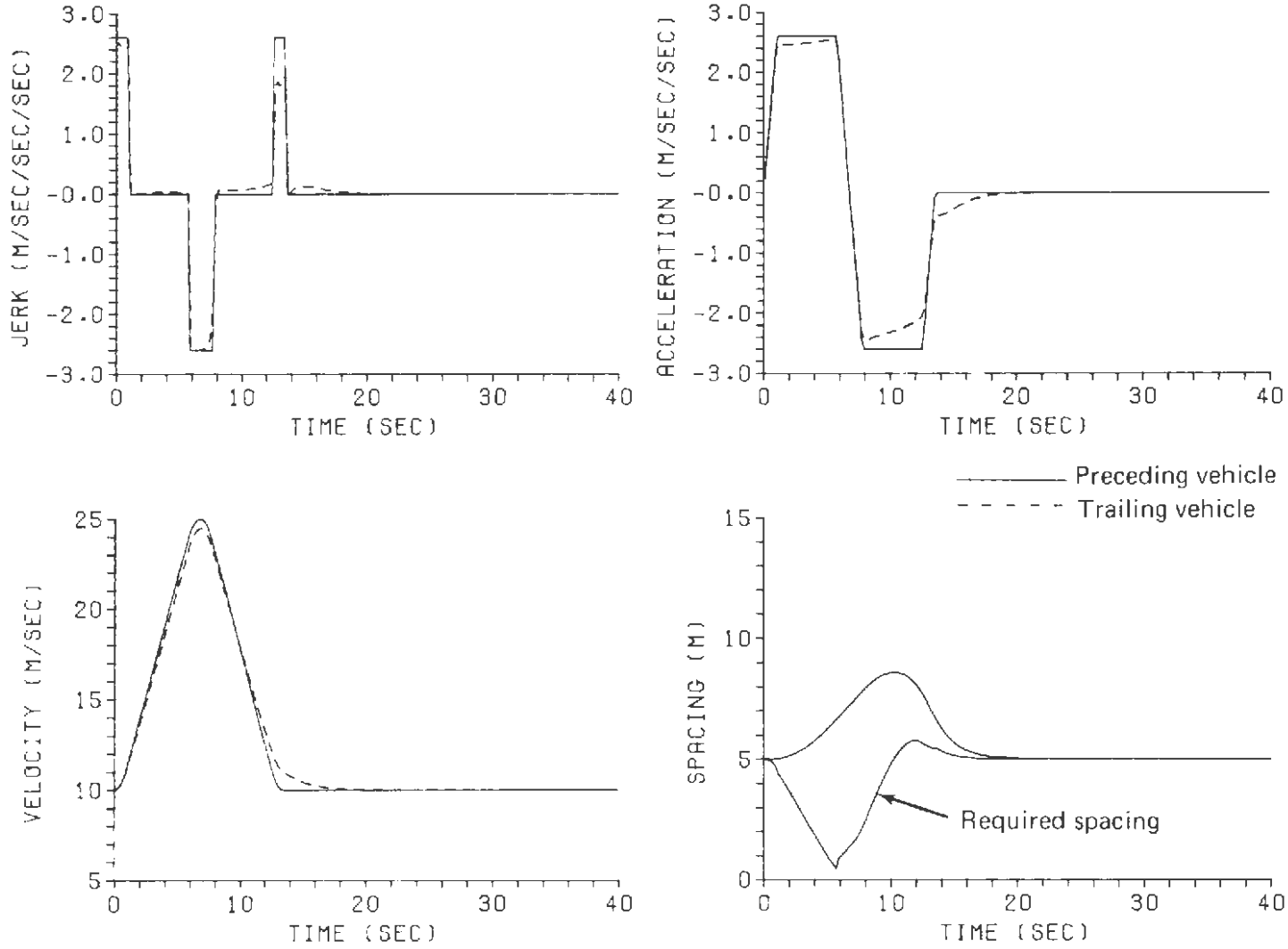

Fig. 44 Suboptimal Control I in Regulator Mode

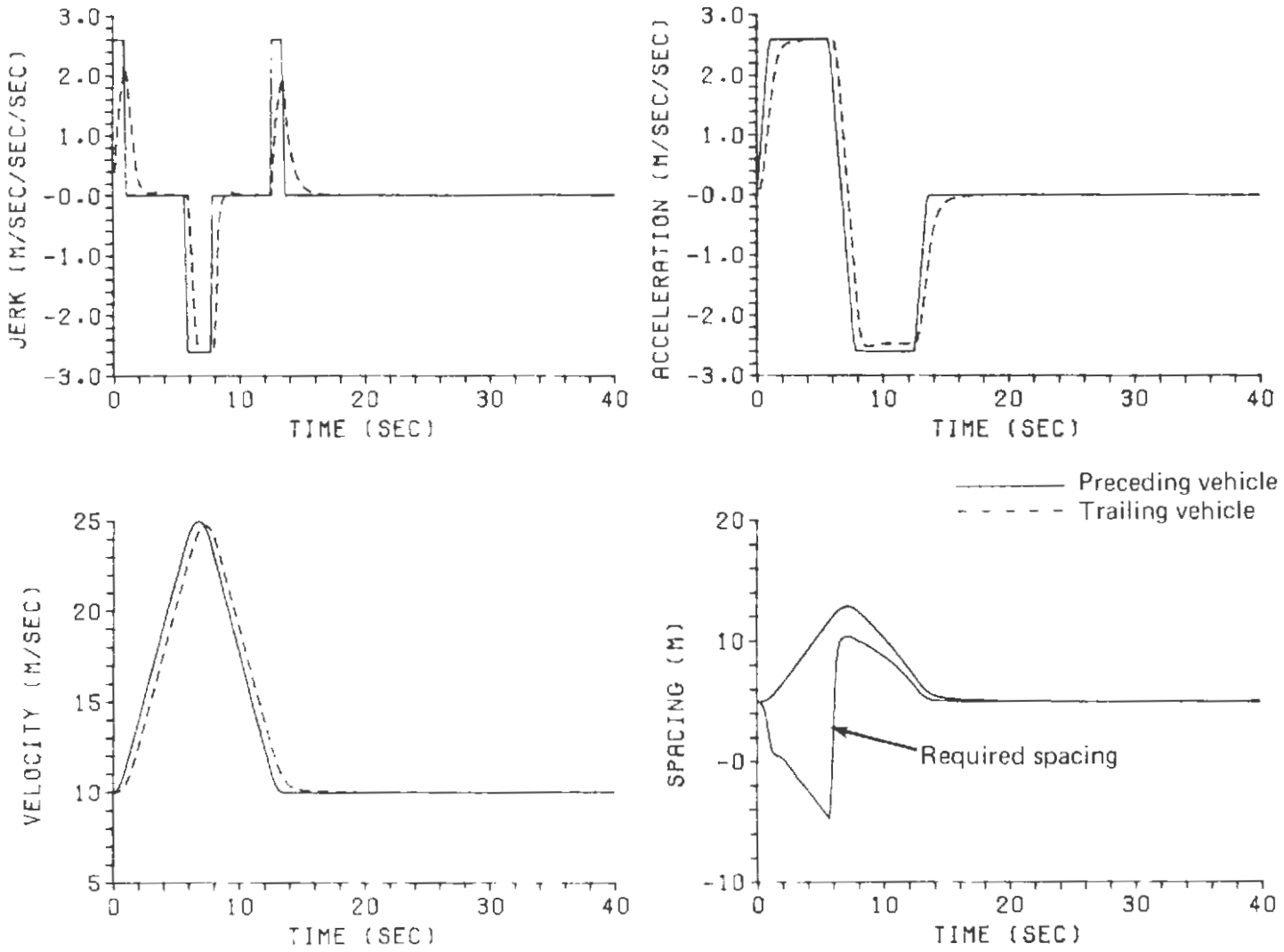

Fig. 45 Suboptimal Control II in Regulator Mode

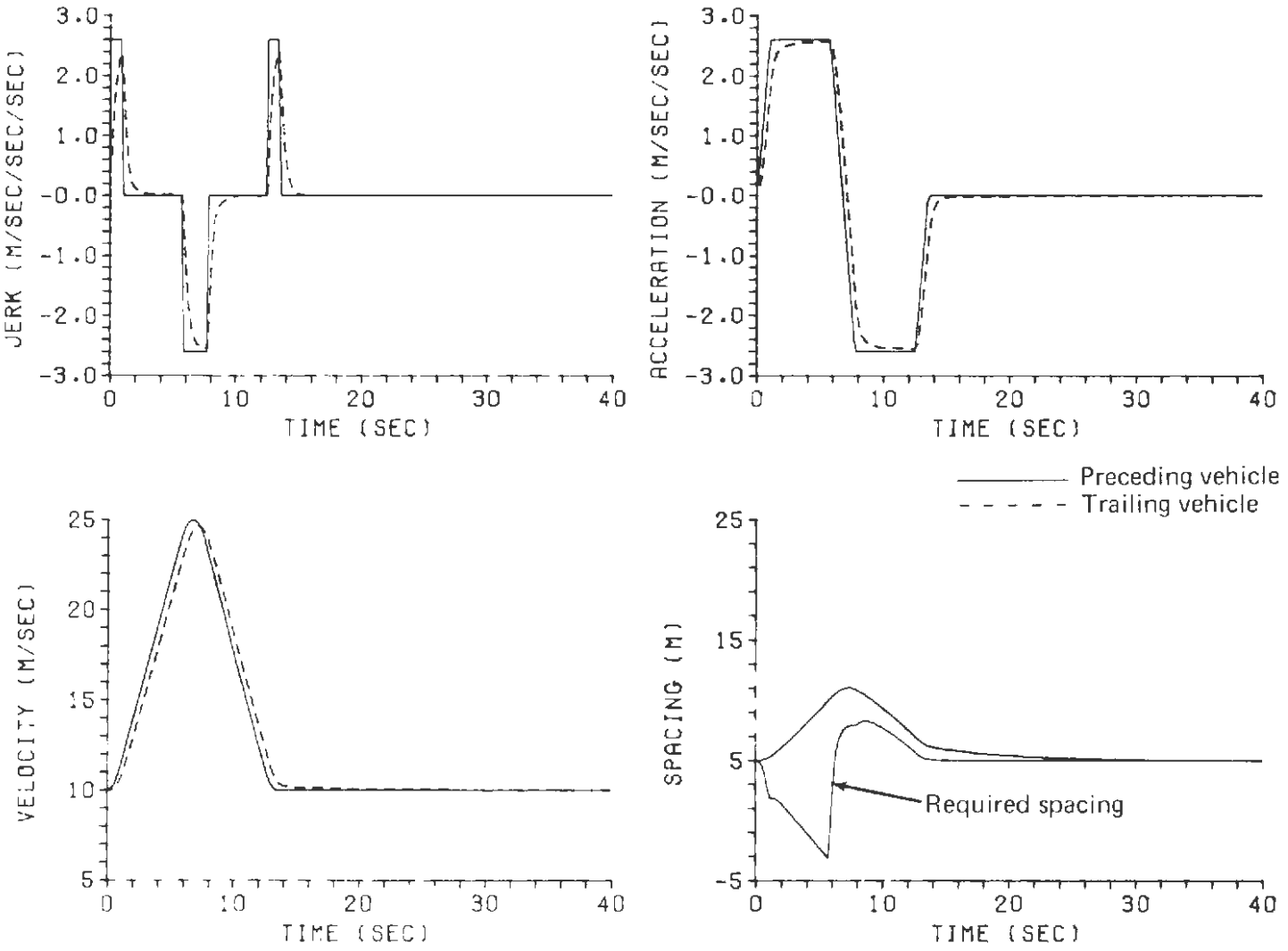

Fig. 46 Suboptimal Control III in Regulator Mode

The headway profiles for suboptimal controls I, II, and III are shown in Fig. 47. The decrease in headway for suboptimal control I demonstrates its effectiveness in following preceding vehicle velocity changes. The results show that suboptimal control II is the most effective in maintaining the desired headway.

The example is repeated for a desired headway of 3 s using suboptimal controls I, II, and III in Figs. 48, 49, and 50, respectively. The headway comparison is shown in Fig. 51.

CONTROLLER PERFORMANCE IN A FIVE-VEHICLE STRING

The performance of the optimal and various suboptimal controls for a string of vehicles is shown through several examples in the following discussion. Suboptimal control I will be dropped from further consideration since it offers no advantage over the optimal control other than some reduced computational complexity. We will show three examples for desired headways of 0.5 and 3 s. The initial conditions for each example may be described with the aid of Fig. 52 with numerical values given in Table 2.

The first example is a simple overtaking maneuver. The optimal control responses for headways of 0.5 and 3 s are shown in Figs. 53 and 54, respectively.

The second example is again a simple overtaking, but at 20 s into the transition the lead vehicle decelerates on limits to 10 m/s. The resulting responses with h = 0.5 s for the optimal control and suboptimal controls II and III are shown in Figs. 55, 56, and 57, respectively. At a desired headway of 3 s the optimal control response is shown in Fig. 58 and suboptimal control II response is shown in Fig. 59.

Finally, an example with speed-up maneuvers will be shown. The initial conditions for example 3 are shown in Table 2 with all vehicles at the desired headway. At t = 0 the lead vehicle accelerates to 25 m/s and then immediately decelerates to 15 m/s. At t = 15 s the lead vehicle accelerates to 20 m/s and immediately decelerates to 10 m/s. The response curves for suboptimal control II are shown in Fig. 60 with h = 0.5 s and in Fig. 61 with h = 3 s.

In all of the above cases the string response is satisfactory with no indication of instability.

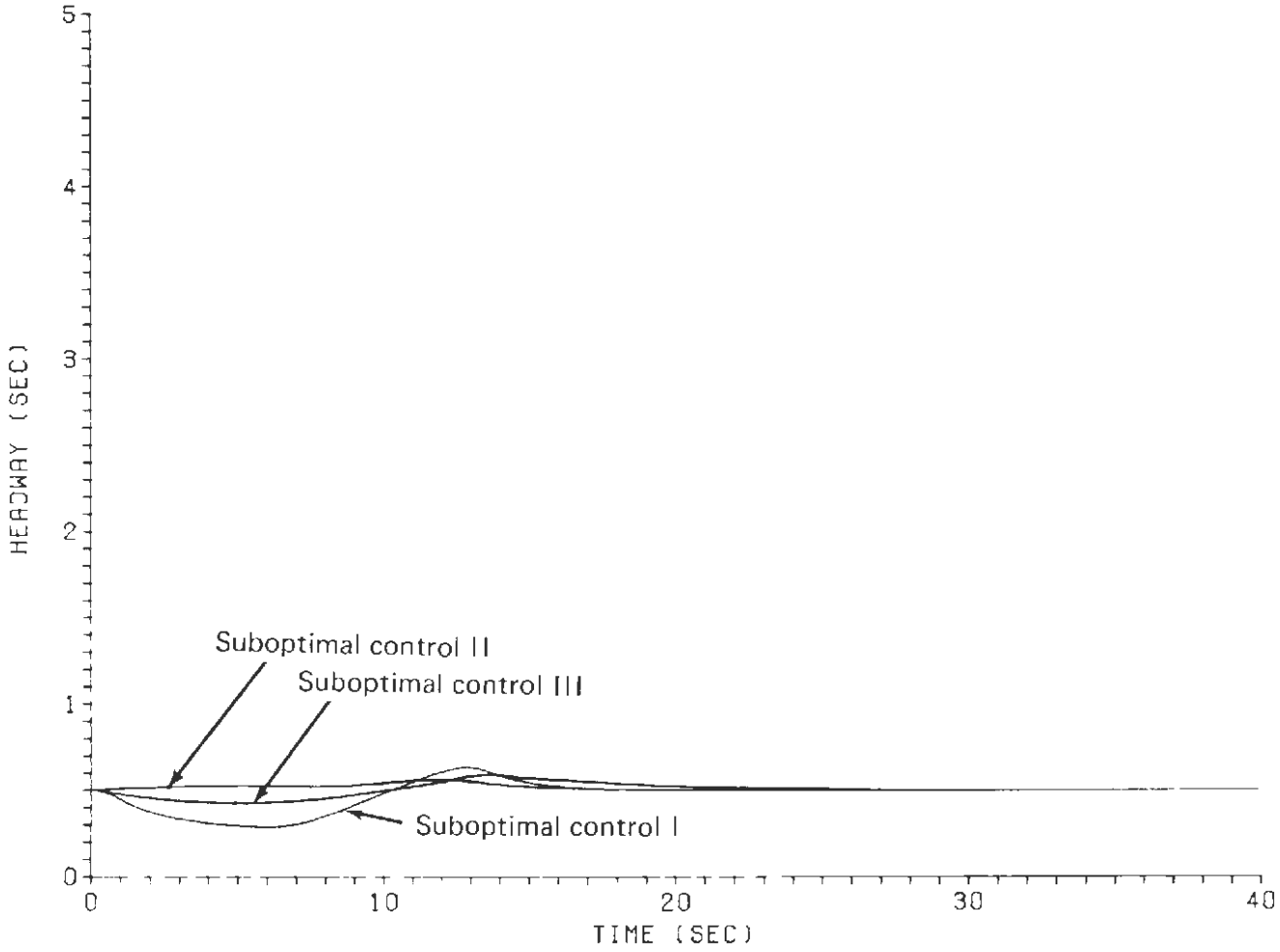

Fig. 47 Headway Profiles in Regulator Mode

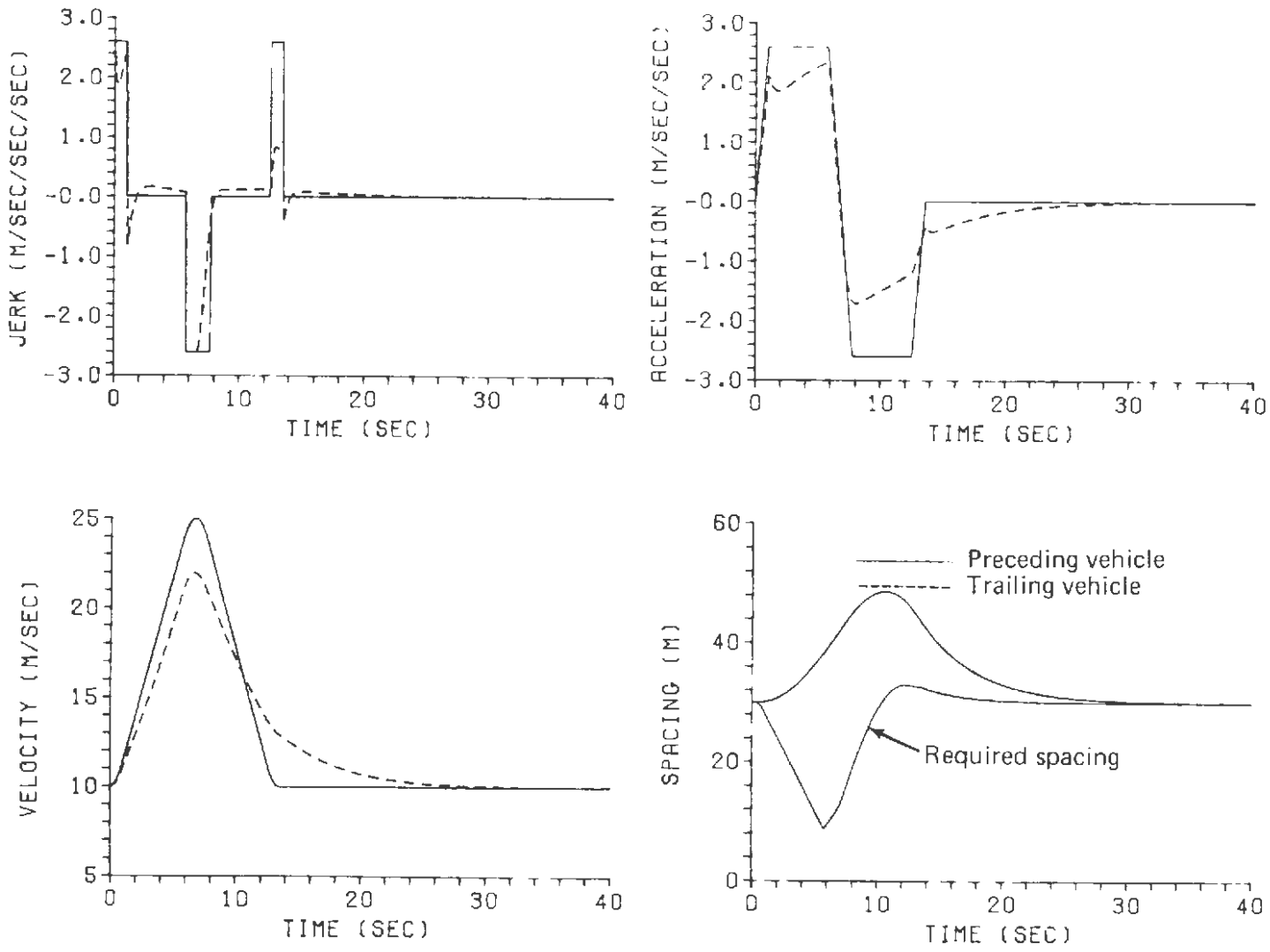

Fig. 48 Suboptimal Control I in Regulator Mode for h = 3 s

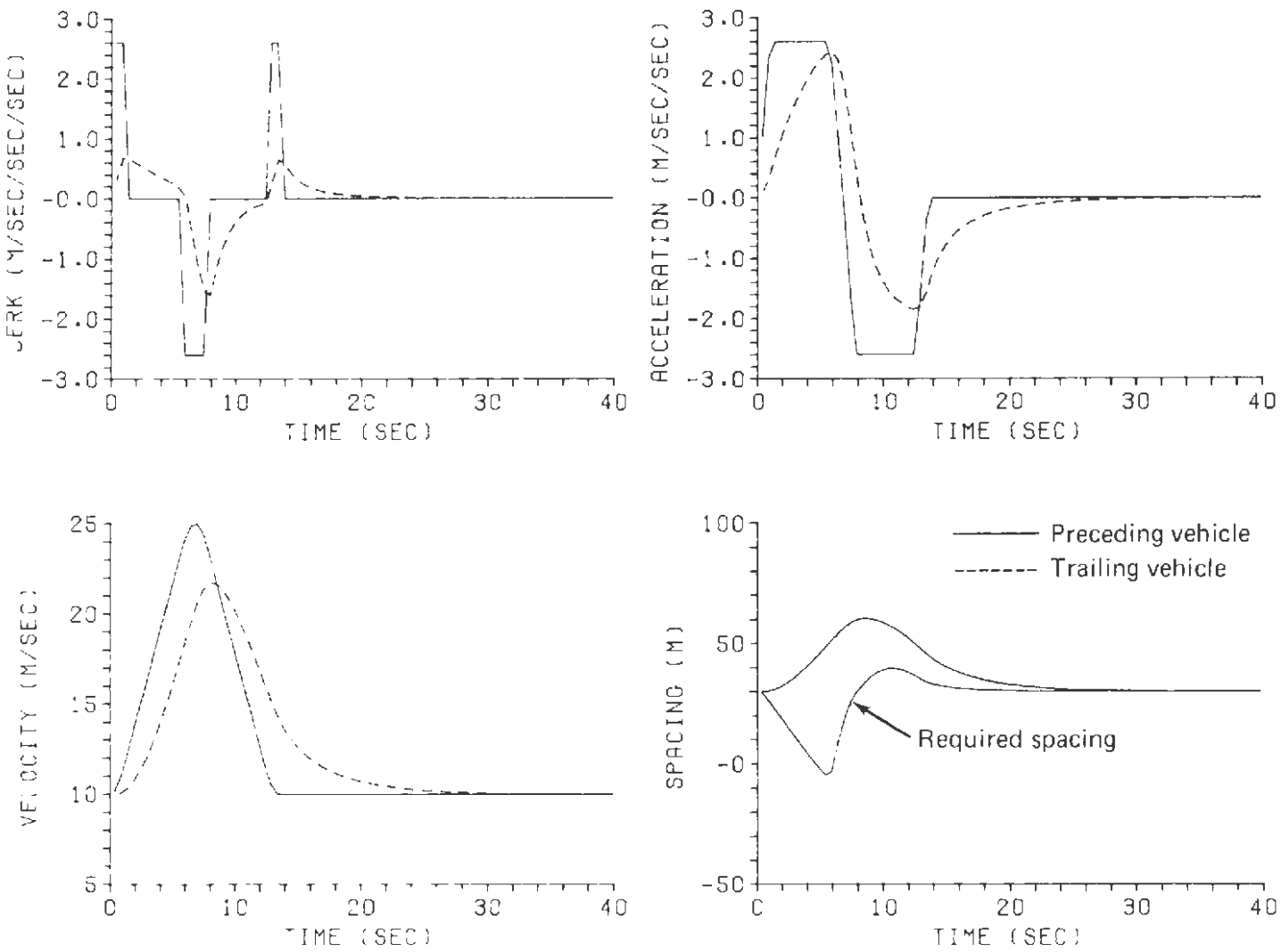

Fig. 49 Suboptimal Control II in Regulator Mode for h = 3 s

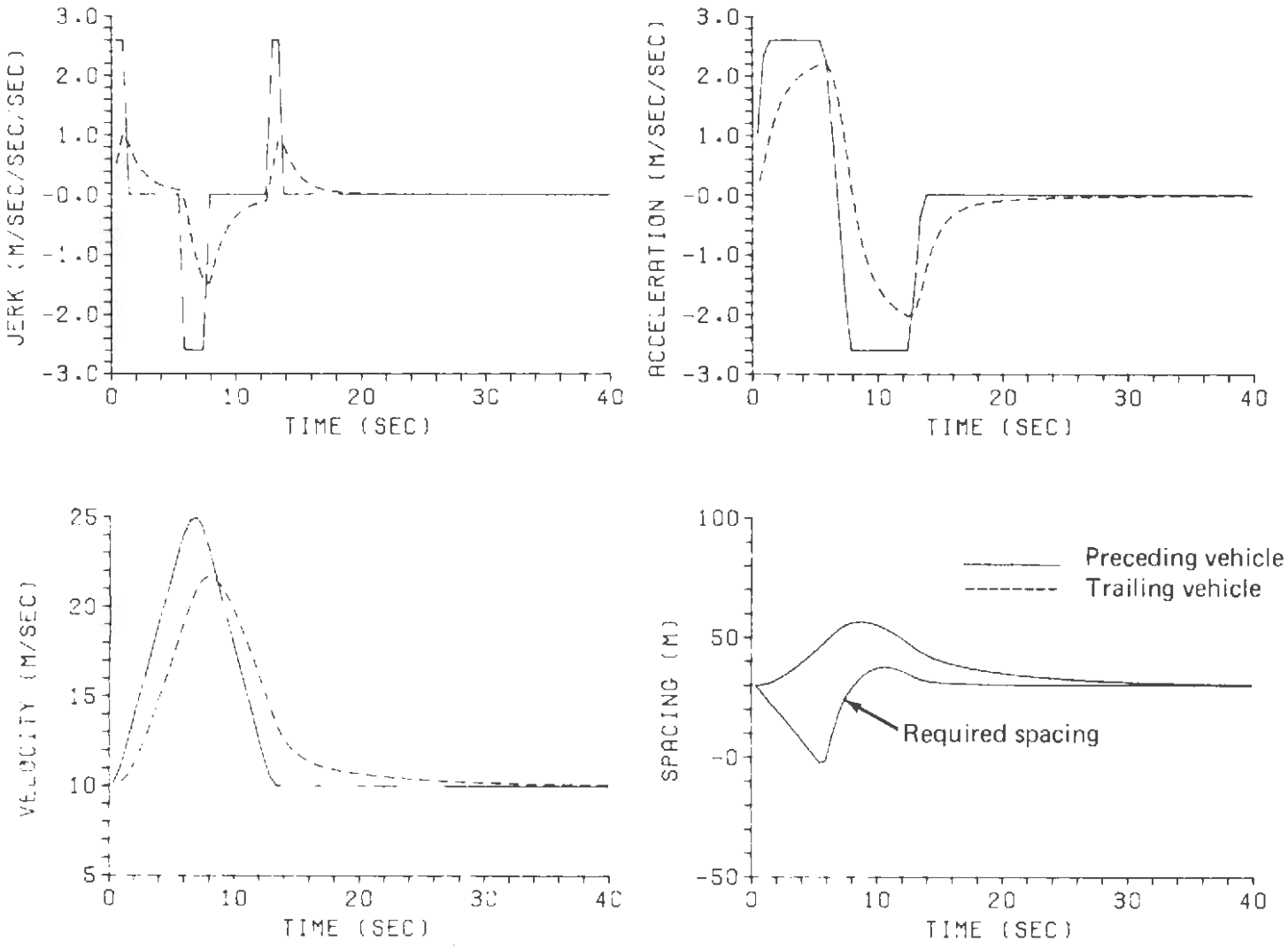

Fig. 50 Suboptimal Control III in Regulator Mode for h = 3 s

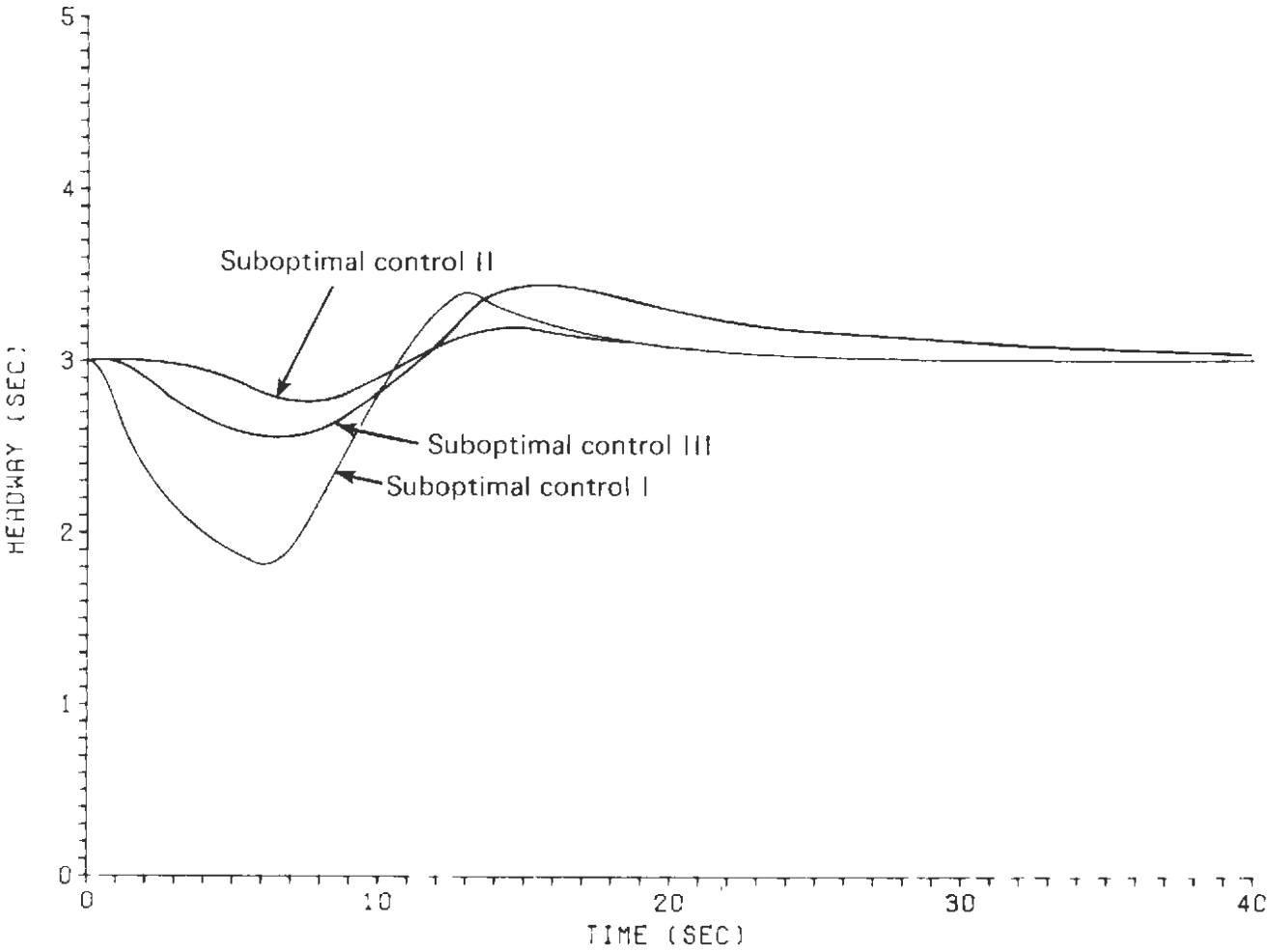

Fig. 51 Headway Profiles in Regulator Mode for h = 3 s

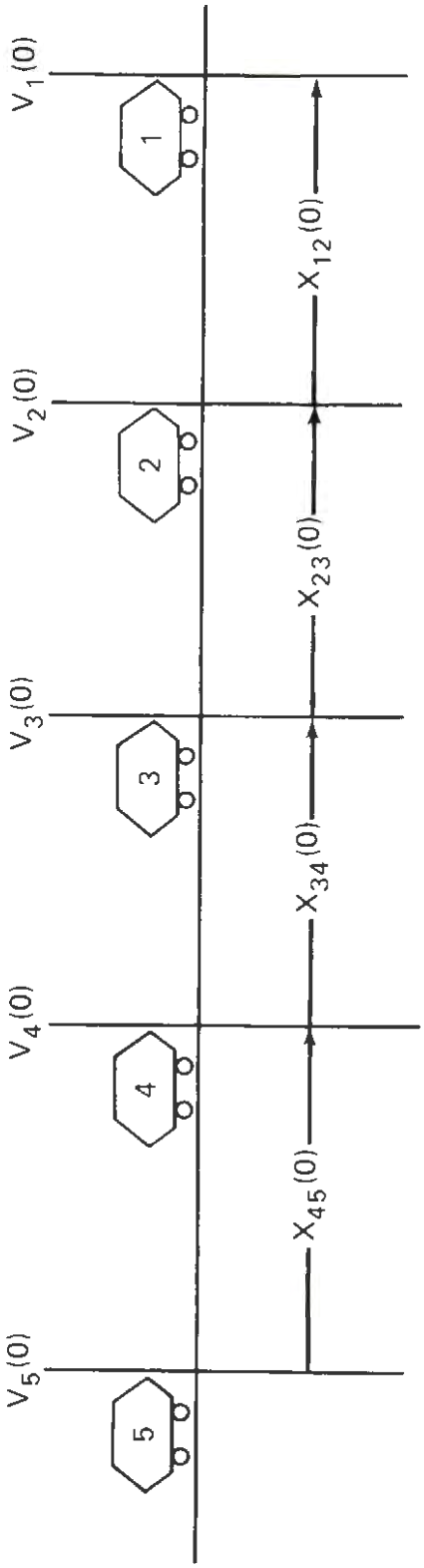

Fig. 52 Initial Conditions for a Five-Vehicle String

Table 2

Initial Conditions for Five-Vehicle String Examples

		Velocity (m/s)					Spacing (m)			
Example	Headway (s)	V_1	V_2	V_3	V_4	V_5	$X_{12}(0)$	$X_{23}(0)$	$X_{34}(0)$	$X_{45}(0)$
1	0.3	10	20	20	20	20	100	60	60	60
	3	10	20	20	20	20	120	100	100	100
2	0.5	15	25	25	25	25	100	50	50	50
	3	15	25	25	25	25	140	100	100	100
3	0.5	20	20	20	20	20	10	10	10	10
	3	20	20	20	20	20	60	60	60	60

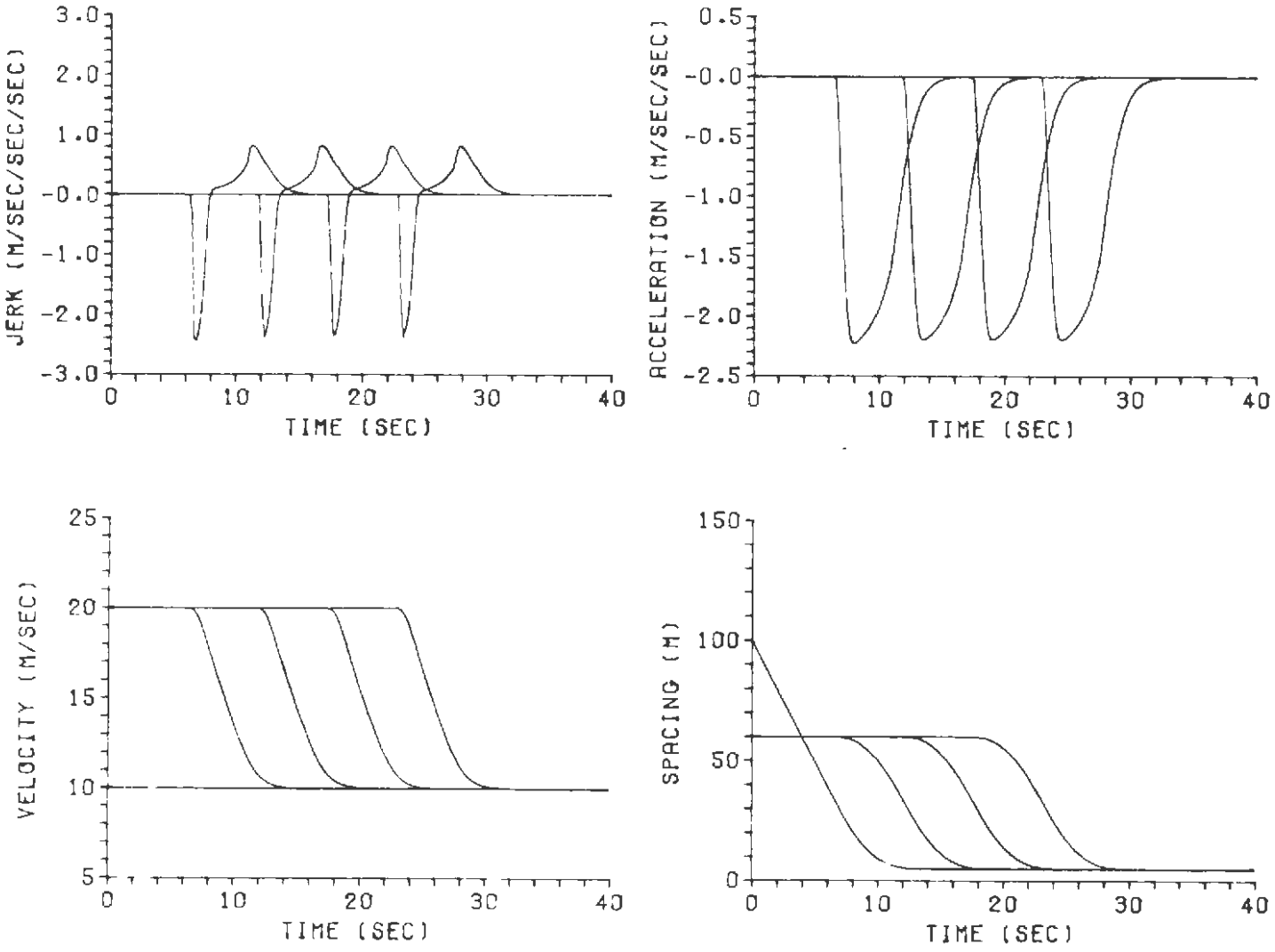

Fig. 53 Optimal Control Response for Example 1 with h = 0.5 s

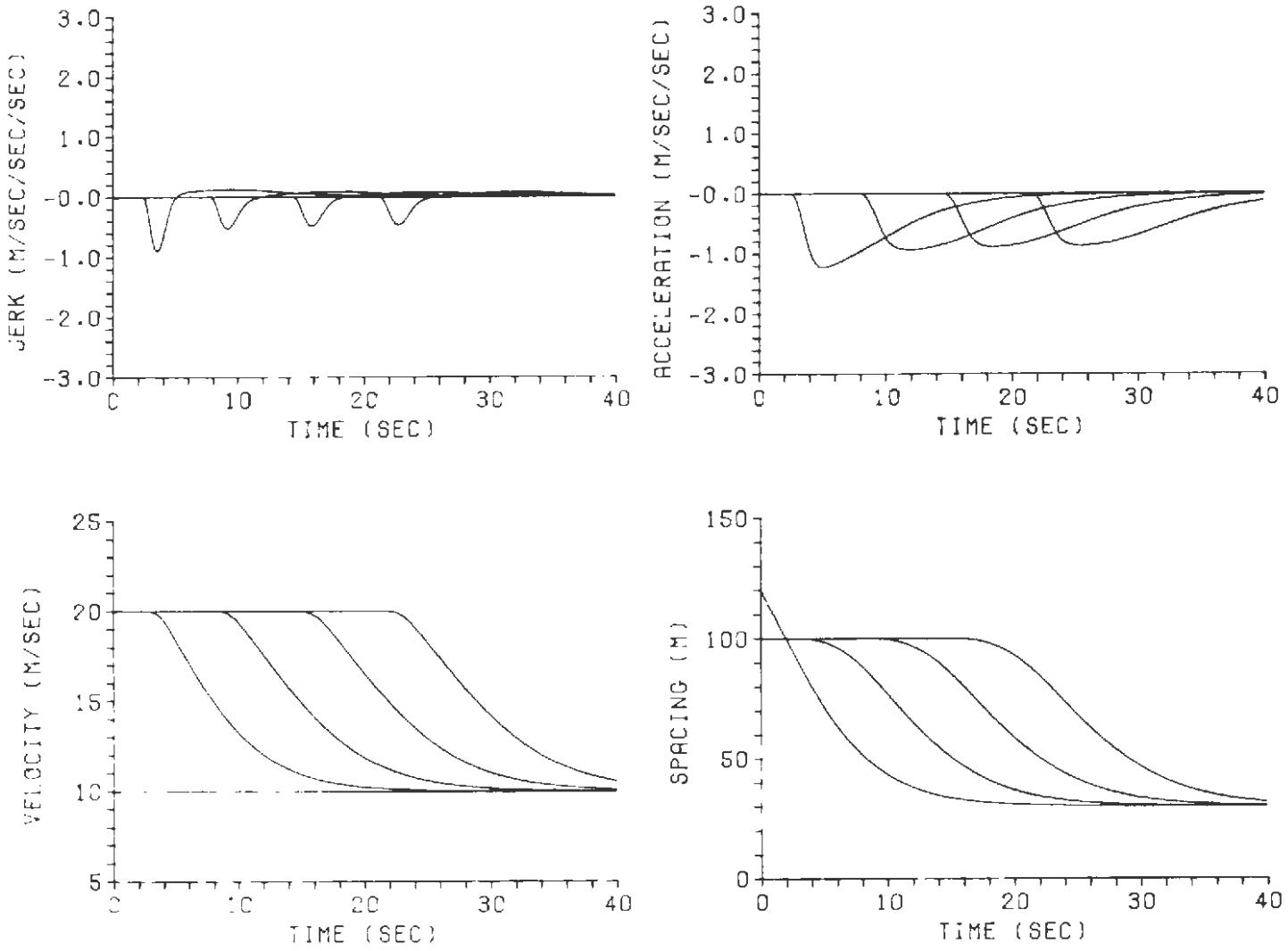

Fig. 54 Optimal Control Response for Example 1 with h = 3 s

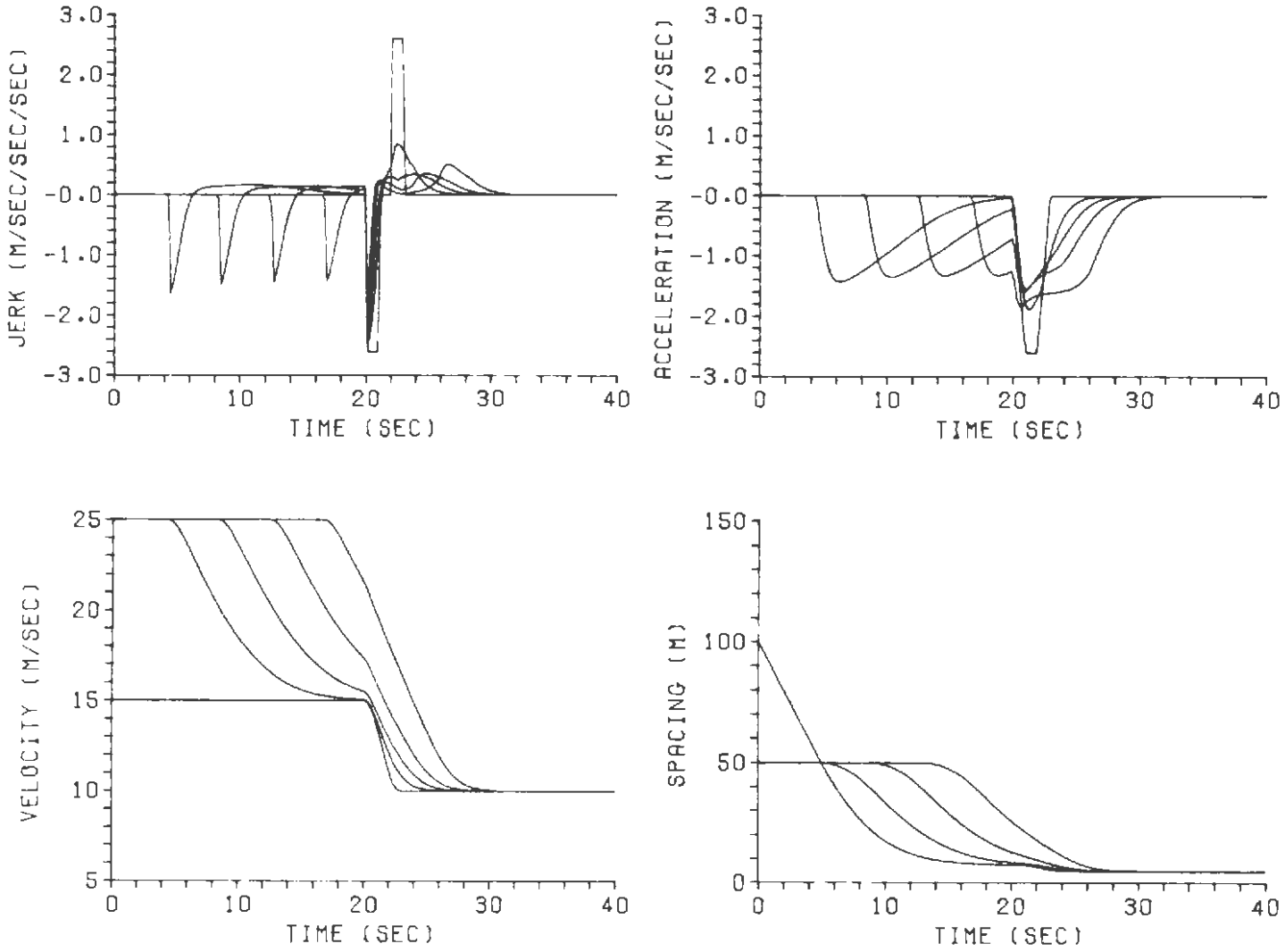

Fig. 55 Optimal Control Response for Example 2 with h = 0.5 s

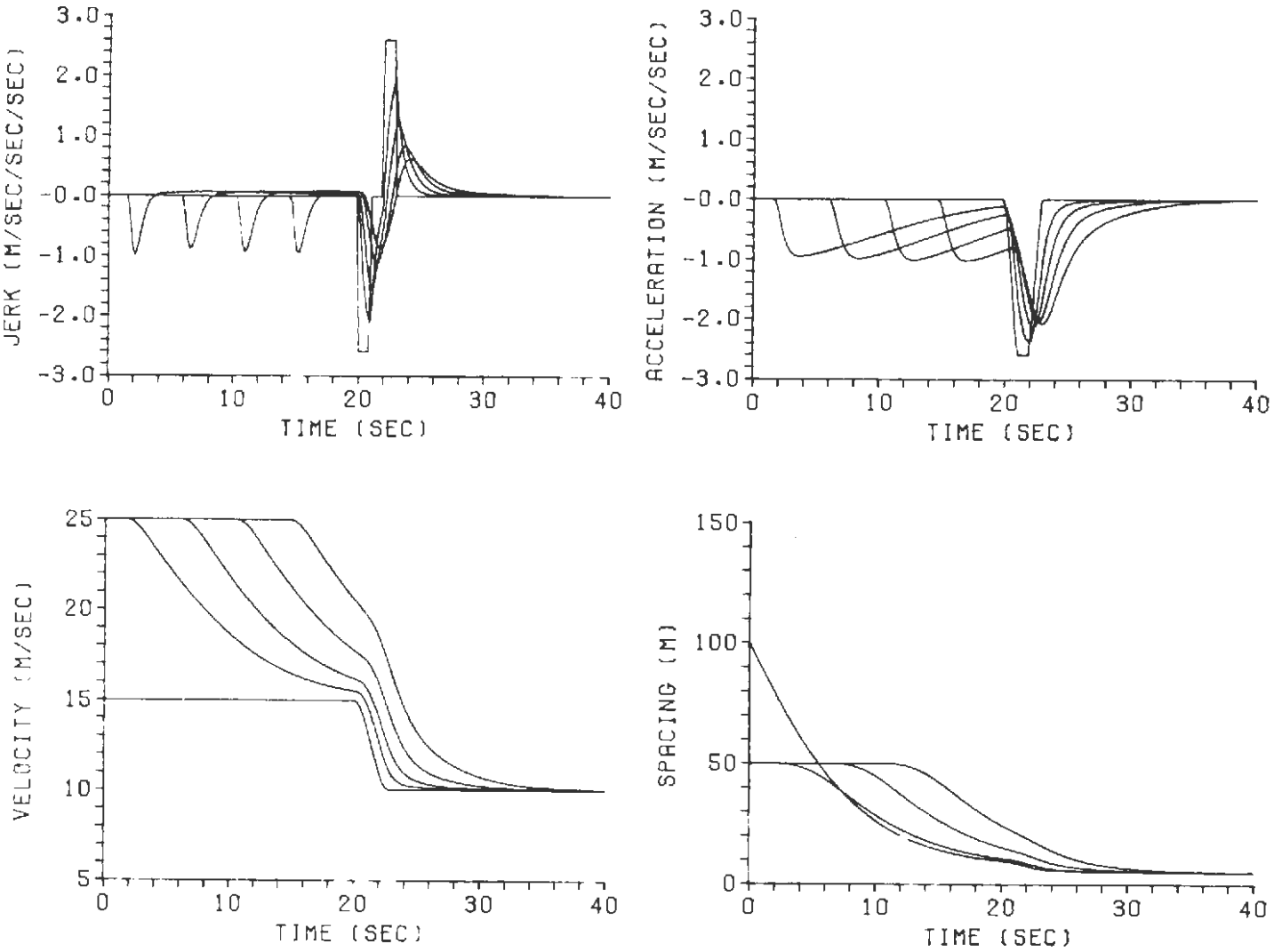

Fig. 56 Suboptimal Control II Response for Example 2 with h = 0.5 s

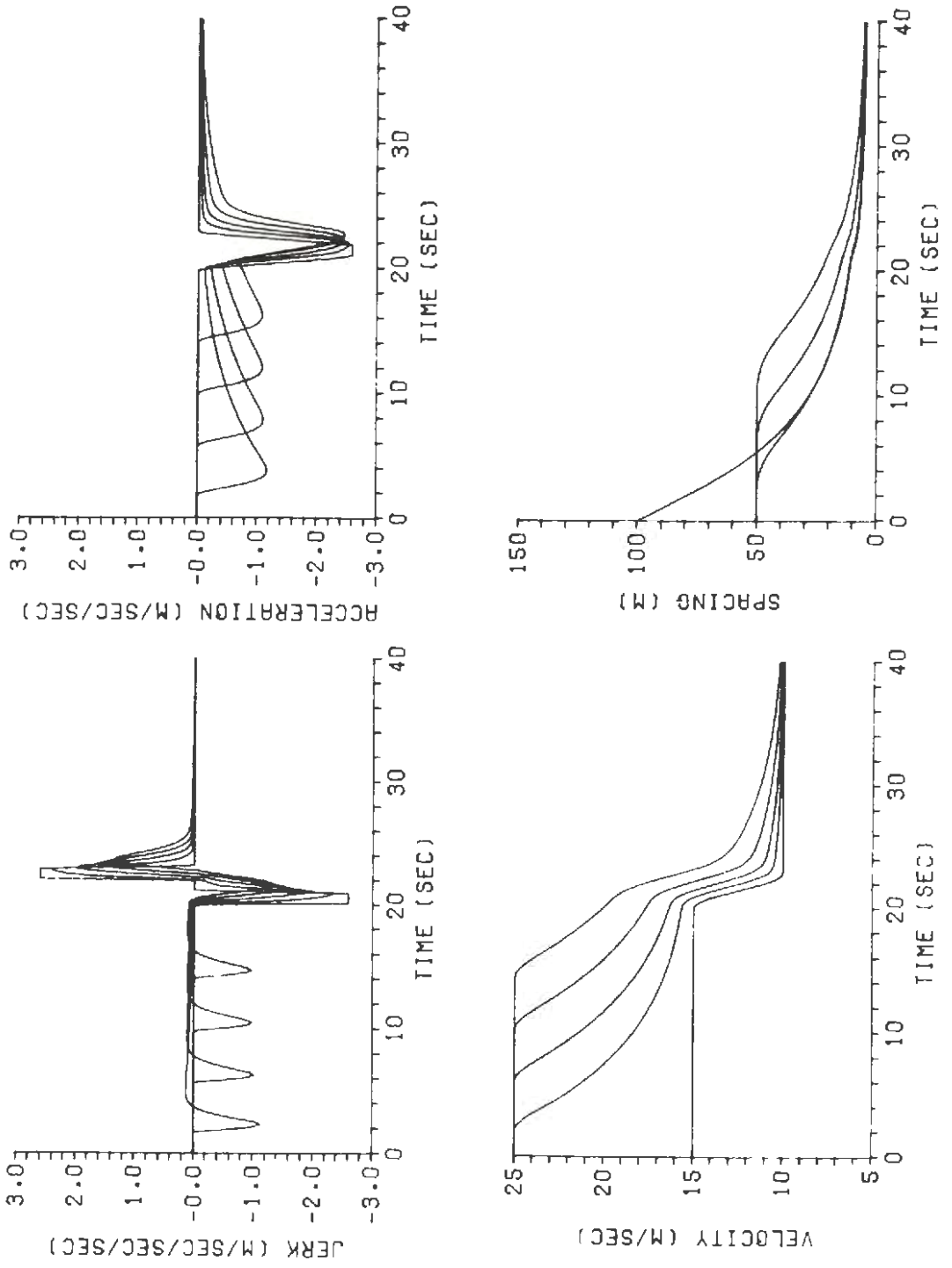

Fig. 57 Suboptimal Control III Response for Example 2 with h = 0.5 s

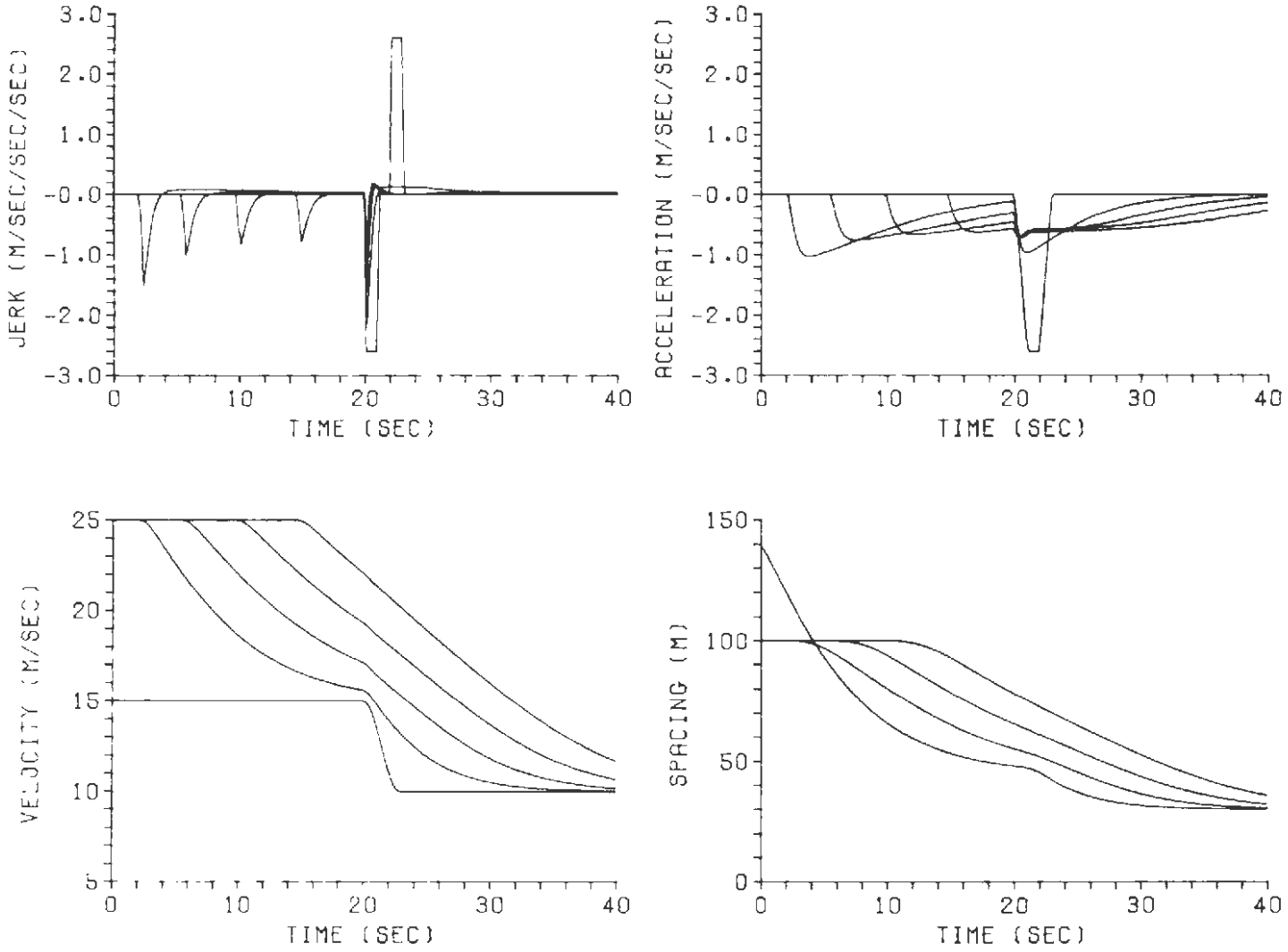

Fig. 58 Optimal Control Response for Example 2 with h = 3 s

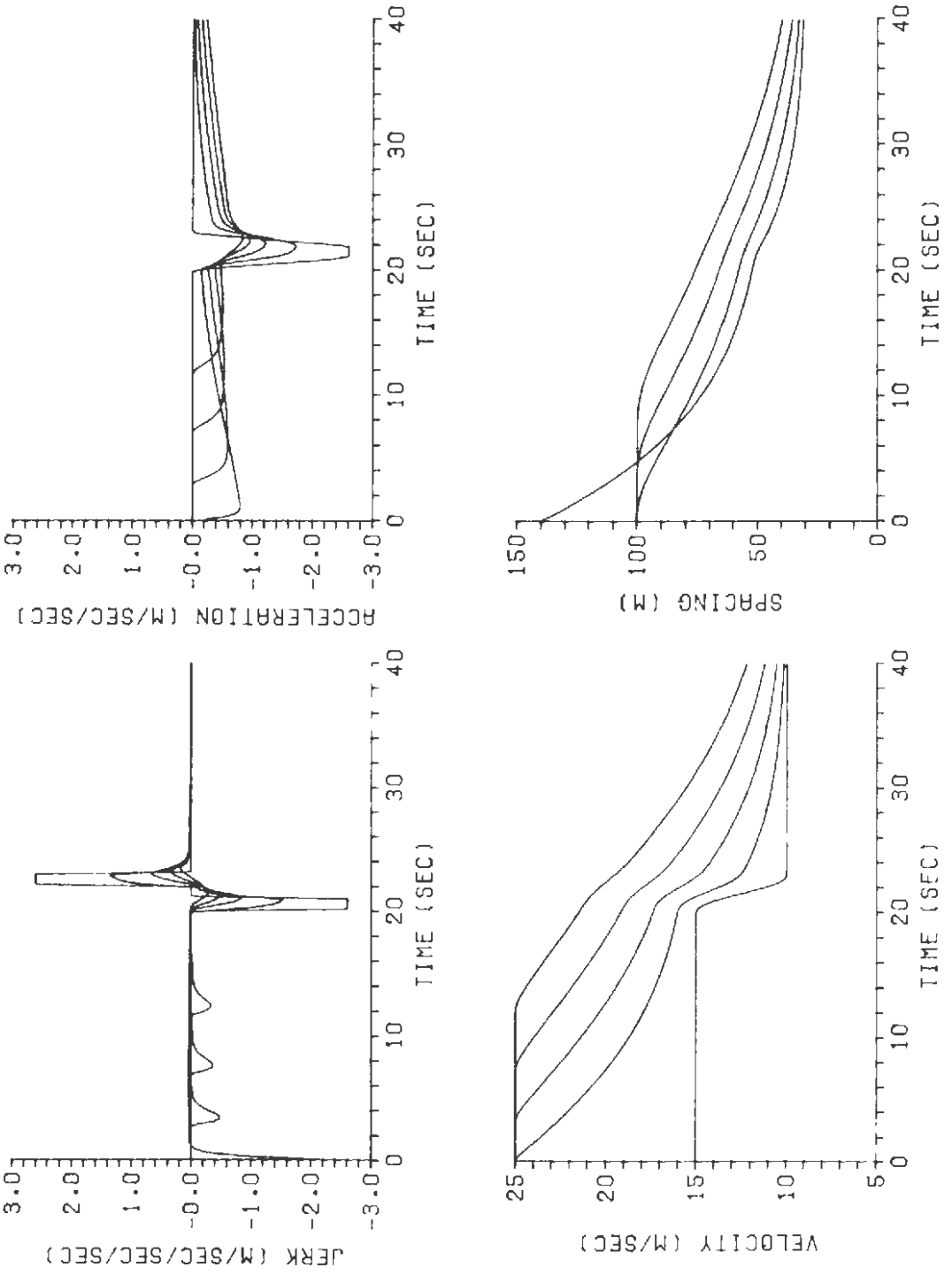

Fig. 59 Suboptimal Control II Response for Example 2 with h = 3 s

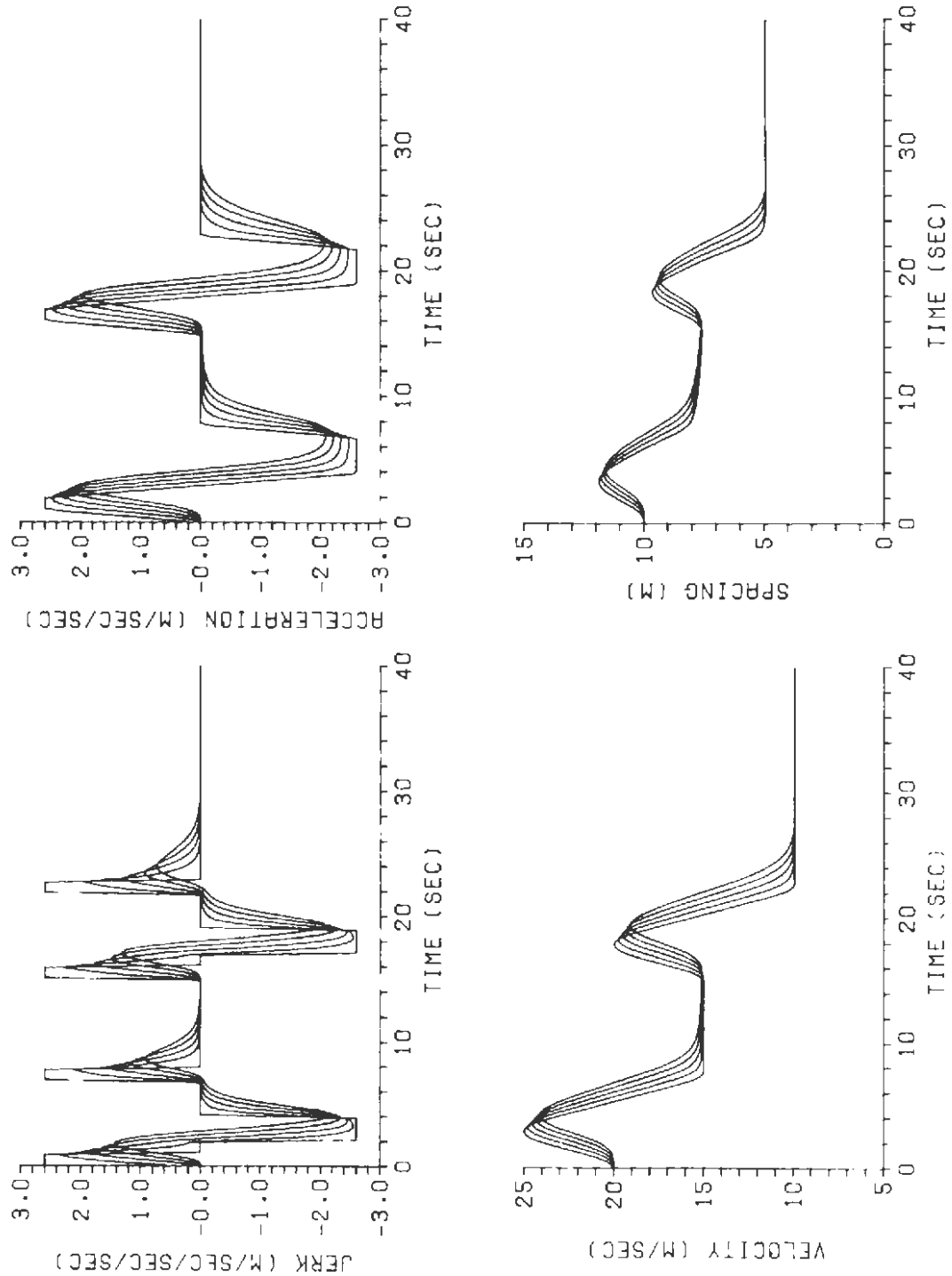

Fig. 60 Suboptimal Control II Response for Example 3 with h = 0.5 s

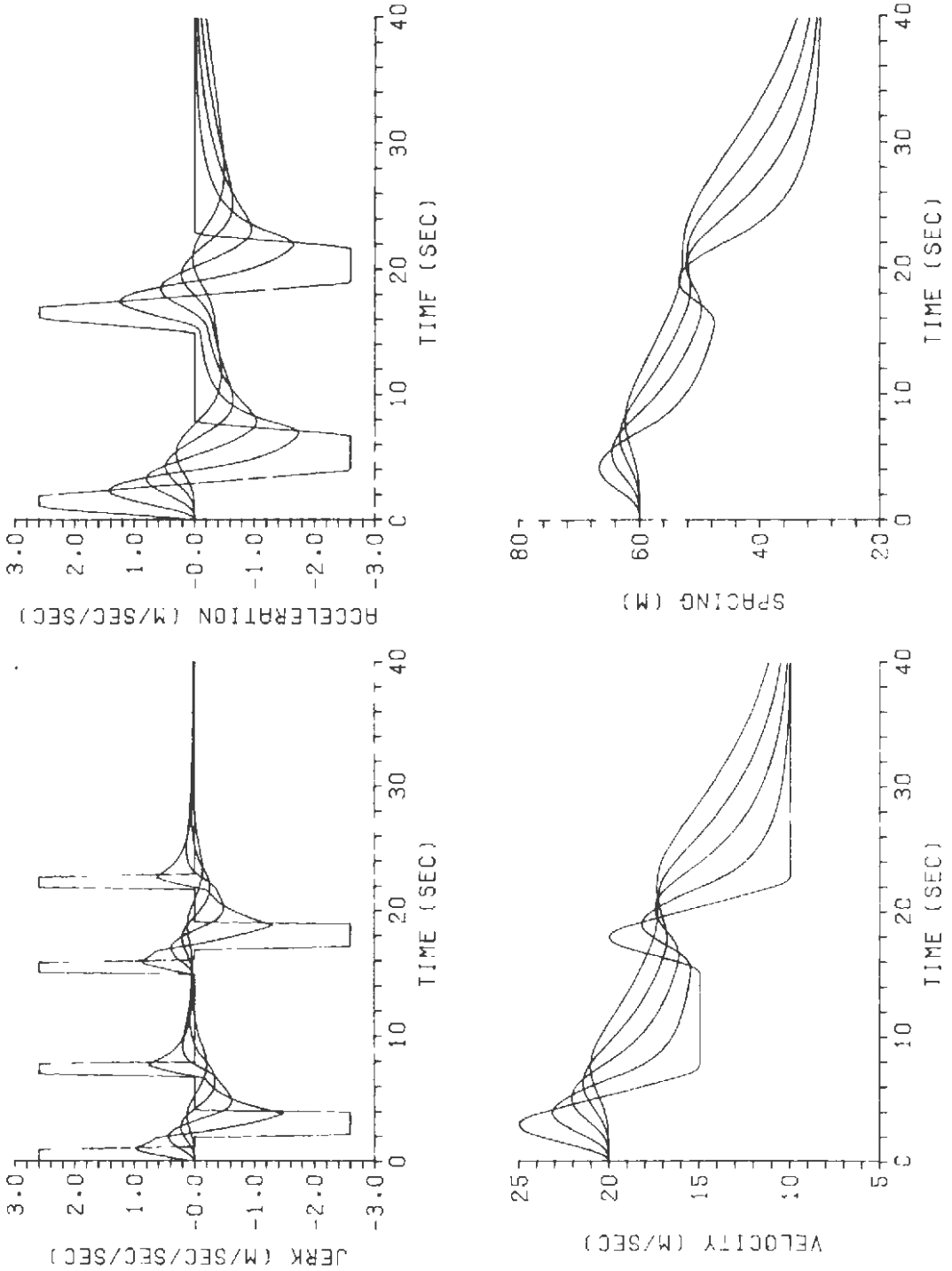

Fig. 61 Suboptimal Control II Response for Example 3 with h = 3 s

8. CONCLUSIONS

A vehicle-following control law may be designed by explicitly considering the state constraints that define the capabilities of each vehicle. The imposed jerk and acceleration limits that assure passenger safety and comfort dictate a kinematic constraint, thus leading to the nonlinear controller derived in Section 4. The resulting control law is optimal in the sense that the vehicle precisely follows the spacing required to prevent the possibility of collision. However, it is not minimum in time for any given initial condition since we are constraining the vehicle to follow a velocity-command mode until it is necessary to switch to the vehicle-following mode. Subsequently, as the vehicle transitions to the nominal headway, the control is then minimum time.

We have also shown that the kinematic constraint may be modified to enable the controller to act as a regulator at nominal headway. The relatively small degradation in performance due to this modification for typical overtaking situations warranted its adoption as what we term "optimal control."

Although the optimal control law could be implemented in terms of the on-line computational requirements, several suboptimal controls were derived with the aim of reducing the informational requirements. That is, optimal control requires preceding-vehicle velocity, acceleration, and jerk while the suboptimal needs only spacing, velocity error, and acceleration error in addition to trailing vehicle velocity and acceleration. Each suboptimal control is based on successive simplification of the kinematic constraint to produce a control such that the maintained spacing is greater than the required spacing except at nominal headway, where they are equal. Suboptimal control III resulted in linear time-invariant feedback, which could be analyzed in the frequency domain to ensure string stability. The operation of suboptimal control III is, in effect, to null the velocity error. Consequently, the kinematic constraint is satisfied while preceding vehicle maneuvers can be followed. In terms of reducing headway, suboptimal control III was found to require approximately two to three times the optimal-control time span for some overtaking situations. On the other hand, suboptimal control II requires less time (66% of suboptimal control III time) with only a small increase in complexity. Suboptimal control I requires no less information than the optimal but the computational complexity is somewhat simplified. Consequently, of the control laws considered, suboptimal control II seems to be the most attractive in terms of simplicity and performance.

In general, the kinematics associated with a vehicle-following automated-guideway transit system defines a constraint region in state space that may be used to generate control laws to follow the boundary of the allowable region. If a new boundary is defined within the allowable region, it may provide a simplification of the corresponding control and, therefore, may be a usable solution. The viability of the solution depends upon the completeness of the original constraint definition. Thus, extension of the technique to problems such as merging requires a total description of the kinematic requirements involved. The kinematic requirements will then dictate a control that assures safety and optimum performance.

9. RECOMMENDATIONS FOR FUTURE STUDY

The technique presented in this study has been shown to admit a workable solution to the vehicle-following problem at short headways. However, additional verification of its applicability to a real system leads to the suggested areas for investigation outlined below.

Computer simulation studies should include a vehicle plant model in the system. The sensitivity of the resulting controller to parameter changes, wind, grade, and loading may then be evaluated.

The configuration of a controller in a real system through determination of digital-analog tradeoffs and vehicle-wayside control allocation should be investigated. In particular, vehicle performance may be evaluated in terms of implementation costs such as data rate, quantization error, and time delay.

The problem of measurement accuracy affects the above two areas. That is, a trade-off exists between vehicle performance and the accuracy of wayside information (i.e., the accuracy of the absolute measurement rather than the effects of sampling, quantization, etc.). The resulting requirements will strongly affect system costs and the manner in which measurements are obtained.

The use of this control technique in emergency operation, merging, and injection of vehicles onto the guideway would provide uniformity in control for all situations. Consequently, this suggests a simplified controller as opposed to a collection of ad hoc procedures to handle these various conditions.

REFERENCES

1. W. S. Levine and M. Athans, "On the Optimal Error Regulation of a String of Moving Vehicles," IEEE Trans. Autom. Control, Vol. AC-11, No. 3, July 1966.

2. M. Athans, W. S. Levine, and A. H. Levis, "On the Optimal and Suboptimal Position and Velocity Control of a String of High Speed Moving Trains," MIT Electronic Systems Laboratory Report PB 173640, November 1966.

3. E. P. Cunningham and E. J. Hinman, "Approach to Velocity/Spacing Regulation and the Merging Problem in Automated Transportation," Joint Transportation Engineering Conference, Chicago, IL, October 1970.

4. S. J. Brown, Jr., "Design of Car-Follower Type Control Systems with Finite Bandwidth Plants," Proc. Seventh Annual Princeton Conference on Information Sciences and Systems, March 1973.

5. R. E. Fenton et al., "Fundamental Studies in the Automatic Longitudinal Control of Vehicles," DOT-TST-76-79, July 1975.

6. G. B. Stupp, H. Y. Chiu, and S. J. Brown, "Feasibility of Vehicle-Follower Controls for Short-Headway AGT Systems," APL/JHU TPR-035, December 1976.

7. G. N. Saridis and Z. V. Rekasius, "Design of Approximately Optimal Feedback Controllers for Systems with Bounded States," IEEE Trans. Autom. Control, Vol. AC-12, No. 4, August 1967.

8. G. N. Saridis, "On the Exact and Approximate Solutions of the Optimal Control Problem with Bounded State Variables," Ph.D. dissertation, Purdue University, Lafayette, IN, August 1965.

9. A. Bryson and Y. Ho, Applied Optimal Control, John Wiley & Sons, New York, 1975.

Appendix A

DISTANCE AND TIME REQUIREMENTS FOR A VEHICLE MANEUVER

As discussed in Section 3 there are two possible on-limit vehicle maneuvers designated maneuvers 1 and 2 in Fig. 3. For a given vehicle acceleration, A, and velocity, V, the distance and time required to attain a desired final velocity, V_f, is given below for each maneuver profile. In addition, the conditions that dictate a particular maneuver are given in terms of A and V.

MANEUVER 1: $\frac{1}{2} A^2 + J_s (V - V_f) \geq A_s^2$

$$d_r = \frac{1}{8A_s J_s^2} A^4 + \frac{1}{3J_s^2} A^3 + \frac{A_s}{4J_s^2} A^2 + \frac{1}{2A_s J_s} A^2 V + \frac{AV}{J_s} + \frac{A_s}{2J_s} V + \frac{V^2}{2A_s} - \frac{V_f^2}{2A_s} + \frac{A_s V_f}{2J_s}$$

$$t_t = \frac{A_s + A}{J_s} + \frac{A^2}{2A_s J_s} + \frac{V - V_f}{A_s}$$

MANEUVER 2: $\frac{1}{2} A^2 + J_s (V - V_f) \leq A_s^2$

$$d_r = -\frac{1}{6J_s^2} (A - A')^3 + \frac{A}{2J_s^2} (A - A')^2 + \frac{V}{J_s} (A - A') + \frac{A'^3}{3J_s^2} - \frac{A'}{J_s} \left[\frac{1}{2J_s} (A^2 - A'^2) + V \right]$$

where

$$A' = -\left| \frac{1}{2} A^2 + J_s (V - V_f) \right|^{1/2}$$

$$t_r = \frac{A - 2A'}{J_s}$$

Appendix B

KINEMATIC BOUNDARY CONTROLS

The control that keeps a vehicle on the kinematic boundary was given in Section 4 by Eq. 13. The control requires the partial derivative of the constraint function with respect to each of the vehicle states, V_T, V_P, A_T, and A_P. For each vehicle, there is a set of partial derivatives corresponding to each of the two possible vehicle maneuvers. These may be calculated from the equations given in Appendix A as follows.

MANEUVER 1: $\frac{1}{2} A^2 + J_s (V - V_{min}) \geq A_s^2$

$$\frac{\partial d_r}{\partial V} = \frac{1}{2A_s J_s} A^2 + \frac{A}{J_s} + \frac{A_s}{2J_s} + \frac{V}{A_s}$$

$$\frac{\partial d_r}{\partial A} = \frac{1}{2A_s J_s} A^3 + \frac{1}{J_s^2} A^2 + \frac{A_s}{2J_s^2} A + \frac{V}{A_s J_s} A + \frac{V}{J_s}$$

$$\frac{\partial t_r}{\partial V} = \frac{1}{A_s}$$

$$\frac{\partial t_r}{\partial A} = \frac{1}{J_s} + \frac{A}{A_s J_s}$$

MANEUVER 2: $\frac{1}{2} A^2 + J_s (V - V_{min}) \leq A_s^2$

$$\frac{\partial d_r}{\partial V} = - \frac{A^2}{2J_s A'} + \frac{A}{J_s} - \frac{A'}{2J_s} - \frac{V}{A'}$$

$$\frac{\partial d_r}{\partial A} = - \frac{A^3}{2J_s^2 A'} + \frac{A^2}{J_s^2} - \frac{AA'}{J_s A'} - \frac{AV}{J_s A'} + \frac{V}{J_s}$$

$$\frac{\partial t_r}{\partial V} = \frac{1}{A'}$$

$$\frac{t_r}{A} = \frac{1}{J_s} - \frac{A}{J_s A'}$$

$$A' = -\sqrt{\frac{1}{2} A^2 + J_s (V - V_{min})}$$

SYMBOLS

A_P	preceding vehicle acceleration
A_s	service acceleration limit
A_T	trailing vehicle acceleration
$c(\underline{x})$	kinematic constraint function
δ_1	magnitude of $c(\underline{x})$ at which full positive service jerk is applied
δ_2	smoothing parameter in acceleration limiter
δ_3	magnitude of $c(\underline{x})$ at which full negative service jerk is applied
Δ	equal to δ_1 and δ_3 when $\delta_1 = \delta_3$
d_r^P	distance required for preceding vehicle to decelerate to minimum line speed
d_r^T	distance required for trailing vehicle to decelerate to minimum line speed
$\underline{g}(x)$	constraint vector
h	time headway
J_P	preceding vehicle jerk
J_s	service jerk limit
J_T	trailing vehicle jerk
k	selected gain in suboptimal controller
$N(A,\omega)$	describing function; a function of input amplitude and frequency
S	vehicle spacing
t_r^P	time required for preceding vehicle to decelerate to minimum line speed
t_r^T	time required for trailing vehicle to decelerate to minimum line speed

u_B	nonlinear boundary control
u_{KB}	kinematic boundary control
u_R	linear regulator control
u'_R	modified linear regulator control for switch-on
V	vehicle velocity
V_{max}	maximum line speed
V_{min}	minimum line speed
V'_{min}	modified minimum line speed to prevent singularity in control
V_P	preceding vehicle velocity
V_T	trailing vehicle velocity
$W(\underline{x})$	scalar weighting function for dual mode controller
$W_1(\underline{x})$	scalar weighting function for u_{KB} and negative $c(\underline{x})$
$W_2(\underline{x})$	scalar weighting function for acceleration limiter
$W_3(\underline{x})$	scalar weighting function for u_{KB} and positive $c(\underline{x})$
X_P	preceding vehicle position
X_T	trailing vehicle position
ϵ	equal to $-c(\underline{x})$
ξ	damping
ω_n	natural frequency